

**THE REPUBLIC OF TURKEY  
BAHCESEHIR UNIVERSITY**

**VALIDATION OF THE FIRST TURKISH  
AXIAL-FLOW LEFT-VENTRICULAR  
ASSIST DEVICE (LVAD) USING  
PARTICLE IMAGE VELOCIMETRY (PIV)**

**Master Thesis**

**SINA DADGAR**

**ISTANBUL, 2014**



**THE REPUBLIC OF TURKEY  
BAHCESEHIR UNIVERSITY**

**THE GRADUATE SCHOOL OF NATURAL AND APPLIED  
SCIENCES M.S. ELECTRONICS ENGINEERING**

**VALIDATION OF THE FIRST TURKISH  
AXIAL-FLOW LEFT-VENTRICULAR  
ASSIST DEVICE (LVAD) USING  
PARTICLE IMAGE VELOCIMETRY (PIV)**

**Master Thesis**

**Sina Dadgar**

**Supervisor: Assoc. Dr. SARPER ÖZHARAR**

**ISTANBUL, 2014**

**THE REPUBLIC OF TURKEY**

**BAHCESEHIR UNIVERSITY**

**THE GRADUATE SCHOOL OF NATURAL AND APPLIED SCIENCE  
M.S. ELECTRONICS ENGINEERING**

**VALIDATION OF THE FIRST AXIAL-FLOW LEFT-VENTRICULAR  
ASSIST DEVICE USING PARTICLE IMAGE VELOCIMETRY (PIV)**

**SINA DADGAR**

**December 17, 2014**

This thesis has been approved by the Graduate School of Natural and Applied Sciences.

Assoc. Prof. NAFİİZ ARICA  
Graduate School Director

I certify this thesis meets all the requirements as a thesis for the degree of Master of Science.

Yrd. Doç. DR. AYÇA YALÇIN ÖZKUMUR  
Program Coordinator

This is to certify that we have read this thesis and we find it fully adequate in scope, quality and content, as a thesis for the degree of Master of Science.

Examining Committee Members

Signature

Thesis Supervisor  
Assoc. Prof. SARPER ÖZHARAR

-----

Member  
Prof. Dr. EROL SEZER

-----

Member  
Assoc. Prof. KAMURAN KADIPAŞAOĞLU

-----



## ABSTRACT

### VALIDATION OF THE FIRST TURKISH AXIAL-FLOW LEFT-VENTRICULAR ASSIST DEVICE USING PARTICLE IMAGE VELOCIMETRY (PIV)

SINA DADGAR

Electronics Engineering

Thesis Supervisor: Assoc. Dr. Sarper Özharar

December 2014, 93 Pages

Heart Failure (HF) is a major cause of mortality in 21<sup>st</sup> century modern life. HF is the case when human cardiovascular system cannot satisfy body's metabolic needs with enough pressure and flow. End Stage Chronic Heart Failure (ES-CHF) can only be treated by Heart Transplantation (HT), but due to insufficient number of available donor hearts, Mechanical Circulatory Support Systems (MCSS) have been used to support ES-CHF patients. Left-Ventricular Assist-Devices (LVAD) being one type of MCSSs, support Left Ventricle's (LV) function by pumping blood from LV to aorta in one direction. Depending on the patient's situation, LVADs can be implanted on patient's body for different purposes. Mostly, LVADs are developed in a few 1<sup>st</sup> world countries and lack of local LVADs in Turkey results in high expenses for importing them. As a result, developing countries like Turkey should design its own LVAD and properly learn its management during R&D phase. So, a study was initiated to construct an innovative domestic LVAD in 2009.

A virtual prototype was designed in SolidWorks CAD software and its hemodynamic and hemolysis characteristics were tested in Computational Fluid Dynamics (CFD). Then, physical prototype is constructed based on that design to validate the virtual results. Hemodynamics of the prototype including head pressure and hydraulic efficiency will be tested in actual laboratory environment over a Cardio Vascular Mock Circuit (CVMC).

This thesis mainly focuses in flow field acquisition (hemocompatibility) over the physical prototype using Particle Image Velocimetry (PIV) method. In the design process of an LVAD, flow field acquisition is an important stage since it can inspect the presence of backflow, eddies, flow separation, and high shear stress which may cause hemolysis or stagnant and statis which may cause coagulation. Instantaneous flow field acquisition is also helpful to observe transition time and calculate the velocity vectors in different parts of physical prototype.

PIV is a high speed photography-based flow visualization technique which is used to evaluate fluid velocity patterns at high spatial resolution. It's a quantitative method who develops the velocity streamlines of the flow in every single point of flow by tracking suspended particles in fluid.

What makes this study unique in its own kind is this project employs a 2-D PIV system to characterize the flow field inside a pump where both axial and tangential velocities exist throughout the pump. Whereas, most of similar studies in literature are using 3-D stereoscopic PIV systems which are much more expensive than 2-D PIV systems.

Probe inside the pump requires transparent shroud to allow laser light access the floating particles and illuminate them and camera look into those particles. This desires the pump to be motor-less and make it dependent on an External Driving Mechanism (EDM).

**Keywords:** Left Ventricular Assist Devices, Particle Image Velocimetry, Computational Fluid Dynamics, 3-D Integration Using 2-D PIV System, Flow Field Acquisition

## ÖZET

### İLK TÜRK EKSENEL-AKIŞLI SOL-VENTRİKÜL DESTEK POMPASININ (SVDP) PARÇACIK HIZI GÖRÜNTÜLEME (PHG) TEKNİĞİYLE VALİDASYONU

SINA DADGAR

Elektrik Elektronik Muhendisliği

Tez Danışmanı: Döç. Dr. Sarper Özharar

Aralık 2014, 93 Sayfa

Kalp yetmezliği 21inci yüzyılın modern yaşam tarzında yaygın bir ölüm nedenidir. Kalp yetmezliği insan kardiyovasküler sisteminin vücuda yeterli metabolik ihtiyaçları gereken akış ve basınçla karşılayamaması demektir. “Son Dönem Kronik Kalp Yetmezliği” yalnızca kalp nakliyle tedavi olabilir, fakat donör sayısının gerekenden daha az olması nedeniyle mekanik kan dolaşım sistemleri “Son Dönem” kalp hastalarını kurtarmak için kullanılmaktadır. Sol Ventrikül Destek Pompaları (SVDP) bir çeşit Mekanik Kan Dolaşım Sistemi olarak, Sol Ventrikülün fonksiyonunu ventrikülden aorta kan basmakla destekler. Hastanın durumuna bağlı olarak SVDPler hastaların kalbine farklı nedenlerle implant yapılır. Genelde SVDPler 1inci dünya ülkelerinde üretiliyor ve Türkiyede yerel SVDP olmadığı için ithal etmesi yüksek maliyetli olmaktadır. Sonuç olarak, Türkiye gibi gelişen ülkelerin kendi SVDPlerini tasarlaması ve üretimini ArGe aşamasında öğrenmesi önemlidir. Bu sebeplerle yerli bir SVDP üretme araştırmaları 2009da başladı.

SolidWork’de sanal bir prototip tasarlanmış ve onun hemodinamik ve hemokompatibilite karakteristikleri Hesaplamalı Akışkanlar Dinamiğinde (HAD) test edilmiştir. Sonra sanal tasarımın sonuçlarını onaylamak için o tasarıma dayanarak fiziki bir prototip üretilmiştir. Protitipin Hemodinamik özelliklerini laboratuvarında bir Kardiyovasküler Mock Devresi üzerinde test edilecek.

Bu tez fiziki prototipin üzerindeki akış alanını Parçacık Hızı Görüntüleme metoduyla karakterize etmeyi amaçlamaktadır. SVDP tasarım sürecinde akış alanını karakterize etmek bir önemli adımdır, çünkü bu şekilde geri akım, girdap, akış ayrılımını gibi istenmeyen durumların olup olmadığı anlaşılmaktadır. Anlık akış alanı karakterize etmenin bir başka avantajı pompanın farklı bölgelerindeki geçiş süresi ve hız vektörlerinin hesaplanabilmesidir.

PHG, akışkanın hız motiflerini yüksek uzaysal çözünürlükte değerlendirmek için kullanılan yüksek hızlı fotoğrafçılık tabanlı bir ölçüm metodudur. PHG akışkanın hız çizgilerini pompanın her bölgesindeki parçacıkları takip ederek bulan nicel bir metottur.



Bu arařtırmayı diđer arařtırmalardan farklı kılan nokta, yksek maliyetli olan 3 boyutlu stereoskopik PHG kullanmak yerine, dřk maliyetli iki boyutlu bir PHG sistemi ile  boyutta lm yapılmıř olması ve bu yntemle pompa iindeki eksenel ve teęet hız vektrlerinin bulunmasıdır.

Pompanın i kısmını arařtırmak iin dıř kaplamasının řeffaf olmasını gerekmektedir ki ıřık sıvıdaki paracıkları aydınlatırsın ve paracıklar kamera tarafından grntlensin. Bu sebeple de pompanın motorsuz olması ve bir dıř tahrik mekanizması ile alıřtırılması gerekmektedir.

**Anahtar Kelimeler:** Sol Ventrikl Destek Pompaları, Paracık Hızı Grntleme, Hesaplamalı Akıřkan Dinamięi, 2-D PIV Sistemiyle 3-D Entegrasyonu, Akıř Alanı Karakterizasyonu

## ACKNOWLEDGEMENTS

First of all, I feel obligated to thank my thesis advisor, Dr. Sarper Özharar for his enduring encouragement. He answered all my questions patiently from the very first moment I met him in Laser Engineering course. I am so thankful to him, because he is the one who made me meet a great man. Dr. Abdurrahman Kamuran Kadıřşaođlu. The man who gave me an opportunity to do research and study in his laboratory. The man who kept reminding me that engineers create that which never existed; The man who thought me that nine women can never bear one a child in a month!

I would also like to express my gratitude to Professor Erol Sezer who helped me understand the language of mathematics. “Bible and Mathematics book are the only books sent to humanity by God” he used to say.

I am deeply grateful to camaraderie and technical supports of my fellow group members, İ.B. Aka and E.G Eken. It would definitely be a boring lab without our usual discussion: How Iranian Safavids and Turkish Ottomans conquered each other’s territories. I also would like to appreciate my roommate, Mr. Hojjat Mahmoudzadeh, to his patience, friendship, help, and our brotherhood.

I would also like to thank my family. My parents and my fiancé, Sandra have done a great job supporting and encouraging me and I am pretty sure that I would never be able to finish this thesis without their love.

Last but not least, I would like to thank Scientific and Technologic Research Council of Turkey (TUBITAK) who supported this study.

And finally, I would like to dedicate my thesis to all those scientists, medical doctors, generous people, and charities who are spending effort by doing research, donating money and etc. to help and save our angels (including Lilly Fernanda) from Congenital Diaphragmatic Hernia (CDH); just for the sake of humanity.

Istanbul, 2014

Sina Dadgar

## TABLE OF CONTENTS

<b>1. INTRODUCTION.....</b>	<b>14</b>
<b>1.1 HEART FAILURE (HF).....</b>	<b>14</b>
<b>1.2 HEART TRANSPLANT (HT).....</b>	<b>14</b>
<b>1.3 MECHANICAL CIRCULATORY SUPPORT SYSTEMS (MCSS).....</b>	<b>16</b>
<b>1.4 BLOOD PUMP TECHNOLOGY.....</b>	<b>18</b>
1.4.1 Flow Type.....	18
1.4.2 Bearing Design.....	19
1.4.3 History.....	19
<b>1.5 LVAD RESEARCH IN TURKEY.....</b>	<b>23</b>
1.5.1 Kucuksu and Lazoglu – Heart Turcia.....	23
1.5.2 Toptop and Kadipasaoglu (Axial Flow, Second Generation).....	23
<b>1.6 AXIAL-FLOW LEFT-VENTRICULAR ASSIST DEVICE (LVAD).....</b>	<b>23</b>
1.6.1 Main Components.....	24
1.6.1.1 Inducer.....	24
1.6.1.2 Rotor.....	25
1.6.1.3 Diffuser.....	25
1.6.2 Bearings.....	25
1.6.3 Permanent Magnets.....	26
<b>1.7 PROCESS TO DEVELOP AN LVAD.....</b>	<b>26</b>
1.7.1 Particle Image Velocimetry (PIV).....	27
1.7.2 Cardiovascular Mock Circuit (CVMC) Test.....	29
<b>1.8 LITERATURE REVIEW AND GAP.....</b>	<b>31</b>
1.8.1 PIV Measurements of HeartQuest Ventricular Assist Device.....	34
1.8.2 Stereo-PIV Measurement of the Flow inside a Pulsatile Pump.....	35
<b>1.9 PROJECT FIELD .....</b>	<b>37</b>
<b>1.10 DESING CRITERIA.....</b>	<b>38</b>
1.10.1 Hemodynamical Performance.....	38
1.10.2 Hemocompatible Criteria.....	38
1.10.3 Mechanical Criteria of EDM.....	39
<b>2. MATERIALS AND METHODS.....</b>	<b>40</b>
<b>2.1 PIV CHAPTER.....</b>	<b>40</b>

2.1.1 Tracer Particles.....	40
2.1.2 Illumination System.....	42
2.1.2.1 Illumination Source.....	42
2.1.2.2 Light Sheet Formation.....	45
2.1.3 Imaging System.....	46
2.1.3.1 Camera.....	47
2.1.3.2 Lens.....	49
2.1.3.2.1 Iris Diaphragm.....	50
2.1.3.2.2 Focusing Ring.....	50
2.1.4 Pixelization or Resolution.....	52
2.1.5 Magnification Factor (MF) and Region of Interest (ROI).....	53
2.1.6 Synchronization.....	55
2.1.7 Processing Software.....	56
2.1.7.1 Masking.....	57
2.1.7.2 Filtering.....	58
2.1.7.2.1 Median Filter.....	58
2.1.7.2.2 High-Pass and Low Pass Filters.....	58
2.1.7.3 Background Elimination.....	59
2.1.7.4 Post-Processing Tool.....	60
2.2 EXTERNAL DRIVING MECHANISM (EDM).....	62
2.3 COMPLEMENTARY COLORS AND PUMP PAINTING.....	64
2.4 TRIGGERING.....	66
2.5 RADIAL SYMMETRY.....	68
2.6 MATHEMATICAL MODELING.....	69
3. RESULTS.....	72
3.1 INDUCER.....	72
3.2 ROTOR.....	77
3.3 DIFFUSER.....	81
4. CONCLUSION.....	87
5. DISCUSSION AND FUTURE WORKS.....	90
6. REFERENCES.....	91

## LIST OF FIGURES

Figure 1.1: Survival rates after transplantation.....	15
Figure 1.2: Adult and pediatric heart transplants – Number of transplant by year.....	15
Figure 1.3: Annual distribution of heart transplantation in Turkey.....	16
Figure 1.4: An LVAD in patient’s body and its inner design.....	17
Figure 1.5: Axial and Centrifugal Flow Pumps.....	18
Figure 1.6: Hemopump.....	20
Figure 1.7: DeBakey.....	20
Figure 1.8: Jarvik 2000.....	21
Figure 1.9: An Axial-Flow LVAD implanted on a patient.....	23
Figure 1.10: An Axial-Flow LVAD.....	24
Figure 1.11: An Axial-Flow LVAD (DeBakey).....	24
Figure 1.12: Design Process of an LVAD.....	27
Figure 1.13: Illustration of PIV test and its setup.....	28
Figure 1.14: A real photo taken from seeded particles, suspended in fluid.....	28
Figure 1.15: Post-processed velocity vectors of Figure 1.14.....	29
Figure 1.16: SolidWorks Drawing of used Chambers.....	30
Figure 1.17: A Mechanical Heart Valve.....	30
Figure 1.18: Air Compressor.....	30
Figure 1.19: Desired Pressure Plot.....	31
Figure 1.20: Schematic of the Pump Geometry and PIV Setup.....	34
Figure 1.21: Comparison of PIV and CFD Results.....	35
Figure 1.22: Schematic of the Stereo PIV Setup and Illuminated Planes.....	36
Figure 1.23: Tangential and Axial Velocity Planes.....	36
Figure 1.24: Volumetric Streamlines.....	37
Figure 2.1: Polyamide Particles in Natural color.....	41
Figure 2.2: Polyamide Particles.....	41
Figure 2.3: Illustration of operation terms of Double Pulses.....	43
Figure 2.4: LED System and Head.....	45
Figure 2.5: Light Sheet Forming Lens.....	46
Figure 2.6: Light Sheet Forming Lens.....	46
Figure 2.7: 2-D mapping between particles in fluid and images.....	47

Figure 2.8: Image pairs and post-processed outcome.....	48
Figure 2.9: PW vs. ET.....	48
Figure 2.10: front and back view of Nano-camera.....	49
Figure 2.11: Microscopic Lens.....	49
Figure 2.12: CA, SA, CC, and SC.....	50
Figure 2.13: Concept of sequential planes over the pump.....	51
Figure 2.14: Iris Diaphragm and Focusing Ring.....	52
Figure 2.15: Illustration of the Concept of Pixels.....	52
Figure 2.16: Illustration of ROI and Corresponding Pixels.....	53
Figure 2.17: Periphery of rotor.....	54
Figure 2.18: Synchronization system.....	55
Figure 2.19: Synchronizer.....	56
Figure 2.20: Masking system.....	58
Figure 2.21: Masking and Filtering.....	59
Figure 2.22: Background and Background Elimination.....	60
Figure 2.23: Different WS.....	60
Figure 2.24: Interrogation of First Image Pair over Inducer Part.....	61
Figure 2.25: Velocity Contours.....	62
Figure 2.26: Pump Components and Transparent Shroud.....	63
Figure 2.27: Drawing of EDM.....	64
Figure 2.28: EDM.....	64
Figure 2.29: Color Wheel.....	65
Figure 2.30: Pump in Different Colors.....	65
Figure 2.31: Effect of Magenta.....	65
Figure 2.32: Illustration of Background in Rotary and Stationary Parts.....	66
Figure 2.33: Desired Synchronization LPS, Camera, and External Trigger.....	67
Figure 2.34: Symmetric nature of the Pump.....	68
Figure 2.35: Consecutive sub-regions.....	68
Figure 2.36: Virtual Representation of Velocity Streamlines.....	70
Figure 2.37: 3-D Reconstruction from two 2-D Vectors.....	70
Figure 2.38: Illustration of Velocity Streamlines Over Inducer.....	71
Figure 3.1: Velocity Vector Illustration over the Inducer.....	72

Figure 3.2: Virtual Velocity Streamlines over the Inducer.....	73
Figure 3.3: Physical Velocity Streamlines over the Inducer.....	74
Figure 3.4: Physical Velocity Streamlines over the Inducer.....	75
Figure 3.5: Physical Velocity Streamlines over the Inducer.....	75
Figure 3.6: Inducer Blade Effect on Particles from CFD.....	76
Figure 3.7: Inducer Blade Effect on Particles from PIV.....	77
Figure 3.8: Corresponding vertical and Horizontal Planes.....	78
Figure 3.9: Virtual Velocity Streamlines over the Rotor acquired by ANSYS.....	79
Figure 3.10: Physical Velocity Streamlines over the Rotor.....	80
Figure 3.11: Virtual Velocity Streamlines over Rotor know from ANSYS.....	81
Figure 3.12: Preliminary results over Diffuser (First Housing).....	82
Figure 3.13: First Housing Shroud.....	83
Figure 3.14: Second Housing Shroud .....	84
Figure 3.15: Velocity Vectors over Diffuser (Second Housing).....	85
Figure 3.16: Velocity Contours over Diffuser in 4 planes.....	86
Figure 4.1: Physical Velocity Streamlines over the Inducer (all planes).....	88
Figure 4.2: Physical Velocity Streamlines over the Diffuser.....	88
Figure 4.3: Physical Velocity Streamlines over the Rotor.....	89

## LIST OF TABLES

Table 1.1: Properties of Different PIV Techniques.....	33
Table 2.1: Comparing laser and LED illuminating sources.....	44



## ABBREVIATIONS

BF	:	Back Flow
Bi-VAD	:	Both Ventricular Assist Devices
CA	:	Chromatic Aberration
CAD	:	Computer Aided Design
CC	:	Chromatic Correction
CFD	:	Computational Fluid Dynamics
CVMC	:	Cardiovascular Mock Circuit
EDM	:	External Driving Mechanism
ES-CHF	:	End Stage Chronic Heart Failure
ET	:	Exposure Time
FDA	:	Food and Drug Administration
HF	:	Heart Failure
HSP	:	High Speed Photography
HT	:	Heart Transplant
ILA	:	Intelligent Laser Applications
LDV	:	Laser Doppler Velocimetry
LED	:	Light Emitting Diode
LPS	:	LED Pulsing System
LV	:	Left Ventricle
LVAD	:	Left-Ventricular Assist Device
MCCC	:	Mechanical Circulatory Support Systems
MF	:	Magnification Factor
ND-YAG	:	Neodymium-Doped Yttrium Aluminum Garnet
NIH	:	Normalized Index of Hemolysis
PD	:	Pulse Distance
PIV	:	Particle Image Velocimetry
PRP	:	Pulse Repetition Period
PW	:	Pulse Width
RI	:	Refractive Index
RMS	:	Root Mean Square
ROI	:	Region of Interest

RPM	:	Revolutions per Minute
RVAD	:	Right Ventricular Assist Device
R&D	:	Research and Development
SA	:	Spherical Aberration
SC	:	Spherical Correction
TAH	:	Total Artificial Heart
THI	:	Texas Heart Institute
WS	:	Window Size

## **1. INTRODUCTION**

This thesis is a small part of development and manufacture of a Left Ventricular Assist Device (LVAD) for heart failure patients. LVAD is a pump which supports Left Ventricle's (LV) objective by pumping blood from LV to aorta in one direction. It was first invented to be transplanted in patient's body as temporary assistance during heart failure or permanent assistance to regulate blood circulation. [1]

### **1.1 HEART FAILURE (HF)**

HF is case that heart is unable to provide enough blood to satisfy body's metabolic needs. It can be a distortion of beat, low blood pressure, insufficient contractility in heart's muscles, and inborn problems. HF causes the blood flow to be slower in heart itself and all over the body and results less nourishment of oxygen and nutrients to tissues. [2] [3] Subsequently, heart's performance, especially LV's who feed circulatory system by pumping blood directly to aorta, decreases. Nowadays, HF is one of the most dangerous, prevalent, and mortal diseases all over the world particularly in western modern societies where unhealthy foods, machinery life, and lack of mobility is common. Up to 5.7 million cases suffer from cardiovascular diseases in US where at least 20 percents of them have end stage HF. Annually, 500,000 new cases are added to this data which reveals that prevalence is increasing. [4] Similarly, more than 5 million cases of HF had been reported from European Countries. [5]

HF is heart's dysfunction which causes damages on heart muscle. There are some methods for recovering patients with heart dysfunction. One is medication and the other is surgery. Since medication is a temporary method and surgery is not practical in emergencies, these methods are not completely useful. However, heart becomes incurable when it gets to last stage chronic failure. Thus, patients with last stage HF must get heart transplantation being the only solution remaining.

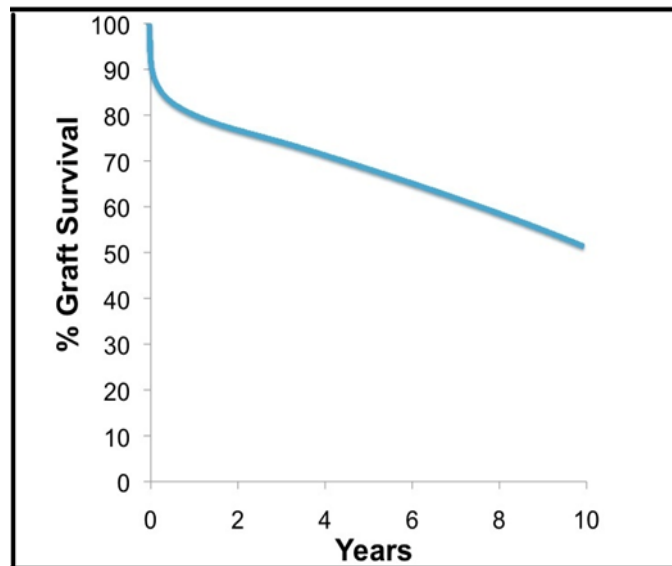
### **1.2 HEART TRANSPLANT (HT)**

A HT or cardiac transplant is a surgical organ transplantation operation which removes the disabled heart of the patient with end stage heart failure (ESHF) and

replaces it with a healthy heart from a deceased donor. Annually, 3500 – 4500 hearts are transplanted worldwide and their survival rate is between 80 and 46 percent from the 1st year to 10<sup>th</sup> year of transplantation. [6]

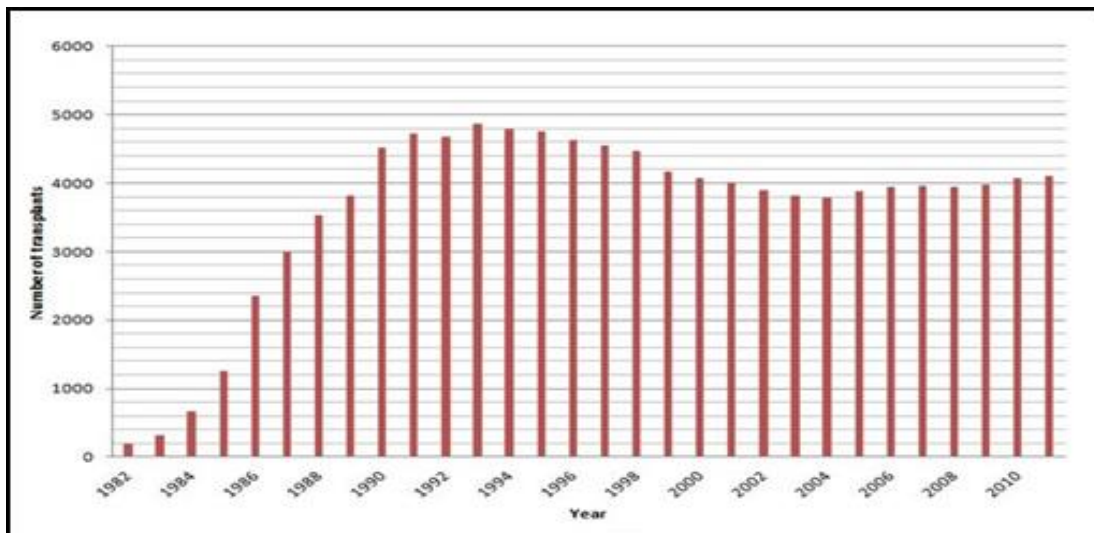
The registry of international society for heart & lung transplantation reveals that heart transplants increased from 187 cases in 1982 to 4096 in 2011 worldwide.

**Figure 1.1: Survival rates after transplantation**



*Source: THE NEW ENGLAND [7]*

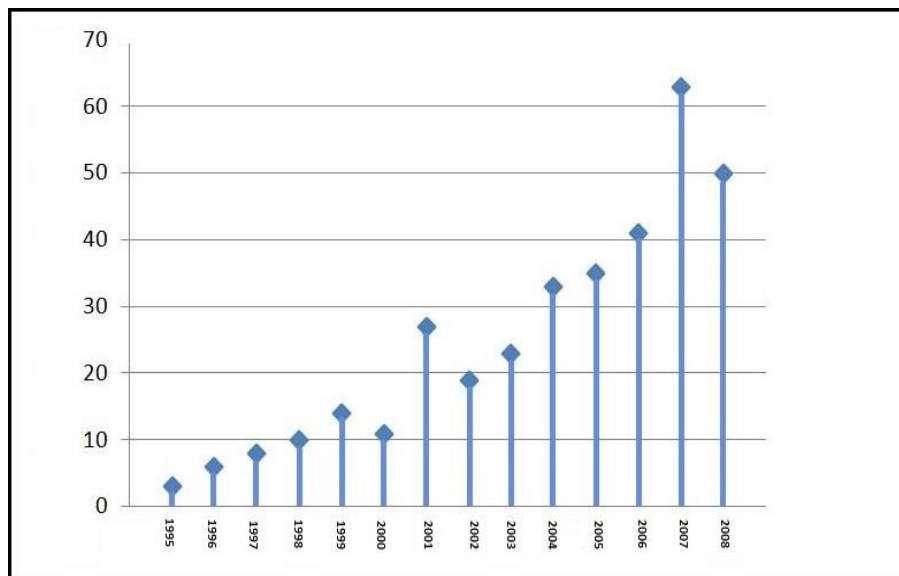
**Figure 1.2: Adult and pediatric heart transplants Number of transplant by year**



*Source: ISHLT [8]*

According to statistics, from 1995 to 2008 in Turkey, 424611 patients had HF and 11percents of them reached last stage of HF. Moreover, 46511 of them needed immediate heart transplant, however only around 50 hearts annually were taken out and ready for transplantation. So the rest of the patients had to wait until available organs could be found for transplantation and unfortunately most of them died in 2 years. All these numerical data reveals that there are needs for Mechanical Circulatory Support Systems as a better treatment for patients with ESHF.

**Figure 1.3: Annual distribution of heart transplantation in Turkey**



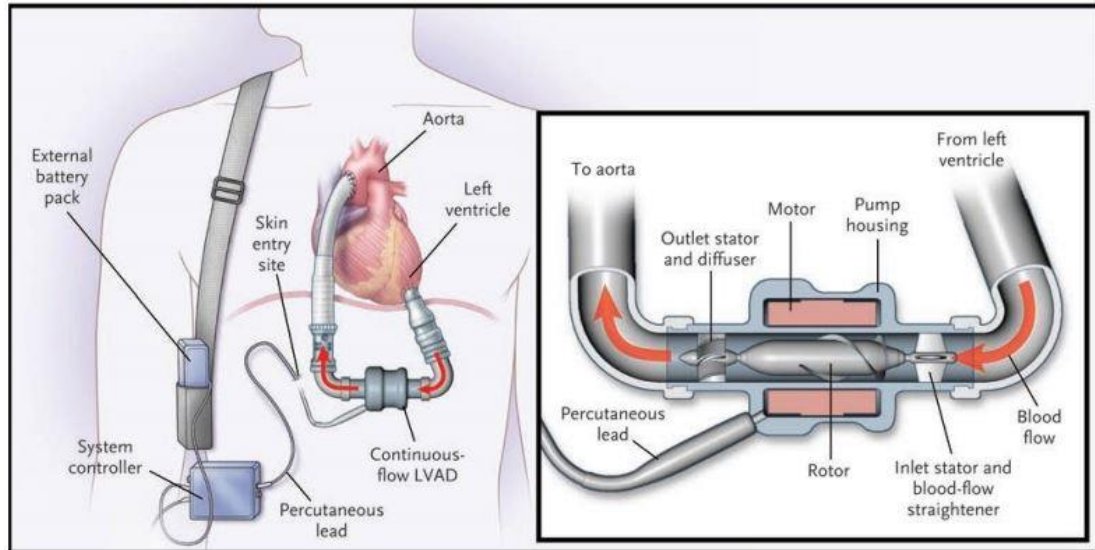
Source: BMC Public Health [9]

### 1.3 MECHANICAL CIRCULATORY SUPPORT SYSTEM (MCSS)

MCSSs are used to keep patients alive with different goals. They are cardiac recovery after open heart surgery, myocardial infraction, after heart transplantation with the acute graft failure, or as a bridge to transplantation in heart transplant candidates [10]

MCSSs re pumps which are broadly used to support the failing LV. LVAD is a type of MCSSs implanted between LV and aorta which its input is connected to LV and output to Aorta.

**Figure 1.4: An LVAD in patient's body and its inner design**



*Source: NEW ENGLAND JOURNAL OF MEDICINE [11]*

LVADs which are battery-operated mechanical pumps are surgically implanted in heart-failed patients with employing a left atrial venous cannula and an aortic one. [12] It helps LV (main pumping chamber of the heart) to pump blood to the rest of the body and as a result, it increases survival period of victims while they are in waiting list of transplantation. Furthermore, since LVADs are also feeding other organs – such as lungs and kidneys – health after heart transplantation increases.

In 1930s, Carrel and Lindbergh developed an in-vitro fabricated heart like apparatus for keeping different organs of body alive out of it. They took out hearts, kidneys, adrenal glands, thyroid glands, and spleens of animals to learn about their function and structure over several years.[13] Later on, some animal studied continued in Russia and USA in 1940s. However human knowledge about MCSSs entered to a meaningful modern era when Gibbon developed the heart-lung machine in 1953 which was advanced for cardiopulmonary bypass. [8]

Nowadays, LVAD sizes had decreased from room sizes to tiny hand held sizes. This portability option gives the patients the opportunity to be discharged earlier compared to past. Moreover, new types of LVADs are providing long lasting good life quality without further transplantations.

According to statistics, using MCSs as a therapy for managing ESHF had a steady increase. Emerging data are evident for Assist Devices being more preferable than inotropes when classified by generation, LVADs being more favorable than RVADs, Bi-VADs or TAHs by assistance modality, and continuous flow devices being more fruitful than pulsatile pumps by device type.

(RVADs and Bi-VADs are MCSs which support right ventricle and both ventricles respectively and TAH stands for Total Artificial Heart)

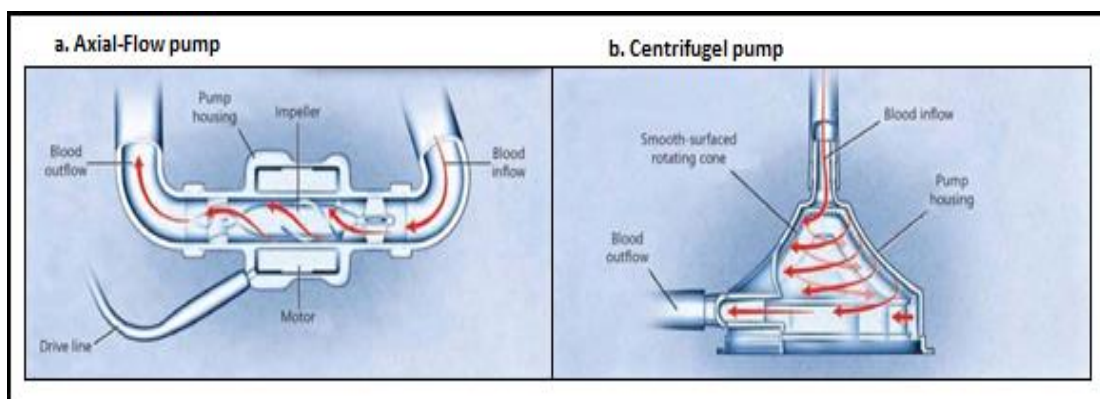
## 1.4 BLOOD PUMP TECHNOLOGY

Numerous types of heart pumps were designed and invented to reduce HF's negative effects on human cardiovascular system by supporting and pumping blood flow. These heart pumps are classified according to their flow type or their bearing design. [14]

### 1.4.1 Flow Type

- i. Pulsatile Flow (Displacement pumps)
- ii. Continuous Flow
  - a. Axial Flow
  - b. Centrifugal Flow (Radial)
  - c. Mixed Flow (Diagonal)

**Figure 1.5: Axial and Centrifugal Flow Pumps**



*Source: Advanced HF [15]*

## **1.4.2 Bearing Design**

- i. First generation: Non-blood contacting (with diaphragm and unidirectional valves)
- ii. Second generation: Blood Contacting
- iii. Third Generation: Magnetically or hydrodynamically levitated

## **1.4.3 History**

### **i. HeartMate I (Pulsatile, First Generation)**

The HeartMate I is a pneumatic LVAD which its operation depends on a pusher plate beating 120 times in a minute to produce pulses to feed 10 L/min blood flow to Aorta. Its width, height, and weight are respectively 110mm, 40mm, and 1190gr. In order to prevent coagulation of blood, the surface of blood contact was covered by sintered titanium.

### **ii. Abiomed (Pulsatile, First Generation)**

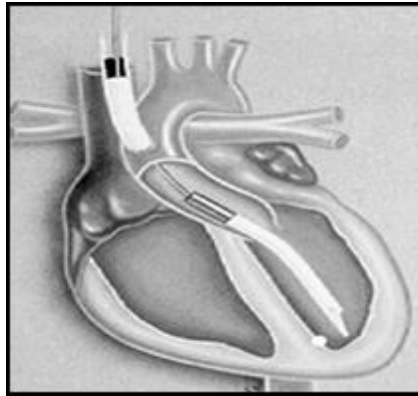
Abiomed which is a pulsatile LVAD, developed in Aachen-Germany. It has 6.4 mm diameter, 60mm length. It is able to feed up to 7L/min blood to Aorta in 100 mmHg with 30percents of hydraulic efficiency.

### **iii. Hemopump (Axial flow, Second Generation)**

Hemopump is a catheter type LVAD which was invented by Dr. Rich Wampler and experimentally tested at the Utah Artificial Heart Institute. Being of the first developing axial pumps who developed and approved its clinical studies in Food and Drug Administration (FDA), is a state of art cardiac assist device for patients with coronary bypass surgery. Its rotational speed is from 17,000 to 26,000 Revolutions Per Minute (RPM) supplying 3.5 to 4.5 liters per minute. FDA approved the clinical studies of Hemopump in 1988. It is now being produced under the trade name Impella.



**Figure 1.6: Hemopump**

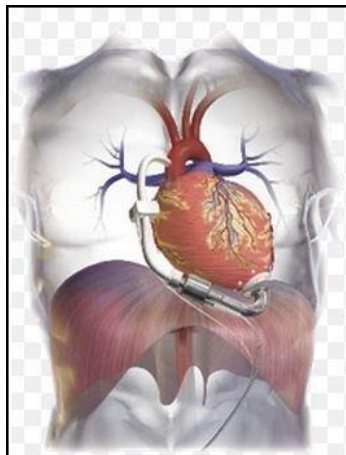


*Source: ASAIO [16]*

**iv. Micromed DeBakey VAD (Axial Flow, Second Generation)**

DeBakey VADs are miniature-sized axial-flow blood pumps which mimic the function of LV. Being 25 mm in diameter by 75 mm in length; Micromed DeBakey VAD requires 10 Watts input power for 10,000 RPM. This rotational speed enables the pump to produce 5-6 liters per minute at a pressure of 100 ml of mercury.

**Figure 1.7: DeBakey**



*Source: Spinoff [17]*

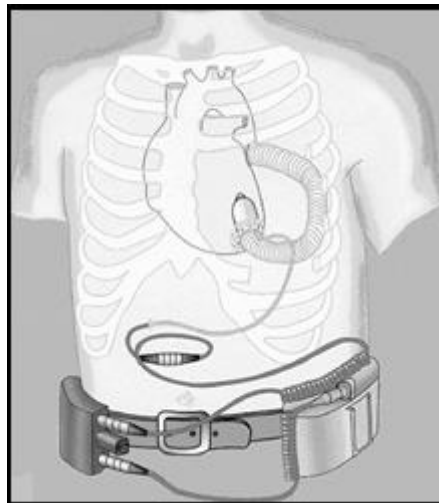
DeBakey pump consists of a stationary diffuser and inducer and a rotatory impeller which is able to rotate from 7,500 to 12,500 RPM and supply flow up to 10 liters per minute. In 2000, FDA approved the clinical study of MicroMed DeBakey VAD in multiple centers in United States.

In September of 2002 at a conference in Japan, more updated statistics indicated that pump has supported many patients from different heart centers and countries in an acceptable manner.

**v. Jarvik 2000 (Axial flow, Second Generation)**

Transcoil Incorporated, the Oxford Heart Center, and Texas Heart Institute (THI) has been progressing the Jarvik 2000 for adults since 1988. Jarvik 2000 which is an axial flow pump is 25 mm in diameter, 55 mm in length with a mass of approximately 85 grams. Regulated by a pulse width-modulated brushless DC motor controller, the impeller of Javarik 2000 is able to rotate from 8,000 to 12,000 delivering 2 to 7 L/min with 100 mmHg pressure. Figure 1.8 illustrates how Javarik 2000 is connected to a power supplying system with a power cable through abdominal wall.

**Figure 1.8: Jarvik 2000**



*Source: ASAIO [16]*

From 1991 to 1999, Javarik 2000 was implanted for 37 healthy calves in THI to evaluate its performance. Results revealed that there is negligible amount of hemolysis.

**vi. HeartMate II (Axial Flow, Second Generation)**

Produced by Thoratec Co. and THI, HeartMate II is a 40mm diametric, 60mm long, and 375 grams axial flow LVAD. It can generate 3-4 L/min flow in 80-100 mmHg while rotating 8000-9000 rpm. Its magnets are located into the rotor center and just like the DeBakey, it contains ceramic bearings. Animal trials started in 1997 and it was first implanted on a patient on July 2000. According to experiments, it got an acceptable Normalized Index of Hemolysis (NIH) for human physiology.

**vii. HeartMate III (Centrifugal, Third Generation)**

Designed and produced by Thoratec Co. in California-USA, HeartMate III is a magnetically levitated centrifugal heart pump for long term use. Its mass is 475 gr and optimizations in in-vitro tests revealed that it has the capability to pump up to 7 L/min of blood in 135 mmHg. HeartMate III rotates around 4500-5000 rpm and has 30 percent of hydraulic efficiency.

**viii. HeartWare (Centrifugal, Third Generation)**

Produced in Florida-USA, HeartWare is a magnetically levitated centrifugal LVAD which is 50mm in diameter and 145 grams. This device is able to operate at 1800-4000 rpm and produce 10 L/min. Clinical trial of this LVAD started in 2008 and it was implanted on 700 patients worldwide until the data was published in 2011.

In Turkey, LVADs are not produced and a limited number of them are imported from European Zone countries and/or United States of America. Their price including hospitalization costs and disregarding either bridge transplantation therapy or destination therapy is around 500,000 US dollars. [18] As a result, R&D of a domestic LVAD is a national necessity for Turks due to this exorbitant price and low clinical success of imported LVADs.

## **1.5 LVAD RESEARCH in TURKEY**

### **1.5.1 Kucukaksu and Lazoglu – Heart Turcia (Centrifugal, Third Generation)**

Prof. Dr. İsmail Lazoğlu and Prof. Dr. Süha Küçükaksu from Koç University started their program to develop a Turkish centrifugal LVAD called Heart Turcia which its in-vitro blood tests are still ongoing.

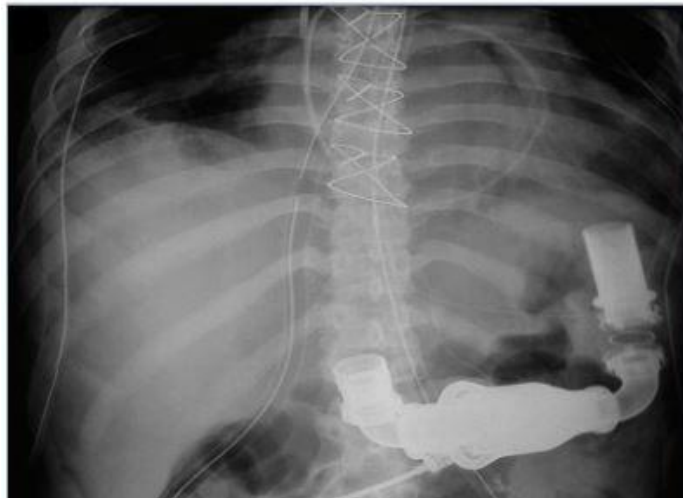
### **1.5.2 Toptop and Kadipasaoglu (Axial Flow, Second Generation)**

Dr. Kamuran Kadıpaşaoğlu and his research team initiated a study in 2009. First Turkish Axial-Flow LVAD was virtually designed and tested in CFD and a physical prototype was manufactured and PIV-CVMC tests are ongoing at the moment. This thesis is a part of the mentioned study.

## **1.6 AXIAL-FLOW LEFT VENTRICULAR ASSIST DEVICE (LVAD)**

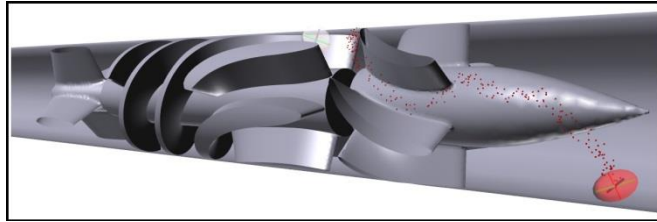
As mentioned earlier, implantation of LVADs in the case of insufficient donors is life saving for patients in ESHF. These miniaturized heart pumps provide high blood flow from LVAD throughout the body. Axil Flow LVADs mainly consists of three fundamental components where two of them are stationary and one is rotary.

**Figure 1.9: An Axial-Flow LVAD implanted on a patient**



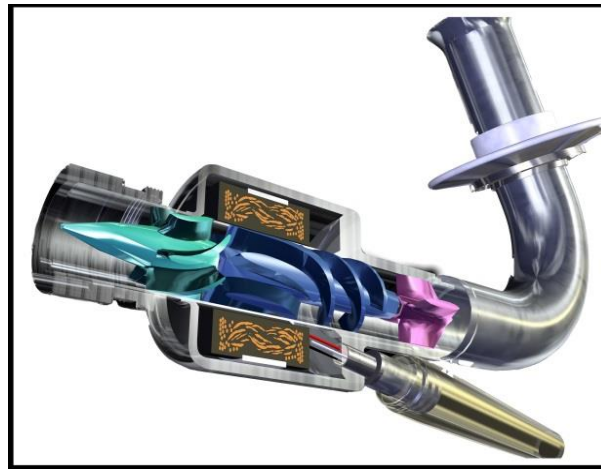
*Source: Technology and Guidelines [19]*

**Figure 1.10: An Axial-Flow LVAD**



*Source: ISRBP [20]*

**Figure 1.11: An Axial-Flow LVAD (DeBakey)**



*Source: Intech [18]*

## **1.6.1 Main Components**

### **1.6.1.1 Inducer**

Being the first component of Axial-Flow LVADs, straightener or inducer regulates the flow field to prevent pre-rotation of flow at rotor inlet. Inducer is located just after the inlet cannula of LVAD and the goal is to get rid of tangential velocity components of flow before it reaches to rotor. Supposing fluid with tangential velocity components reach to rotor, unsteady flow can force the flow move in opposing direction because of motion of rotating part. Presence of inducer parallelizes the flow of blood because the blades of inducer are parallel to the flow. [14]

### **1.6.1.2 Rotor**

Referred to impeller and also propeller in literature, rotor is the next part which fluid meets after inducer. Rotor imparts kinetic energy to fluid with its blades. Rotated by an electromechanical motor, it converts mechanical energy to hydraulic energy (torque and angular velocity to flow and pressure). Thus, rotor is the most important component of an axial-flow LVAD due to its ability to provide energy to the blood flow. Rotor works with a brushless DC motor with embedded permanent magnets. [21] However, in order to allow optical access which will be presented later in this work, the brushless DC electromagnetic motor is removed and replaced by an external driver. So the rotor is rotated with an External Driving Mechanism (EDM).

### **1.6.1.3 Diffuser**

Out-coming fluid from rotor has high tangential velocity due to the rotation of impeller. Diffuser being the third component of axial-flow LVAD can decelerate the tangential velocity, owing to the geometry of its blades. As a result, kinetic energy of fluid gets converted to potential (pressure) energy because of diffuser's special geometry. [14]

### **1.6.2 Bearings**

For Axial-Flow LVADs, choosing the best and most matching bearings to the impeller is also important to assure about hemocompatibility, because hemolysis mostly occurs around bearing where high local stress exists. According to the bearing style and mechanism, pump generations can be classified. 1<sup>st</sup> Generation pumps used bearings isolated by plastic covers from blood. Whereas these plastic covers get destroyed because of exerted fatigue and also bearing oil leaks inside into blood flow and causes lateral problems. In 2<sup>nd</sup> generation pumps, blood lubricates mechanical bearings. However, because of high friction in these regions, hemolysis highly happened again. Finally, 3<sup>rd</sup> generation of pumps employed hydro-dynamic levitation via letting blood to wash bearings; owing to the fact that sizes of red blood cells are bigger than bearing gaps. [21]

### **1.6.3 Permanent Magnets**

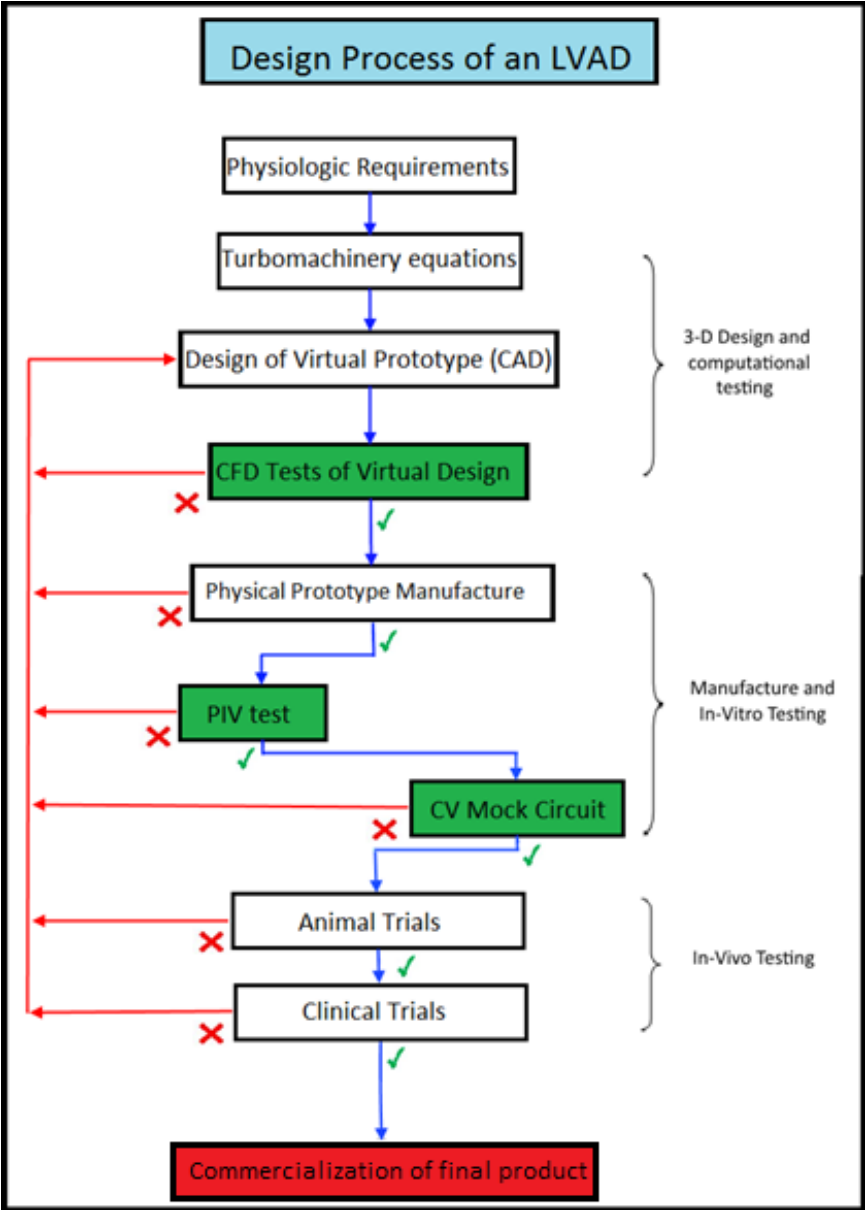
Even-though some blood pumps have the same design, their configurations about electromagnetic brushless DC motor differs. These configurations are reliable on how permanent magnets are located. Used to create magnetic field, permanent magnets are only located on rotary component. It gets interacted with another magnetic field created by copper coils located at stator of DC motor. But as mentioned before, electromagnetic DC motor was removed from this study because of some reasons which will be covered later in this work and an EDM is employed to rotate the pump instead. [21]

### **1.7 PROCESS TO DEVELOP AN LVAD**

From the very first idea of design and development of an LVAD to the last stages which is the commercialization of the final product, there is a long way to cover which may take 5 to 10 years. Firstly, according to physiological requirements, geometric parameters such as cross-sectional area, blade tip, dimensions of hub and tip, number of blades and their attack angle and etc. were calculated considering turbo machinery equations. Then, 3D primitive model of the pump was drawn and designed using Computer Aided Design (CAD) tool. Next step is to virtually study the Hemolysis and Hemocompatibility of designed model with Computational Fluid Dynamics (CFD) solver. Comparing computational and desired results, iterative alterations had continued to find errors to achieve best dimensions for the pump to meet hemodynamical and hemocompatibility criteria. In this project, after necessary iterations, FP1 of K. Toptop was chosen as the best design for manufacturing of physical prototype.

Now, verified physical prototype (FP1 of K. Toptop) is manufactured. In physical tests stage, the aim is to study the performance of FP1 under realistic physical environment and inspect whether it is functioning exactly like in virtual world or not. In order to investigate this, PIV (which is the main topic of this thesis) is used to evaluate FP1 from hemocompatible aspect and the Mock Circuit test will be employed to study it from Hemodynamical aspect.

**Figure 1.12: Design Process of an LVAD**



*Source: Made by Sina Dadgar*

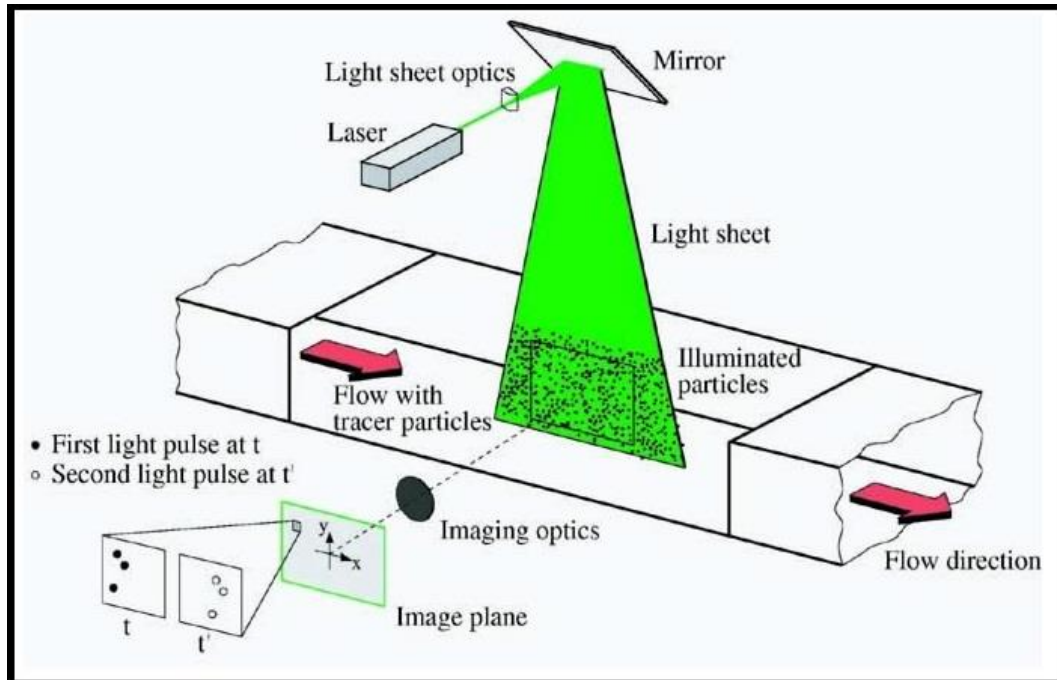
**1.7.1 Particle Image Velocimetry (PIV) Test**

PIV is a high speed photography-based flow visualization technique which is used to evaluate fluid velocity patterns at high spatial and temporal resolution. It is a quantitative method who develops the velocity streamlines of the flow in every single point of flow by tracking suspended particles in fluid. First, the fluid is seeded with light-scattering tracer particles and an illumination system (a laser mostly) spotlights those particles. Then, a camera takes two consecutive photographs to be



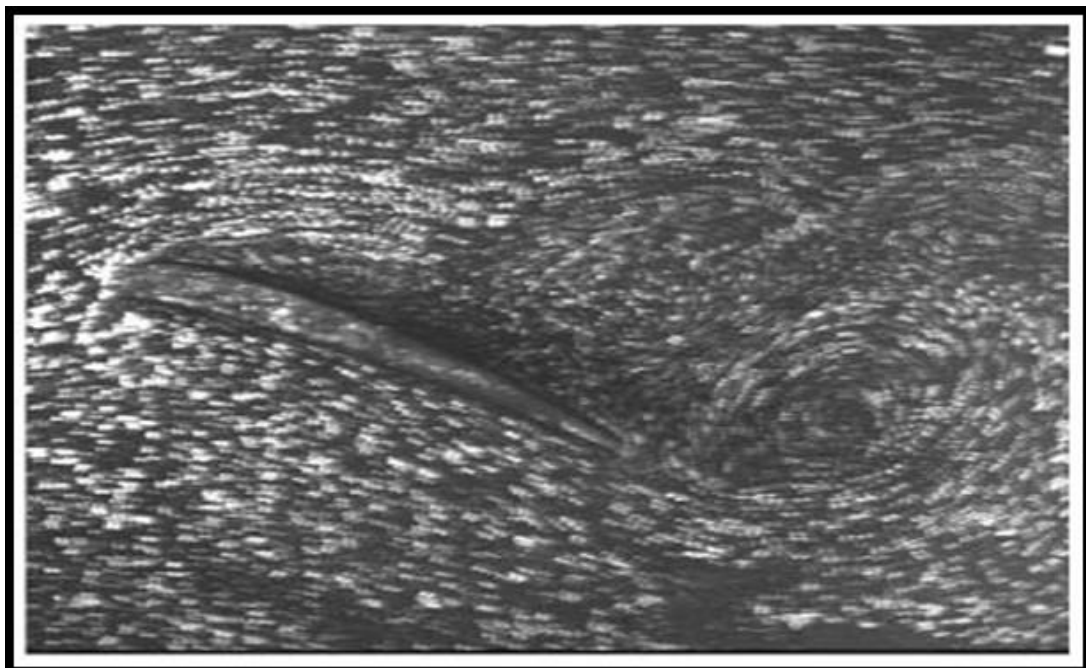
able to capture the behavior of the particles in a specific time period. Given the covered distance and temporal difference of image pairs, velocity vectors of each particle can be calculated by post-processing software.

**Figure 1.13: Illustration of PIV test and its setup**



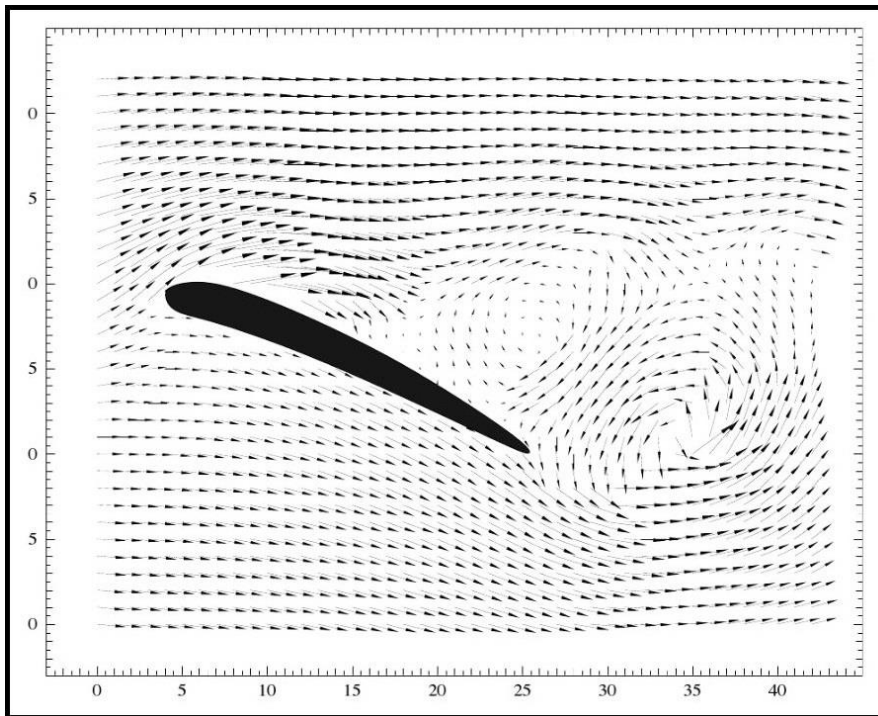
Source: Springer [22]

**Figure 1.14: A real photo taken from seeded particles, suspended in fluid**



Source: Springer [22]

**Figure 1.15: Post-processed velocity vectors of Figure 1.14**



*Source: Springer [22]*

In this study, PIV test is used to acquire the flow field inside the physical prototype of an Axial-Flow Left-Ventricular assist device. Also, it is used to confirm the results from CFD about flow separation, high shear stress, and high velocity gradient regions. If there are gaps between CFD (Computational) and PIV (Physical) tests, 3-D virtual prototype must be modified to eliminate outsized variances to satisfy the design criteria. Once necessary iterations are conducted between virtual and physical designs and optimizations made CFD-PIV results to meet physiological needs and acceptable results converged, the development of LVAD can start a new stage which is called mock circuit.

### **1.7.2 Cardiovascular Mock Circuit (CVMC) Test**

Mock circuit is a hydraulic model of human cardiovascular system. It consists of reservoirs representing the chambers of heart (Ventricles, Atria, and Aorta), unidirectional valves representing human cardiac valves, and an air pressure compressor for creating pulses like a real ventricle.

**Figure 1.16: SolidWorks Drawing  
of used Chambers**



*Source: Eken's Thesis [23]*

**Figure 1.17: A Mechanical Heart Valve**



*Source: Eken's Thesis [23]*

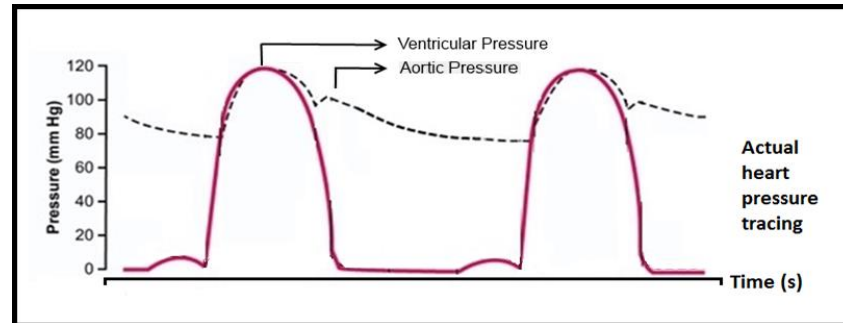
**Figure 1.18: Air Compressor**



*Source: Eken's Thesis [23]*

In this study, CVMC is used to simulate blood circulation of human body in normal and heart failure modes. The aim from this study is to get the same amount of flow and pressure between LV and as a healthy person or a sick person (without and with LVAD implanted in CVMC respectively). CVMC is a tool used to evaluate the pump hemodynamically.

**Figure 1.19: Desired Pressure Plot**



*Source: Eken's Thesis [23]*

In order to make the pump consistent with the performance of the pump and physiologic demands, CVMC is also used as a controller algorithm for manipulate the pump. Later on, according to outcome from CFD-CVMC tests, rotational velocity and torque demands will be recognized and power needed to run the motor will be calculated and final product will be designed and constructed.

After all decent results are gathered from CDF, PIV, and CVMC tests and necessary optimizations are conducted between them, the product can be tested on animals and once acceptable hemodynamics and hemocompatible results are reported, it can be tried on human in clinical trials and hospitals as the last step.

## **1.8 LITERATURE REVIEW AND GAP**

As mentioned before, about 95 percent of the patients with HF in Turkey need MCSSs – mostly LVADs- to survive. Most of these LVADs which are transplanted on patients are imported from manufacturer countries which are USA, Germany, and Japan most of the time and other countries like Turkey have to import them from manufacturer corporations. However, since local researchers and medical doctors of LVAD importing countries are deprived and experienceless during design and

manufacture of the LVADs, they lack clinical practice with patient management in post-operative period. Furthermore, exorbitant prices of imported LVADs cause significant economic burden to countries without technology to develop their own LVAD. As a result, R&D of domestic LVADs for all countries is necessary to remove economic burden and enhance the knowledge about post-operative period.

This goal can be achieved by R&D of numerous devices made by trained professional technicians. The research team of this study still has several steps to complete the prototype and provide it to stocks. As it was mentioned before in section 1.7, virtual design and tests are already accomplished and now a physical prototype is manufactured in order to start the physical tests including PIV and CVMS and finally convey the study to the in-Vivo test.

PIV test in the procedure of physical tests for the validation of LVAD is significant step to validate virtual results in hemocompatible manner. In order to study the behavior of the fluid inside the pump, literatures are using optical and physical techniques. However optical methods have more advantage than physical probes. Firstly, optical methods do not interfere with the fluid whereas traditional mechanical methods distort the flow in negative manners. Moreover, because of optical nature of optical methods, they can probe into the non-accessible regions which mechanical methods are not able to investigate.

Unlike old methods such as Laser Doppler Velocimetry (LDV) which studies the flow in only one single point, PIV is able to quantitatively make simultaneous measurements over the whole flow field. This method also assures that obtained information can be gathered at an effectively instantaneous time. All in all, PIV has approved its precision and advantages and now, it's been more than ten years that this method is used to validate the function of LVADs all over the world. This method helps to investigate the locations with high shear stress and stagnation, both which must be avoided because of their ability of generating hemolysis and thrombosis to meet the design criteria.

Depending on the experiment and nature of the flow being studied, one can decide on the sort of PIV setup to use. Table below illustrates different PIV techniques and their properties.

**Table 1.1: Properties of Different PIV Techniques**

	2D PIV	Stereo PIV	Dual Plane Stereo PIV	Tomographic PIV
Measurement Grid	2D Planar	2D Planar	2×2D 2×Planar	3D Volumetric
Measure Vector Components	2C	3C	3C	3C
Cameras	1	2	4	4(3-6)
Illuminator Light Sheets	1	1	1-2	1

*Source: 14th Symposium of Laser Techniques to Fluid Mechanics [24]*

The very basic PIV technique is the classic simple 2D PIV. The measurement grid in 2D PIV is two-dimensional planar which measures two components of velocity. Usually, 2D PIV is used in laminar flows. Also, in some articles despite to the presence of both axial and tangential velocities, 2D PIV systems are used. However, the outcome in these studies is just several 2-D planar velocities. Interpreting the flow field of a volumetric flow based on 2-D velocity vectors would be difficult and ambiguous.

On the other hand, some researches employ stereoscopic or tomographic PIV techniques where several cameras are focused on a single point to capture the three-dimensional motion of particles providing an additional measurement dimension. Outcome in these studies are in the form of 3-D velocity vectors which eases the study of probable backflows and vortices.

In literature, most of the articles and studies go around either normal 2-D PIV when there is only axial velocity along the pumps or 3-D Stereoscopic PIV (when there are both axial and tangential velocities). Stereoscopic PIV is a method which employs

two cameras to observe the light sheet from different angles and measure three velocity components of fluid in one plane.

Even though the flow field runs volumetric with axial and tangential velocities in this study, a normal LED based 2-D planar PIV has been used because of financial issues. However, the 2-D PIV system is innovatively used to study the volumetric flow by changing the location of camera and illuminator and mathematical methods to reconstruct 3-D velocity vectors.

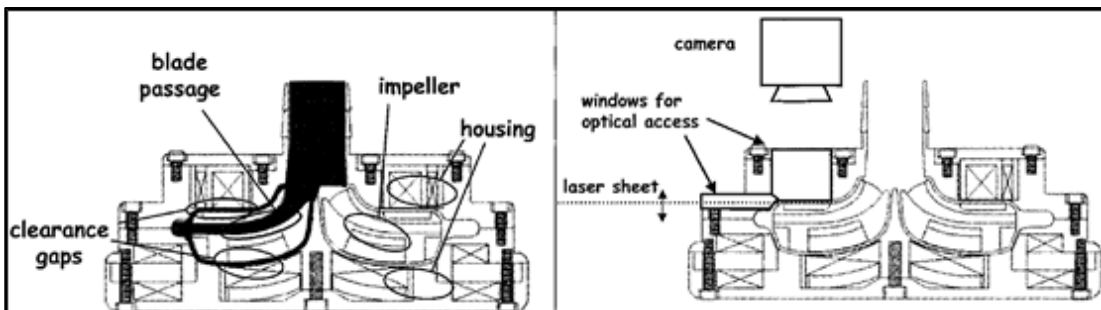
In this study, despite there are axial and tangential velocities together, a 2-D PIV system is used to characterize the flow field inside the pump because of shortage in the grant and this is precisely what makes this study innovate.

### 1.8.1 PIV Measurements of HeartQuest Ventricular Assist Device

This study characterizes the flow within a magnetically centrifugal VAD using a 2-D planar PIV system to identify the regions of stagnation and vortices and refine computational outcome of model.

The third prototype of this pump (CFVAD3) was developed where the four-bladed impeller inside a shrouded delivers 6 L/min at 100 mmHg while running at 2000 rpm. The blood flows through small clearances in each side of the impeller (illustrated in figure 1.20) in the simultaneous presence of radial inward pressure and tangential outward pressure generated by rotating impeller.

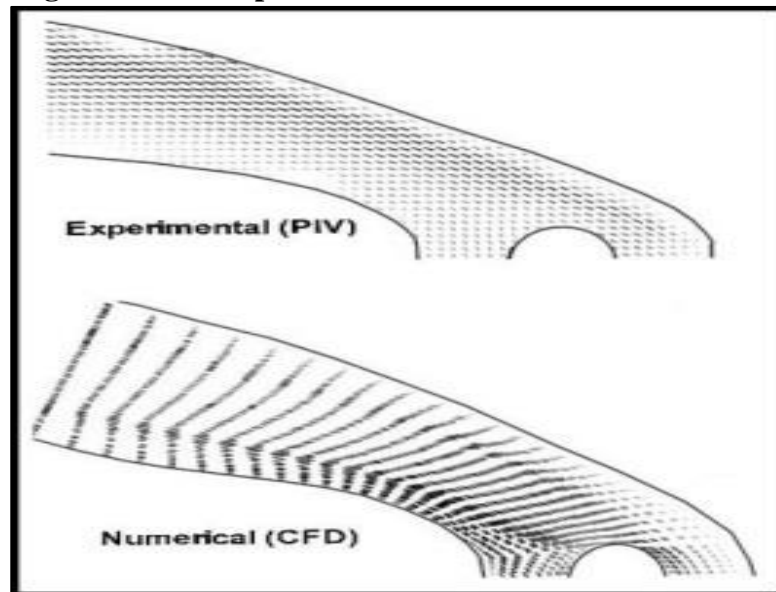
**Figure 1.20: Schematic of the Pump Geometry and PIV Setup**



Source: ASAIO [25]

However, PIV velocity measurements are accomplished in inlet elbow while the measurements in other critical regions are still remaining. Furthermore, the measurement and computed velocity in inlet elbow is 2-D planar velocity vectors which are illustrated in figure 1.21.

**Figure 1.21: Comparison of PIV and CFD Results**



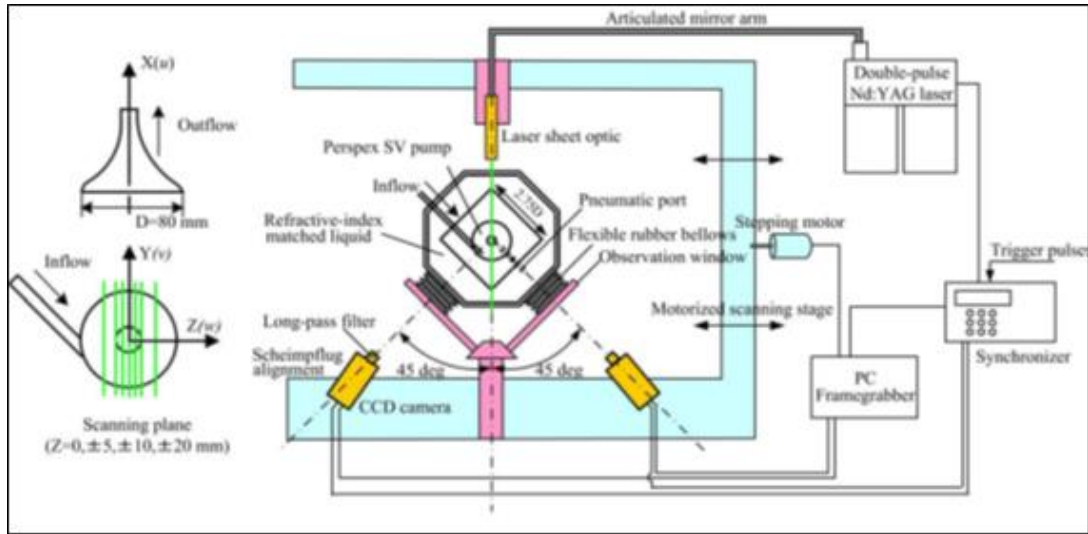
*Source: Blackwell [26]*

### **1.8.2 Stereo-PIV Measurements Of The Flow Inside A Pulsatile Blood Pump**

In this study, a three-dimensional volume mapping of flow field in a pulsatile blood pump is accomplished using a Stereo PIV setup. Dual cameras and laser light sheet are configured to capture the behavior of particles in the volume while imaging systems are aligned in 45-degree with respect to each other.



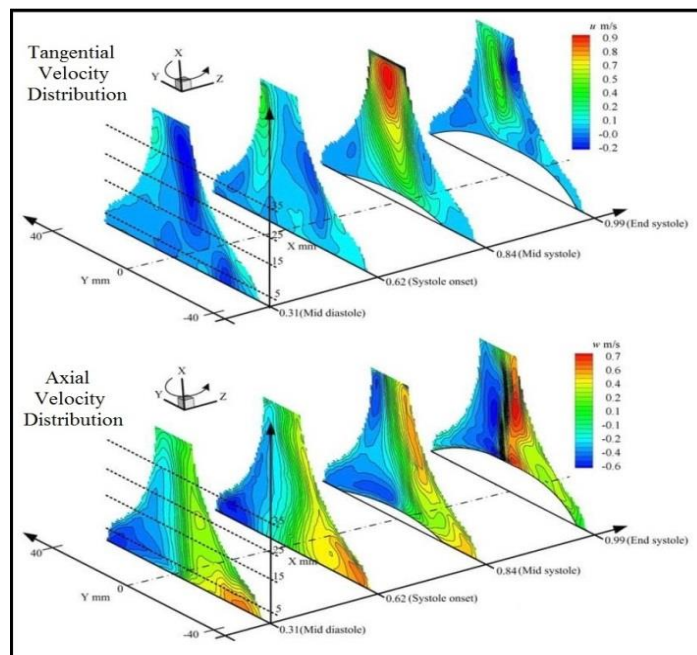
**Figure 1.22: Schematic of the Stereo PIV Setup and Illuminated Planes**



*Source: 13th Symposium of Laser Techniques to Fluid Mechanics [27]*

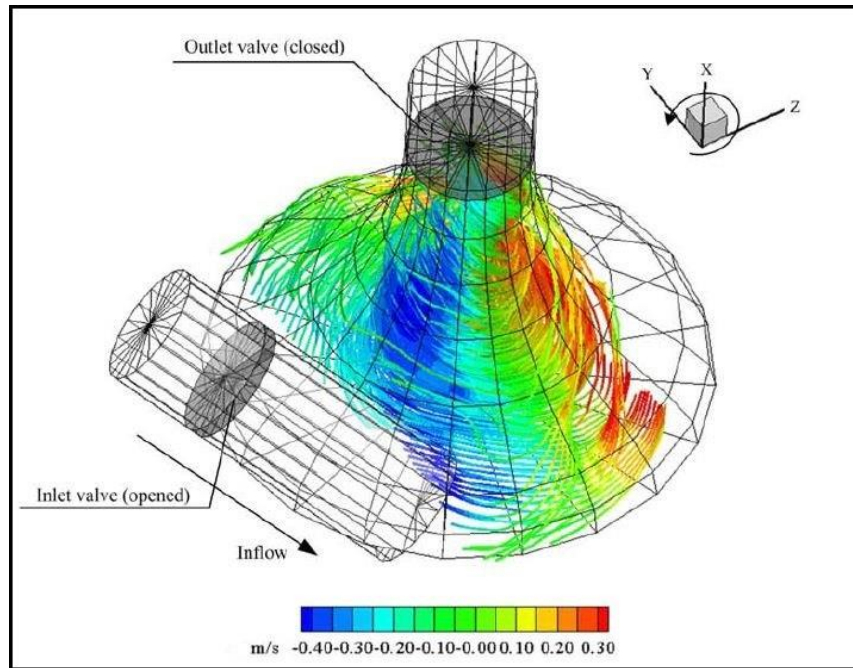
The unsteady behavior of vortices are discussed in several planes in a cardiac cycle and phase-locked plane axial and tangential velocity vectors are acquired (represented in figure 1.23) and using the software, three-dimensional volumetric streamlines are plotted (represented in figure 1.24)

**Figure 1.23: Tangential and Axial Velocity Planes**



*Source: 13th Symposium of Laser Techniques to Fluid Mechanics [27]*

**Figure 1.24: Volumetric Streamlines**



*Source: 13th Symposium of Laser Techniques to Fluid Mechanics [27]*

## 1.9 Project Field

As mentioned before, Dr. Kamuran Kadıpaşaoğlu and his research team started a project in order to develop a new Axial-Flow LVAD and convey it as qualified products ready to implant on patients with HF. Accordingly to Figure 1.12, the project started its virtual design including 3-D design and computational testing on 2009. The project was granted by Scientific and Technologic Research Council of Turkey (TUBITAK-111M243) and in 2 years, 3-D designs and computational tests accomplished and FP1 of K. Toptop was chosen as the best design for manufacturing of physical prototype. In 2013, the physical stage started again with grants from Scientific and Technologic Research Council of Turkey (TUBITAK-111M242) and its aim was to carry the design form virtual world to physical world and do the same hemodynamical and hemocompatible tests. So a virtual prototype of pump was constructed and since it is necessary to do PIV tests which require optical access, a transparent shroud and an External Driving Mechanism was also designed and constructed to be able to start PIV tests. PIV test which is what this thesis focuses on, is used to detect the effects of fluid which cause blood degradation and coagulation (Hemolysis and Thrombosis). The problems which can be generated because of bad hemocompatibility of pump make this significantly clear that PIV must validate the

CFD results. During this thesis, materials and methods of employed optical method will be explained first and later, results and outcomes of experiments will be shared with audiences. After PIV validation, Cardiovascular Mock Circuit (CVMC) will be used to validate the pump's function in hemodynamical manner, and right after that physical stage will be over. For the next stage which is in-Vivo tests, it will be needed to start animal trial and human tests to be ready for commercialization.

The specific research objectives of this thesis are as following:

- i. To provide the volumetric three-dimensional flow field using a 2D PIV setup.
- ii. Compare the outcome from PIV with CFD and declare if physical tests are validating the virtual tests or not.
- iii. Calculate the radial and axial velocities along the pump.
- iv. To inspect and reveal possible regions of backflows and vortices

### **1.10 Design Criteria**

Designed pump must be virtually and physically verified according to physiological criteria. It must create a specific head pressure and flow and also avoid generating backflow, vortex, flow separation, stagnation, and stasis. Also, transparency of shroud must assure the accuracy of gathered data from PIV test.

Furthermore, different parts of EDM need to be aligned and be able to rotate the rotor according to mechanical demands.

#### **1.10.1 Hemodynamical Performance**

- |                        |                                    |
|------------------------|------------------------------------|
| i. Pressure difference | $80 < \Delta P < 120 \text{ mmHg}$ |
| ii. Blood flow         | $3 < Q < 8 \text{ L/min}$          |
| iii. Angular velocity  | $8 < \omega < 11 \text{ Krpm}$     |

#### **1.10.2 Hemocompatible Criteria**

- |             |                                  |
|-------------|----------------------------------|
| i. Backflow | $\text{BF} < 10 \text{ percent}$ |
|-------------|----------------------------------|

ii. Stagnation	Not Tolerated
iii. Statis	Not Tolerated
iv. Flow Seperation	Not Tolerated
v. Eddies	Not Tolerated

### **1.10.3 Mechanical Criteria Of EDM**

i. Shroud	Visually clear~1.3 refractive index
ii. Base (Mount)	Aligned and Stainless

## **2. MATERIALS AND METHODS**

As mentioned before, the objective of this thesis is to study and characterize the flow field of a pump which is going to be the first Turkish Axil-Flow LVAD. Flow field acquisition is a very important stage in the R&D of a heart pump because it can reveal possible regions of high shear stress, flow separation and circulation, and backflow which can lead to blood hemolysis and stagnant and stasis locations to blood coagulation. For this, PIV method is employed to characterize the flow field of a blood analogue through an LVAD. PIV is an optical method which seeds the fluid with light-scattering tracer particles and uses the double pulses of an illumination system to illuminate them. Simultaneously, a synchronized high speed camera takes consecutive image pairs during enlightenment period by illumination source to capture the behavior of particles in a specific time period. Given the covered distance and temporal difference of image pairs, velocity vectors of each particle can be calculated by post-processing software.

In order to study the pump, first the pump components were manufactured and they were shrouded by a transparent housing to enable the optical access which is needed for PIV experiments. This special housing makes the pump dependent on an External Driving Mechanism (EDM) which consists of pump parts, shaft, transparent housing, torque sensor, and a DC motor.

### **2.1 PIV CHAPTER**

#### **2.1.1 Tracer Particles**

The choice of the right seeding material to scatter the light from the laser beam or light sheet is very crucial to the acquisition of successful experimental data in PIV. The fluid must be seeded with particles small enough to follow the flow and big enough to scatter the illuminating light towards the imaging system. Their size is usually a few tens of micrometers in liquids and a few micrometers in gases. [28]

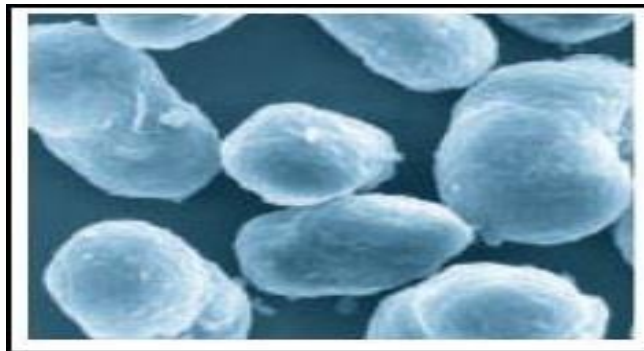
Particles must be homogenously-distributed and must have the same density as the fluid being used in other words they should have neutral buoyancy. Otherwise they

will not follow the flow trajectory as preferred and may settle down or float on the surface. Furthermore, the refractive index (RI) of the particles must be different than the refractive index of the fluid. This is necessary to insure the illuminator light on the fluid flow can reflect the particles towards the camera.

Moreover, monodispersity of particles (having a uniform size distribution) is crucial to obtain same light energy and exposure of particles in all images. Slight differences in dimensions of the particles can cause significant differences.

In this study, Polyamide tracer particles (Polyamide PA12, Vestosint 2157, 50- $\mu\text{m}$  size and 1.016  $\text{g}/\text{cm}^3$  density) are used. They follow the flow with neutral buoyancy and satisfy all dynamical properties needed for a proper PIV measurement. Polyamide is a high-refractive-index polymer. It has a refractive index of  $1.5 \pm 0.05$  which is greater than the refractive index of water (approximately 1.33). [29]

**Figure 2.1: Polyamide Particles in Natural color**



*Source: Vestosint [30]*

**Figure 2.2: Polyamide Particles**



*Source: Taken by Sina Dadgar*

The radius of particles is 25  $\mu\text{m}$  and due to their spherical nature, the volume of each particle is  $0.625 \times 10^5 \mu\text{m}^3$  according to Eq 2.1

$$V_p = \frac{4}{3} \pi r^3 \quad 2.1$$

Standard amount of polyamide particles in fluid is 32 million in one liter. Based on this and the volume of each particle, the volume of the particles needs to be added to fluid is  $2 \times 10^{12} \mu\text{m}^3$  according to Eq 2.2

$$\frac{V}{V_p} = \# \text{ of particles (32 million)} \quad 2.2$$

According to this, the mass of the particles which needs to be added to one liter of fluid is 2.032 grams according to Eq 2.3 considering the density of particles to be  $1.016 \frac{\text{gr}}{\text{cm}^3}$

$$\text{Volume} = \frac{\text{mass}}{\text{density}} \quad 2.3$$

## 2.1.2 Illumination System

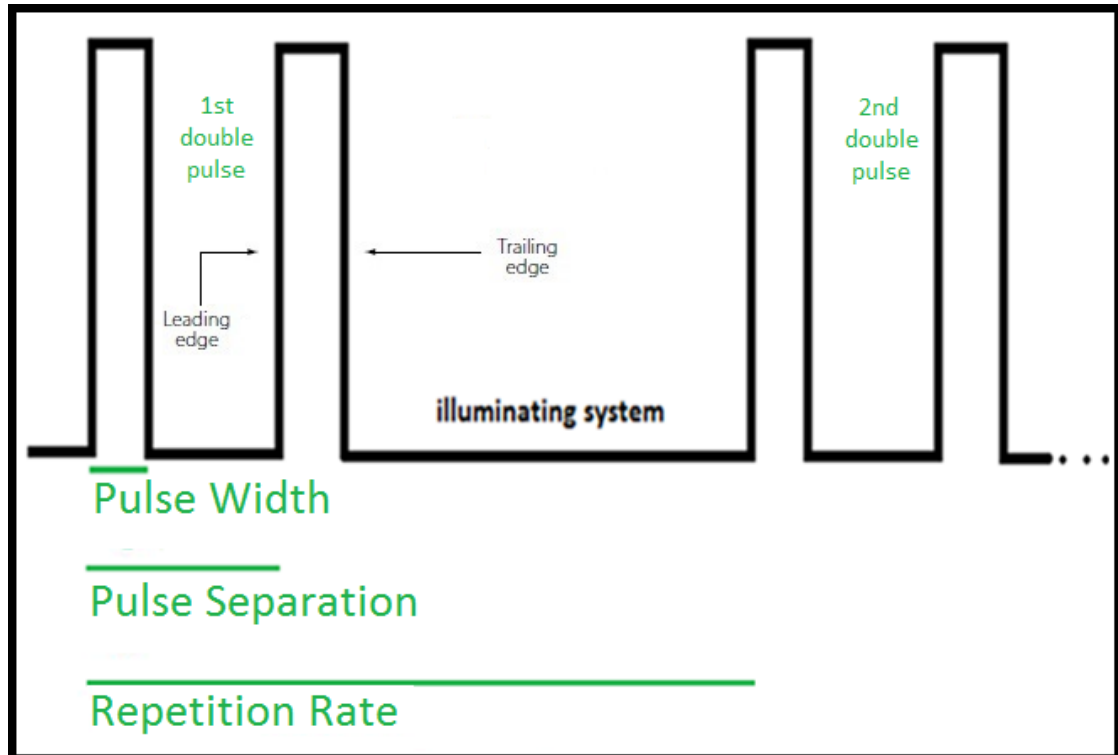
### 2.1.2.1 Illumination Source

Due to the presence of small-sized particles in the fluid, it's needed to employ an intensely high-power light source. Further, these pulses need to be short enough to enhance the ability of the camera to freeze the particles in the obtained images so that they can be analyzed by the software.

The temporal behavior of the double pulses can be characterized by three factors which are Pulse Width (PW), Pulse Separation or Distance (PD), and Pulse Repetition Period (PRP). PW is the time interval between leading edge and trailing edge of a pulse. Doing PIV experiments in high speed floating tests requires PW to be short enough to be able to freeze the particles in acquired images. PD is the time

interval between the first transition of the first double pulse where amplitude of the pulse reaches a certain level and the second transition where pulse amplitude drops to zero. RR stands for the number of double pulses per second. Figure 2.3 illustrates PW, PD, and RR all together.

**Figure 2.3: Illustration of operation terms of Double Pulses**



*Source: Made by Sina Dadgar*

Illumination systems in the terms of operation are classified as laser based systems and LED based systems.

Commercially available PIV optimized laser based systems generate pulse energies ranging from 5 to 500 mJ, and pulse width as short as 10 ns. However, LED Based Systems are weaker and slower than laser based system. Their PW is limited to be 1  $\mu$ s at least and the energy of their emitting pulses is mostly 1 mJ. For PIV experiments, both Laser and LED systems are operating at 532 nm (green light) since the ccd detector of the camera is most sensitive at that wavelength.

Currently, dual-cavity pulsed Neodymium-Doped Yttrium Aluminum Garnet (Nd:YAG) lasers are commonly used for PIV experiments. However, some



researchers have used pulsed Light Emitting Diodes (LEDs) as a low-cost alternative to pulsed laser systems. Table 2.1 compares the characteristics of lasers and LEDs for PIV experiments.

**Table 2.1: Comparing laser and LED illuminating sources**

	Pulse Energy (mJ)	Pulse Duration ( $\mu$ s)	Wavelength (nm)	Repetition Rate (Hz)
Double-Pulsed twin Nd:YAG lasers	20-400	0.005-0.0010	532	10-30
Double-Pulsed LED array	1	0.6-20	532	1-1000

*Source: CAMBRIDGE [28]*

Given the velocity of the fluid, it can be decided to use whether a Laser based or LED based system. Since the pulse width determines the time duration during which the image is taken, it is preferred that the particle moves less than or equal to 1 pixel during the PW. So if the fluid is (or the particles are) running fast (i.e. greater than 3-5 m/s), the illumination system needs to send shorter pulses to capture and freeze the particles. Otherwise, the particles will be imaged as streaks instead of frozen points according to the fundamentals of High Speed Photography (HSP).

In this study, the fluid accelerating component of the pump – rotor – imparts kinetic energy to fluid and makes it to run with the velocity of 10 m/s along the rotor which is equal to 0.01 mm/ $\mu$ s. According to this calculation, the best option is to use a laser based system, but because of financial limitations, it is decided to use an LED based system. It was first considered that this slow illumination source will create streaks, but later on it was decided to increase the Region Of Interest (ROI) to avoid this problem. The concepts of ROI and streaks will be explained in details in chapter 2.1.5.

The LED system which is used in this study is an LED Pulsing System (LPS) Controller with one LED head which was purchased from Intelligent Laser

Applications (ILA) GmbH, Jülich, Germany. It can generate current pulses up to 200 Amps and be controlled by a software using Ethernet. It also can be synchronized to any camera with status signals. This product was manufactured by ILA just for PIV experiments.

**Figure 2.4: LED System and Head**

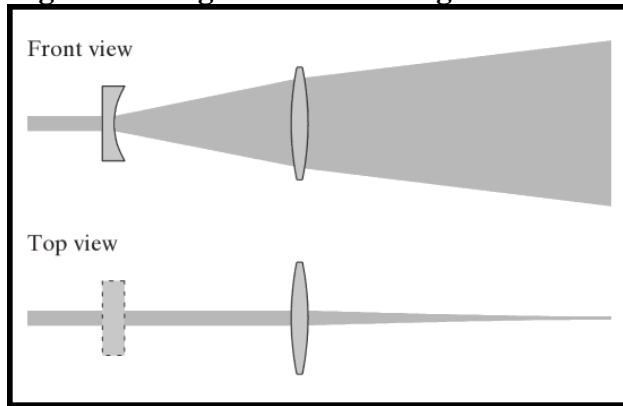


*Source:* Taken by Sina Dadgar

### 2.1.2.2 Light Sheet Formation

Output of a laser or an LED is a cylindrical beam of light. The diameter of the light usually doesn't meet the desired thickness of the light sheet. Since it is needed to illuminate a large region of particles in one plane in measurement domain, it has to be formed in a 2 dimensional sheet of light. For this, "short-focal-length" [28] cylindrical lenses are used to expand the beam in one axis only and keep it collimated in the other dimension resulting in the desired light sheet.

**Figure 2.5: Light Sheet Forming Lens**



*Source: CAMBRIDGE [28]*

The cylindrical lens used to generate 2-D light sheet in this project is manufactured by Intelligent Laser Applications (ILA) GmbH, Jülich, Germany while it has been located inside a cage plate (LCP03-60mm) manufactured by THORLABS Inc.

**Figure 2.6: Light Sheet Forming Lens**



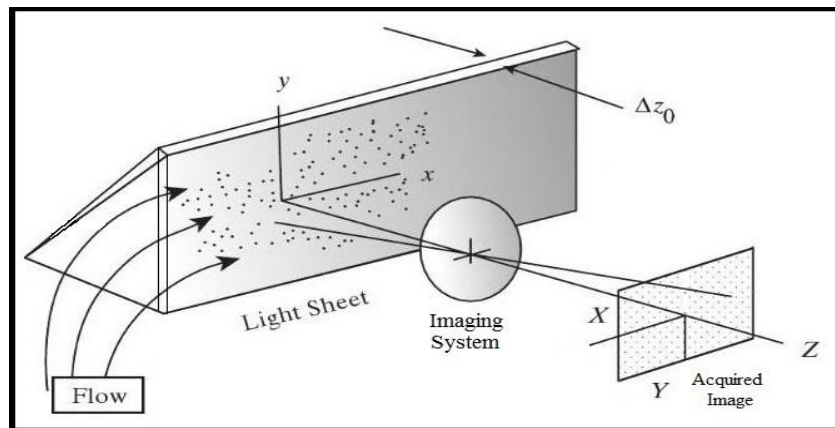
*Source: Taken by Sina Dadgar*

### 2.1.3 Imaging System

Imaging system assigns certain coordinates to each particle in the fluid based on the location in the acquired images. In other words, imaging system of PIV spotlights the location of each particle in fluid and maps them onto corresponding pixels on the images. Since the illumination system is illuminating a thin layer of fluid, the

behavior of particles in posterior and/or anterior planes (posterior and anterior planes will be covered in section 2.1.3.2. and 2.1.5) are not considered in the acquired images. In other words, mapping which has been explained above is from a two-dimensional (not three-dimensional!) particle moving to two dimensional images. Figure 2.7 illustrates how imaging system works in a particle image velocimeter system.

**Figure 2.7: 2-D mapping between particles in fluid and images**



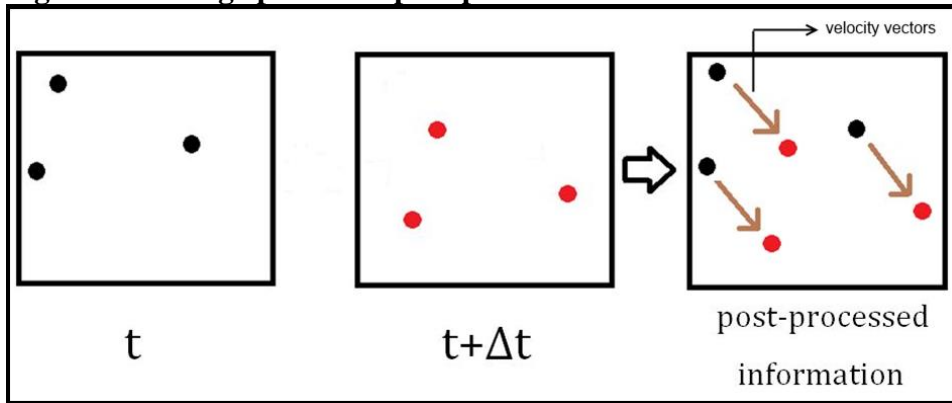
Source: CAMBRIDGE [28]

### 2.1.3.1 Camera

When the LED light sheet is turned on, the particles in the fluid are illuminated as long as the pulse width. During this time, the camera takes the first image. After a time defined by the pulse separation, the second pulse of the pulse pair arrives to the object, and the particles are illuminated for the second time, again for a time equal to pulse width. During this time, the camera takes the second image. As a result an image pair is obtained with a time difference of  $\Delta t$  as shown in Figure 2.8. Based on these information, velocity vectors for each particle can be calculated according to Eq 2.4 by post-processing software, where  $\Delta x$  is the displacement of the particle.

$$V = \frac{\Delta x}{\Delta t} \quad (\text{m/s}) \quad 2.4$$

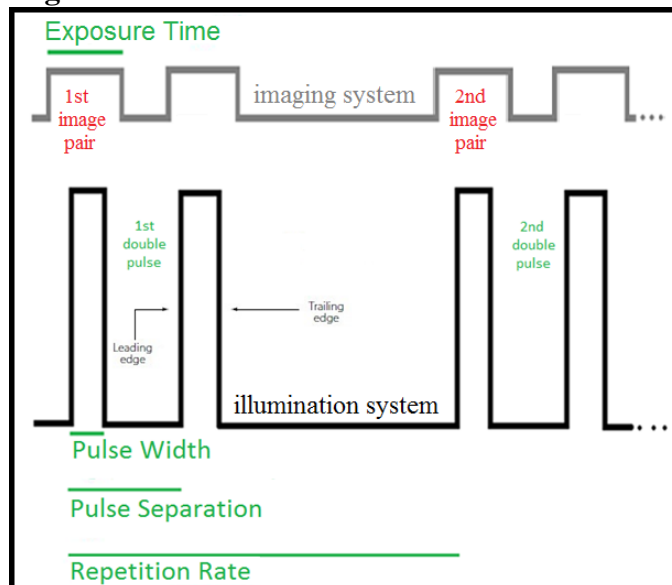
**Figure 2.8: Image pairs and post-processed outcome**



Source: Made by Sina Dadgar

Acquiring image pairs capable of being processed entails on the precise control over camera which is done by Exposure Time (ET). ET is the duration of time that the camera's diaphragm is open and recording the digital photograph. This directly affects the amount of light that reaches to film. In High Speed Photography (HSP), ET must usually be two times greater than PW (the illumination period) to freeze in order to moving object. In other words, there is a linear relationship between illumination period (PW) and imaging period (ET). Figure 2.9 illustrates how ET and PW correspond each other.

**Figure 2.9: PW vs. ET**



Source: Made by Sina Dadgar

The camera which is used in this study has a  $1392 \times 1040$  pixel resolution Nano-camera with exposure time which is able to vary from 5 micro-seconds ( $\mu\text{s}$ ) to 60 seconds which was manufactured by Intelligent Laser Applications (ILA) GmbH, Jülich, Germany.

**Figure 2.10: front and back view of Nano-camera**



*Source: Taken by Sina Dadgar*

### 2.1.3.2 Lens

Since the fluid motion being imaged is seeded with micrometer-sized particles, the optical lens should have large magnification, able to resolve the particles; also it should have a large numerical aperture to collect as much light as possible. Therefore, the camera is equipped with a long-distance microscopic lens to expand the diffraction limited field. The lens which is equipped on the mentioned camera in this project is a K2 model of DistaMax™ which is manufactured by INFINITY photo-optical GmbH, Colorado, USA.

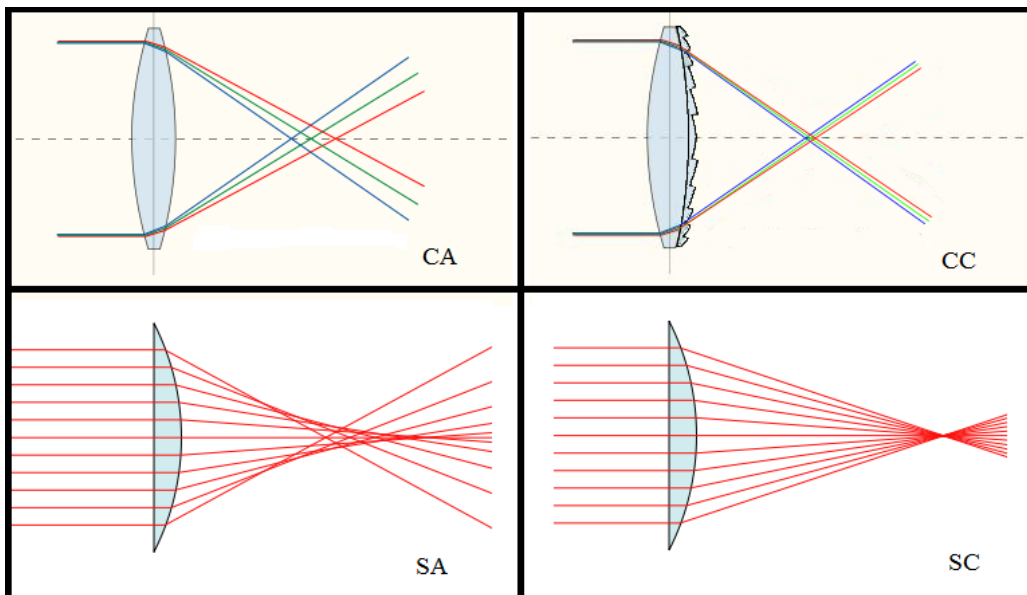
**Figure 2.11: Microscopic Lens**



*Source: INFINITY [31]*

Because of the presence of color distortion (Chromatic Aberration-CA) and light refraction (Spherical Aberration-SA) in high power optical tests such as PIV, the lens happens to provide Spherical Chromatic Correction (CC) and Spherical Correction (SC) in order to acquire high quality images avoiding distortion and refraction. Figure 2.12 illustrates the concept of CA, SA, CC, and SC. Chromatic Aberration happens when light of different wavelength is focused on different points. This happens due to material dispersion resulting in wavelength dependent focal length. However, since in this study a monochromatic light is used, CA is not a critical issue. Spherical Aberration however, is due to height dependent focal length, this happens due to imperfections in the geometrical shape of the lens. [32]

**Figure 2.12: CA, SA, CC, and SC**



*Source: Jones & Bartlett [33]*

### 2.1.3.2.1 Iris Diaphragm

Distamax K2 is equipped with a mechanically controllable iris diaphragm to have the control over light attenuation and depth of focus in the acquired image.

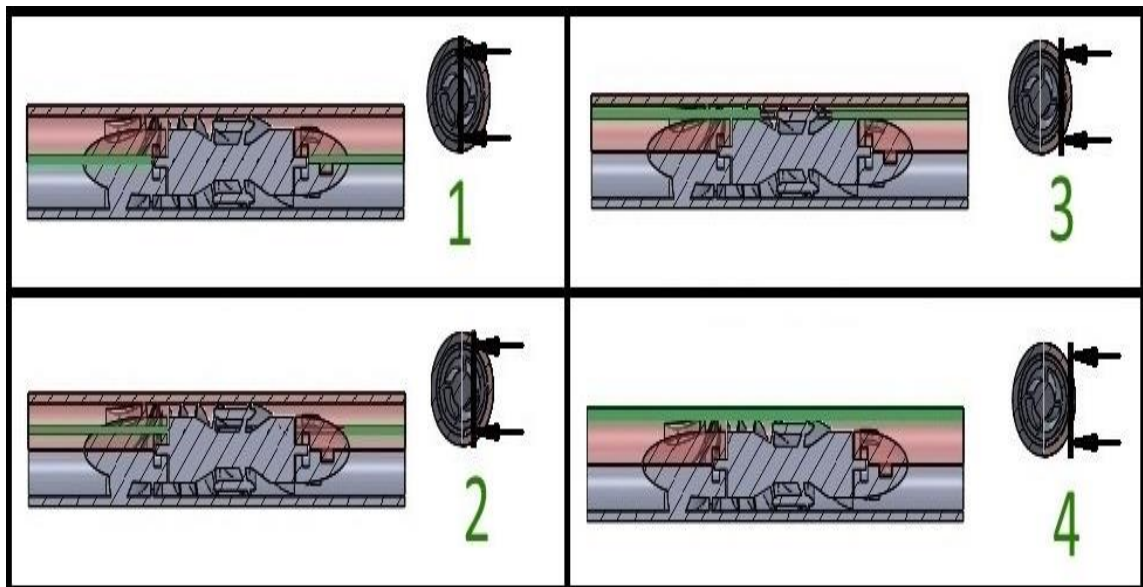
### 2.1.3.2.2 Focusing Ring

As mentioned before, the fluid inside the pump is flowing in three-dimensions since it is travelling inside a volume. However the principle of photography is to take



photographs two-dimensionally in the plane which is focused. In order to gain the information in other planes and avoid losing them, the lens which is equipped on camera has a focusing ring to focus on different planes of pump and allows the PIV system to image different planes. After post-processing, these planes will be combined together using mathematical tools which will be covered in the section 2.6. To focus on a specific plane, the focusing ring must be altered in order to acquire clear images in screen. Altering focusing ring moves the lens plate back and forth and therefore changes the distance from effective center of lens to the image plane of camera. In the meantime, since the LED is illuminating just a thin layer of volume, focusing on posterior and anterior planes require moving the illuminating sheet back and forth so focused camera can acquire images from the illuminated plane. It is known that the more plane number guarantees the better visualization of small vortices; however, since the half of the radius of pump and the width of light sheet is 8 and 2 mm respectively, the PIV experiment is accomplished in 4 planes. Figure 2.13 and 1.14 are illustrating the concept of sequential planes and Iris Diaphragm and Focusing Ring on the Lens.

**Figure 2.13: Concept of sequential planes over the pump**



*Source: Made by Sina Dadgar*



**Figure 2.14: Iris Diaphragm and Focusing Ring**

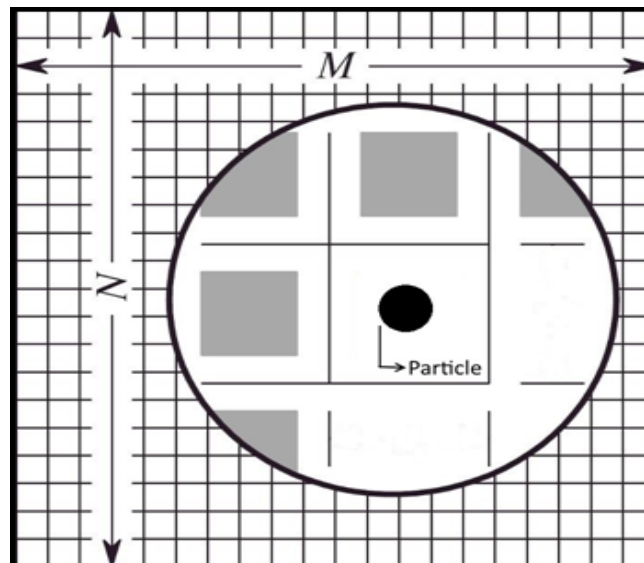


*Source: Made by Sina Dadgar*

#### **2.1.4 Pixelization or Resolution**

The process that leads to acquire exact realistic images from real objects is called Pixelization. First, the acquired image gets sampled by the integration of field over picture elements (pixels). Later on, the intensity of each location in the field gets quantized with the corresponding pixel. Finally, intensity digits of each pixel get stored in the memory of camera and an image becomes available. This is clear that the more pixels in an image make the image clearer. The resolution of camera used in this project is  $1392 \times 1040$ .

**Figure 2.15: Illustration of the Concept of Pixels**



*Source: CAMBRIDGE [28]*

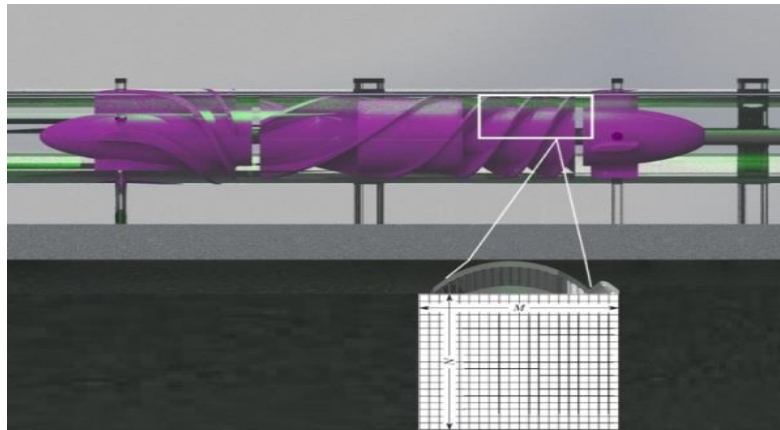
### 2.1.5 Magnification Factor and Region Of Interest (ROI)

In PIV, Magnification Factor (MF) is a tool used to determine the size of an object in real life compared to the image which is captured by a microscopic camera. MF needs to be identified in order to assimilate flow field with visualized flow in images and provide the physical amount of flow speed by post-processing software. Eq 2.5 illustrates the equation of MF.

$$MF = \frac{\text{resolution}}{\text{ROI}} \quad (\text{pixel/millimeter}) \quad 2.5$$

Given the resolution of camera as 1392×1040 and considering ROI to be 18×18mm, MF happens to be approximately 77.33 pixels in one millimeter.

**Figure 2.16: Illustration of ROI and Corresponding Pixels**



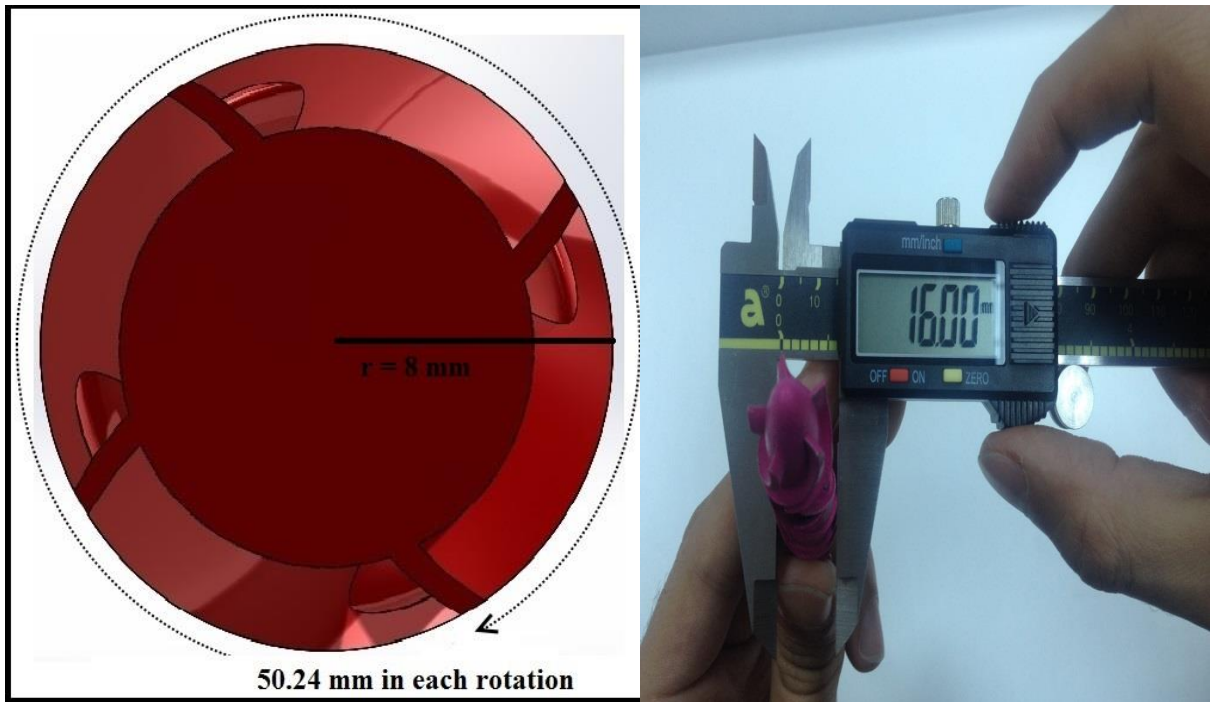
*Source: Made by Sina Dadgar*

The size of the region which camera is looking in order to acquire images is called the Region of Interest (ROI). The size of ROI is directly proportional to the velocity of fluid ( $V_f$ ) and PW.

As mentioned before, in this study the component of the pump, accelerating the fluid, the rotor that is 8mm in diameter – rotates at nominal speed of 8-10 KRPM imparting kinetic energy to fluid and making it to run with the a given velocity which is calculated below. In each rotation, rotor is covering 50.24 mm according to the circumference of a circle which is:

$$C_{\text{circle}} = 2 \pi r \quad 2.6$$

**Figure 2.17: Periphery of rotor**



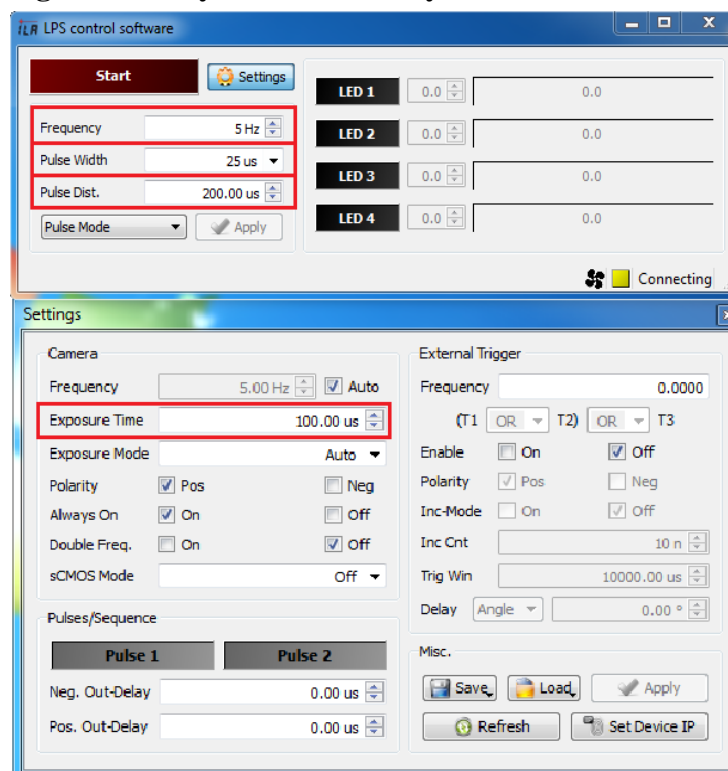
*Source: Made and Taken by Sina Dadgar*

And therefore, in 10,000 rpm, the particles around rotor cover a distance of 502.4 meters per minute or 8 micrometers per each micro second. According to this high velocity of the fluid, illumination and photograph acquisition must be dependently fast to freeze the particles in the acquired images. This means the particles will cover 627.75 micrometers or 0.627 millimeters (which is a significantly large distance to be covered by particles in PIV) in 75 microseconds (as the shortest PW that LED light source can generate). This displacement will show itself as streaks in images if the camera is looking in a 4×4mm ROI. Streaks are generated when the diaphragm of camera is open for a longer time that illuminating sources travel through to frame. But when increasing the ROI from 4×4mm to 18×18mm, the problem related to the streaks in images is solved. It must be noted that laser based systems can generate pulses up to nanoseconds which means that PW would be shorter and there would be no streaks in images. But since Laser based systems are more expensive than LEDs, it was preferred to use an LED based system and increase the ROI to avoid dealing with streaks. Throughout this study, ROI in all acquired images is 18×18mm.

## 2.1.6 Synchronization

The synchronizer plays the role of an external trigger for both the camera and the LED. Controlled by a computer, it dictates and synchronizes the timing and the actions of the laser and camera (i.e. PW, PS, ET, and etc.) Thus the time difference between each pulse of the laser in reference to the camera's timing can be controlled. Figures 2.9 and 2.18 illustrate synchronizer's function.

**Figure 2.18: Synchronization system**



*Source: Made by Sina Dadgar*

The synchronization system being used in current study is an LED Pulsing System (LPS) Controller which is in double pulse mode synchronizable to any camera which is manufactured by Intelligent Laser Applications (ILA) GmbH, Jülich, Germany.

**Figure 2.19: Synchronizer**



*Source: Made by Sina Dadgar*

LED pulsing system is also able to perceive external trigger signals and run illumination and image acquisition simultaneously based on external trigger coming from outer systems. In section 2.4, the concept of external trigger will be covered in details.

### **2.1.7 Processing Software**

The aim from PIV experiment in this study is to acquire the flow field over the pump to reveal the presence of backflow, flow separation, eddies and etc. and also to study the velocity vectors all over the pump to validate the outcome from CFD tests. To do so, particles are seeded in fluid and illuminated two-dimensionally by the double pulses of an LED. Simultaneously, a synchronized camera takes consecutive double images while double pulses from illumination source are illuminating particles. As an outcome from all, there is a set of image pairs which are taken with some time interval where first image representing the initial location of each particle in a given ROI and second image representing the secondary location of same particles in same ROI. Given the time interval between image pairs and distance covered by each particle, velocity vector of each particle can be calculated quantitatively by software. But the concept of velocity for a computerized program is velocity in the terms of the number of pixels covered in a given time. The displacement in the terms of pixels in a given time must be converted to real velocity (i.e. the distance covered in terms of meter) and as explained in section 2.1.5. MF is the tool which corresponds the

distance which particles cover in images and the distance the particles cover in real world. So, Post-Processing software must be equipped with MF tool in order to enhance the precision of calculated velocity vectors.

Furthermore, time interval between image shots must be defined on post-processing tool so it can interrogate how long does it take for particles to cover MF based distances.

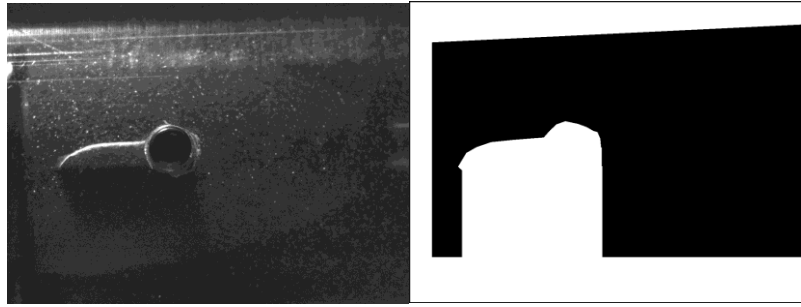
Acquired images by microscopic camera are covering all elements in ROI including particles, pump subsections, and background. They also contain “salt and pepper noises” [34] where there is no light access (like the regions under blade) and/or regions in which there is no flow. In order to achieve trustable outcome from Post-Processing software, some image Pre-Processing manipulations need to be done to eliminate “salt and pepper noises”, mask the regions out of interest, and to eliminate the background. By this, Post-Processing software will consider noise-less images where unwanted regions are masked and particles are highlighted by eliminating the background.

The software which is used in this study is PIVtecILA2C-University usage which was purchased from Intelligent Laser Applications (ILA) GmbH, Jülich, Germany.

#### **2.1.7.1 Masking**

PIVtecILA2C allows the operator to use this tool to specify the regions that are needed to be Post-Processed. In other words, this tool gives the operator the chance to exclude unwanted regions and avoid Post-Processing to be done over those regions. Masking is done simply by dragging and dropping the unwanted regions out of Post-Processing operations. Figure 2.20 illustrates a real image taken by camera from inducer part of pump in left and masked version of the same image in the right hand side where only black parts are going to be considered in Post-Processing.

**Figure 2.20: Masking system**



*Source: Made by Sina Dadgar*

## **2.1.7.2 Filtering**

### **2.1.7.2.1 Median Filter**

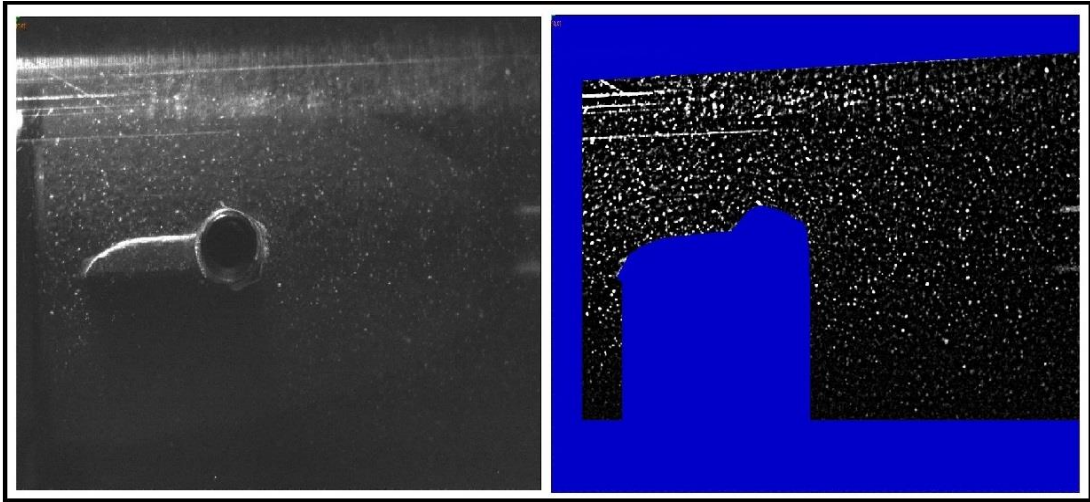
In order to eliminate white and black dots in images which are called “salt and pepper noise”, Median Filter (MF) replaces the value of white and/or black pixels with the gray level of the pixels in the neighborhood of that pixel. This filter reduces the amount of the noise and it has less blurring than other type of filters.  $3 \times 3$  MF is used to Pre-Process all images in this study where  $3 \times 3$  stands for the number of pixels around a specific pixel which is white or black.

### **2.1.7.2.2 High-Pass and Low-Pass Filters**

High and Low-Pass filters respectively transmit high and low frequencies. Low-pass filters are averaging filters which smooth high frequencies and likewise, High-pass filters smooth low frequencies. The high and low-pass Gaussian filters transmit 50 percent of cut off. This bans the presence of diffraction in images so that Post-Processing them results good and trustable outcome. [35]

Figure 2.21 illustrates an image in the left hand side and the presence of Median and High and Low-Pass filters in the right hand side. This figure highlights the importance of filters and their ability to highlight particles (unwanted regions are also eliminated).

**Figure 2.21: Masking and Filtering**



*Source: Made by Sina Dadgar*

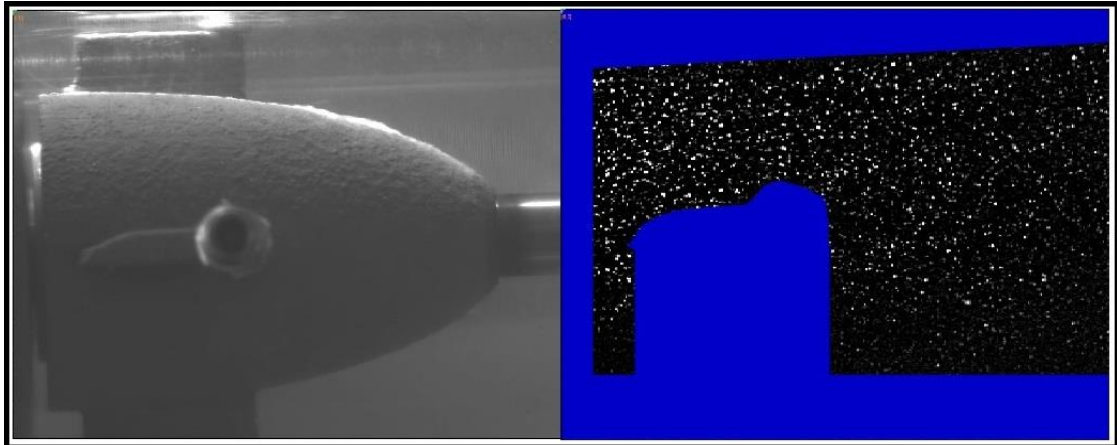
### **2.1.7.3 Background Elimination**

Some portions of the pump which stays in the background of particles can be seen in the figure 2.21. Eliminating them would make it easier for software to detect particles clearly. To do so, PivUtils Scheduler v1.1.9 - Intelligent Laser Applications (ILA) GmbH, Jülich, Germany is used in this project. PivUtils gets the average of every single pixel in 200 acquired image pairs. In outcome, moving parts (particles) of 200 images are eliminated and only the stationary parts of ROI are remained.

Loading this background in Image Pre-Processing tool of PIVtecILA2C, subtracts all pixels from the values in image from background. As a result, all pixels in images look black except particles. In other words, using this tool, images contain only particles and the rest is eliminated. Figure 2.22 illustrates the outcome from PivUtils Scheduler in left side and the effect of background elimination in right side.



**Figure 2.22: Background and Background Elimination**

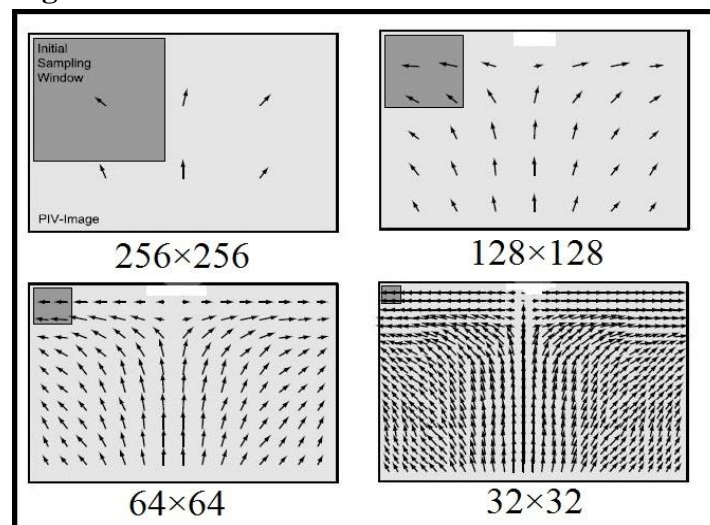


*Source: Made by Sina Dadgar*

#### **2.1.7.4 Post-Processing Tool**

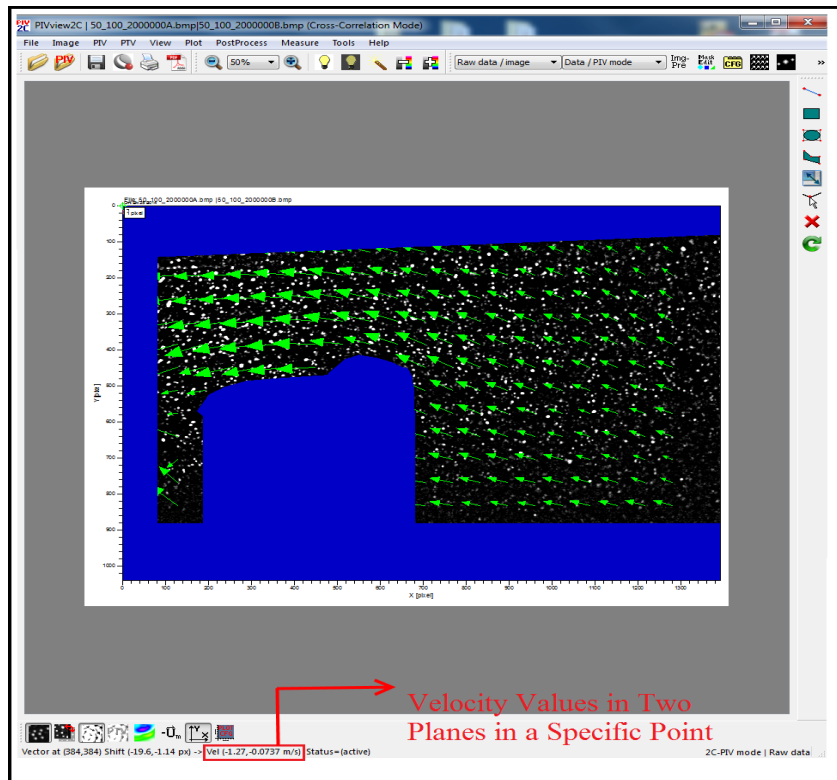
Once MF and pulse delay are defined, regions out of interest are masked, filters are applied, and the background is eliminated, software can start to post-process the images in order to acquire flow field and velocity vectors. Post-processing PIV images defines the number of horizontal and vertical window sizes which are pixels. This defines the rectangular interrogation Window Size (WS) which PIV images are sampled to perform the local cross-correlation. Vector fields can be computed using different interrogation window sizes:  $32 \times 32$ ,  $64 \times 64$ , and  $128 \times 128$ . Figure 2.23 illustrates the differences between different WSs. Based on WS; analyzer interrogates the local cross-correlation over first image pair and illustrates the velocity vector across images.

**Figure 2.23: Different WS**



*Source: Made by Sina Dadgar*

**Figure 2.24: Interrogation of First Image Pair over Inducer Part**

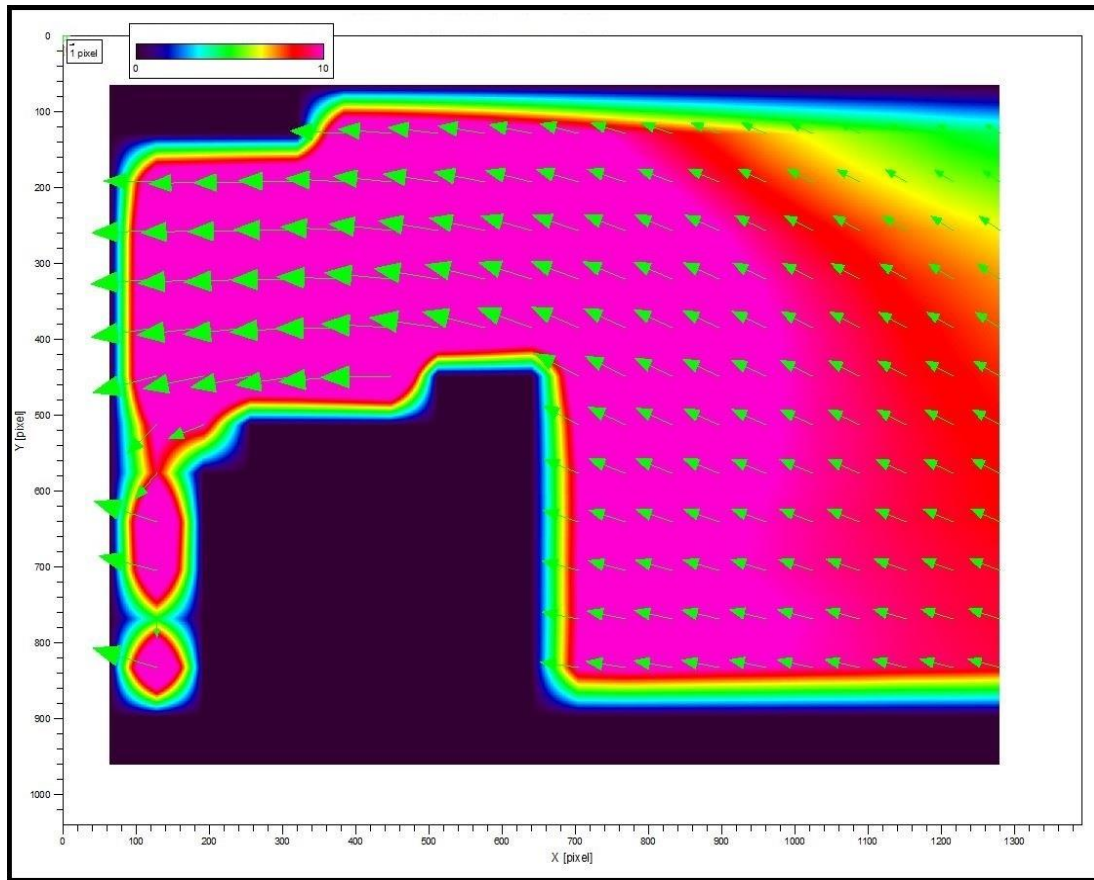


*Source: Made by Sina Dadgar*

Next step is to analyze all image pairs. Batch option processes a large number of PIV images. This proceeding accumulates the mean and Root Mean Square (RMS) of displacement and velocity data and calculates the average velocity vectors for all image pairs which is the real flow field over the region which images are acquired.

The outcome from analyzer has the ability to precisely characterize the velocity magnitude in two directions. It can also quantitatively draw the velocity contours which simplify the visualization of velocity magnitude in different parts of ROI. Figure 2.25 illustrates the velocity contours over inducer where different colors are representing maximum and minimum velocities according to scale.

**Figure 2.25: Velocity Contours**



*Source: Made by Sina Dadgar*

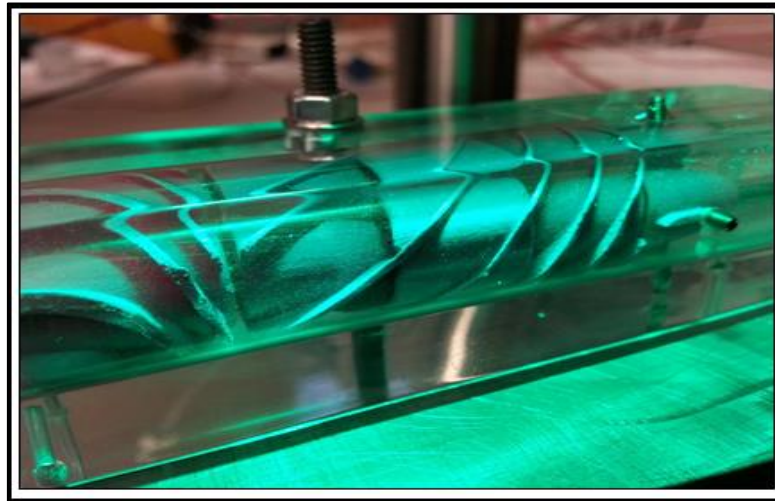
## **2.2 EXTERNAL DRIVING MECHANISM (EDM)**

As mentioned before, PIV method is used to acquire the flow field of an LVAD in this study. Normally, LVADs which are implanted on patients' body work with battery operated permanent magnets. However, in order to study the flow field in physical stage of the R&D of an LVAD using PIV, light of illumination system needs to have access to particles which are seeded in fluid and camera needs to be able to capture the behavior of particles. This can only be done if the housing around pump is transparent which requires removing the permanent magnets. As a result, the pump needs to be spun by an External Driving Mechanism (EDM). EDM consists of different parts which pump components, transparent shroud, driving shaft, torques sensor, and DC motor are the most important parts of it. Sinterly manufactured pump components are circular which requires the inner walls of shroud to be curved. Also, outer walls should be flat to avoid reflection problems. Equation 2.6 describes the backward reflection of light from a surface.

$$R = \left[ \left( 1 - \frac{n_1}{n_2} \right) / \left( 1 + \frac{n_1}{n_2} \right) \right]^2 \quad 2.7$$

In Eq 2.6, R is the ratio of reflected beam power to incident beam power whereas  $n_1$  and  $n_2$  are respectively the RI of the liquid (inside the shroud) and solid (shroud itself). This equation reveals that the reflected beam will be disappeared if the refractive indices are perfectly matched (i.e.  $n_1 = n_2$ ). As a result, the RI of the fluid inside housing material should align perfectly. [36] Shroud housing transparent prototype which was made by mold casting technique [21] has the RI of 1.38 (close enough to the RI of water which is 1.33). This creates 0.22 percent of backwards reflection which is negligible according to the power of LED. Figure 2.26 illustrates pump components inside the transparent shroud during a PIV experiment.

**Figure 2.26: Pump Components and Transparent Shroud**

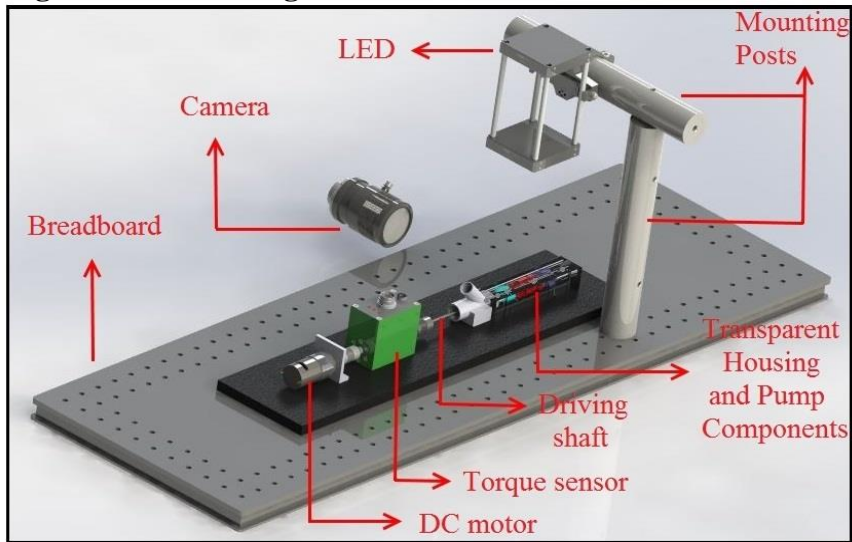


*Source: Aka's Thesis [21]*

Pump Components inside housing is connected to a torque sensor and a DC motor by a driving shaft. This shaft conveys the rotation originating from motor towards the pump components. Also, commanding the desired speed from motor is controlled by a dSPACE data acquisition system.

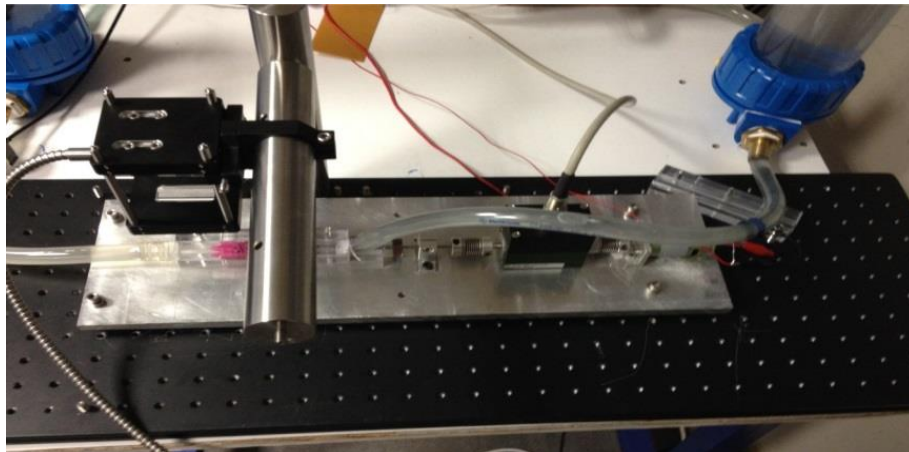
The whole EDM is assembled on a hole tapped opto-mechanical breadboard (PBG51503-THORLABS Austin, Texas, USA). The holes of this breadboard are used to hold the mounting post (P10-THORLABS Austin, Texas, USA) which holds LED above the pump in a stable manner. Figure 2.27 and 2.28 are illustrating a drawing and an image taken from the EDM in the presence of LED light.

**Figure 2.27: Drawing of EDM**



*Source: Made by Sina Dadgar*

**Figure 2.28: External Driving Mechanism**



*Source: Taken by Sina Dadgar*

### **2.3 COMPLEMENTARY COLORS AND PUMP PAINTING**

In this study, LED is running at 532 nm which corresponds to green color in human visible spectrum. While illuminating particles in fluid, it also illuminates the pump components which are made from sandblasted titanium. Thus, any light falling on the rotor is reflected back. However, only light reflected back from particles are considered as signal and light reflected back from pump itself is considered as noise. Therefore, in order to eliminate the reflection originating from pump components, they are painted in their complementary color in “color wheel” [37] which is magenta for green. Figure 2.29 is illustrating the color wheel and complementary colors.



**Figure 2.29: Color Wheel**



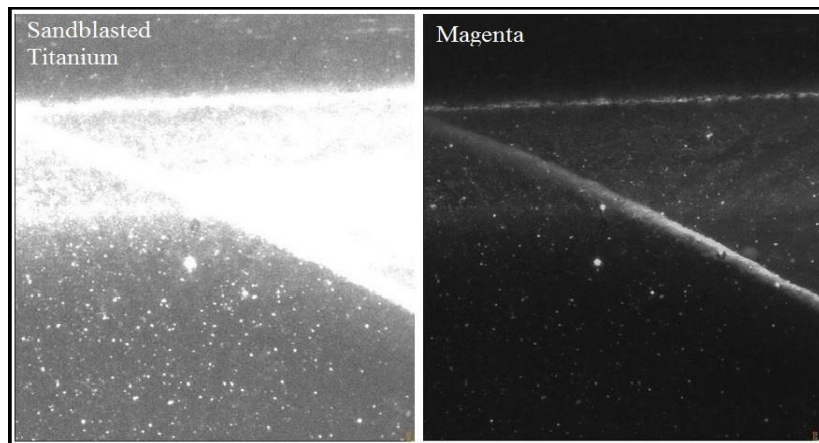
*Source: Routledge [37]*

**Figure 2.30: Pump in Different Colors**



*Source: Taken by Sina Dadgar*

**Figure 2.31: Effect of Magenta**



*Source: Taken by Sina Dadgar*

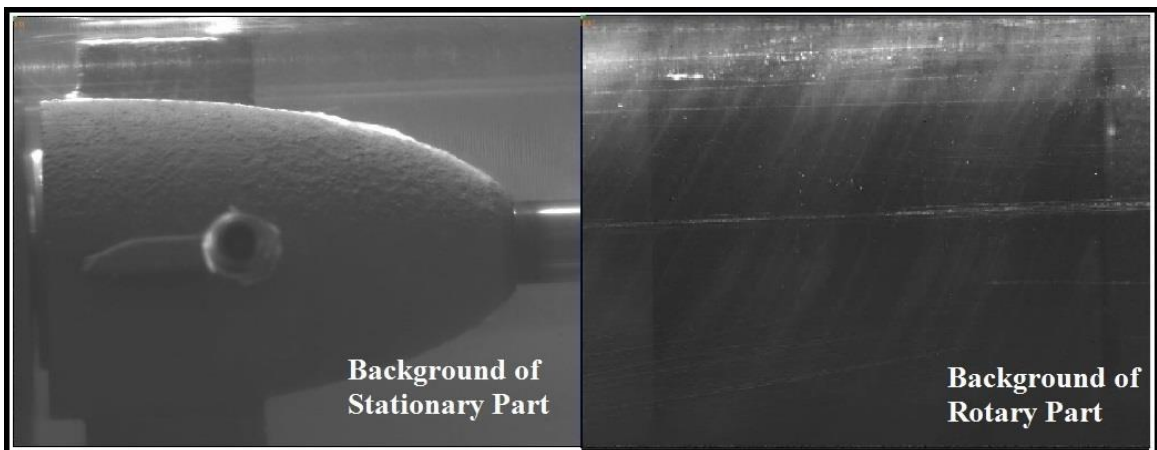
Figure 2.31 indicates the effect of painting pump in magenta. This enhances the ability of software to detect particles easier.

## 2.4 TRIGGERING

As discussed in section 2.1.7.3, background elimination in image pre-processing increases the accuracy of result. Stationary parts (i.e. whatever which has constant location in all acquired 200 image pairs) are eliminated so only particles remain for being processed. For stationary parts of physically manufactured pump (i.e. inducer and diffuser), eliminating background is quiet easy due to their constant locations all the time.

Dissimilarly, since rotary part is spinning all the time, the location of its blades and parts are different in all acquired images and calculated background would be non-frozen. As a result, subtracting the real images from calculated background won't generate pure images where only particles are illustrating because of non-frozen background. Figure 2.32 illustrates calculated background for a stationary part and rotary part (In rotary part the blades are not frozen).

**Figure 2.32: Illustration of Background in Rotary and Stationary Parts**

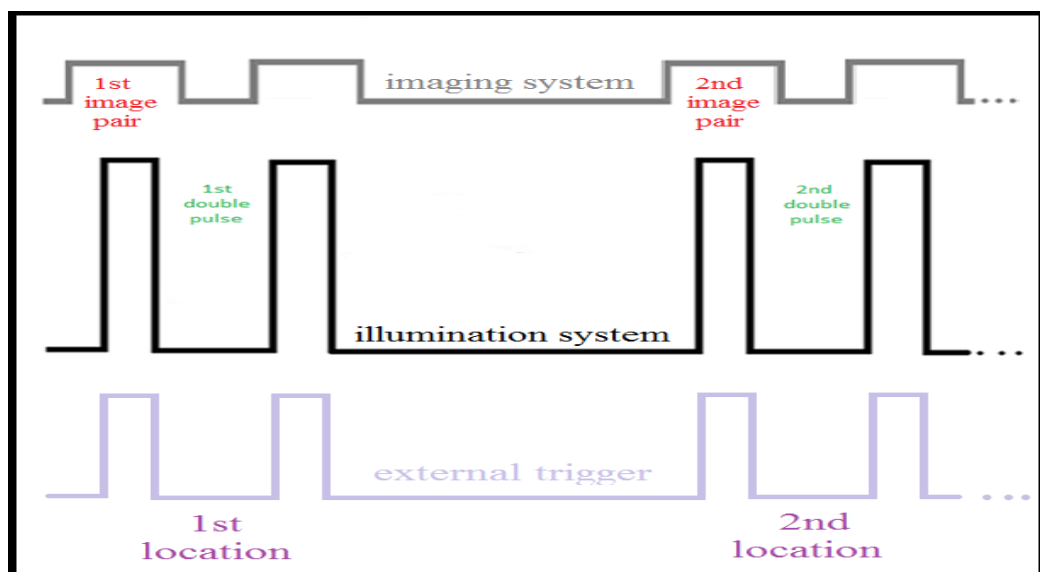


*Source: Made by Sina Dadgar*

In order to avoid acquiring images like Figure 2.32 (which eliminating its background is impossible), each photo must be taken while the rotor is in a given location. To make this happen, an external trigger must come to synchronization unit making all systems (i.e. camera shots, LED fires, and rotor location) run

simultaneously. Without an external trigger, synchronization unit synchronizes camera and LPS (Figure 2.9) to make them work at the same time. However, in the presence of the external trigger, synchronizer commands LED to set the fire according to the frequency of rotor (i.e. when the rotor is in the exact given location) and camera to acquire images when LED light is fired. Figure 2.33 illustrates how three different signals must be synchronized.

**Figure 2.33: Desired Synchronization between LPS, Camera, and External Trigger**



*Source: Made by Sina Dadgar*

However, the EDM is not spinning with a constant speed. Currently, the pump is located between a low and a high pressure reservoir representing only LV and Aorta. Thus preload is continuously changing with respect to the afterload of the pump. Since this problem was not considered and calculated during the design and manufacture process of the EDM, acquiring precise trigger signal to be applied on synchronization unit is impossible. If the taken trigger was accurate, acquired 200 images would be exactly in the same given location with an equal gap between all A and B images. Mentioned problem disabled this research from acquiring images from spinning part (rotor). This research had to study the flow field over rotor by acquiring only one image pair where taking any trigger signal is not necessary. Flow field visualization of anything must be averaged over several image pairs; however,

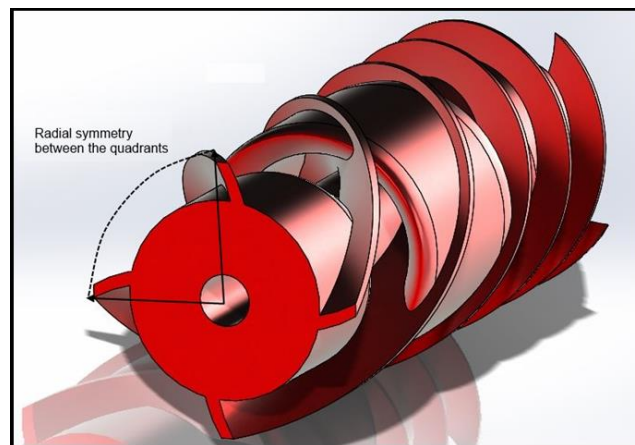


considering the decrease in the precise of result, it can also be characterized by considering one image pair.

## 2.5 RADIAL SYMMETRY

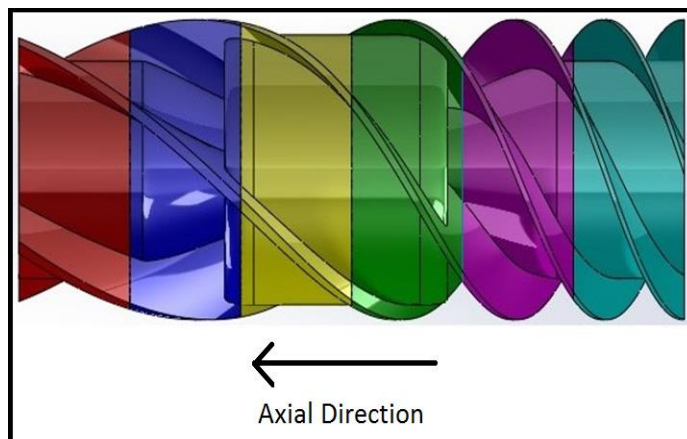
Due to the transverse cross-section of the pump which is composed of 4 symmetric quadrants, only one quadrant is considered in six consecutive sub regions in the axial direction of flow. The reason which pump is divided into six subsections which are illustrated in figure 2.35 in different colors is because the field of view of camera is limited to 7 mm.

**Figure 2.34: Symmetric nature of the Pump**



*Source: Aka's Thesis [21]*

**Figure 2.35: Consecutive sub-regions**



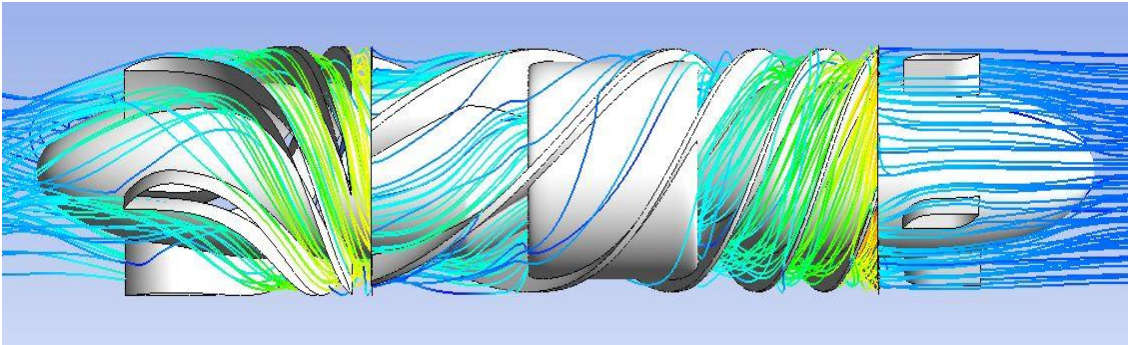
*Source: Made by Sina Dadgar*

So PIV experiment needs to be repeated for every subsection. To do so, camera and LED need to be slidable in the radial direction of the components of pump (i.e. to gather data from all subsections which are illustrated in different colors in figure 2.33). However, the flow is not planer but volumetric. In order to gather data from anterior planes, the LED is slided back and forth and camera is focused in different planes using focusing ring which was explained in details in section 2.1.3.2.2.

## **2.6 MATHEMATICAL MODELING**

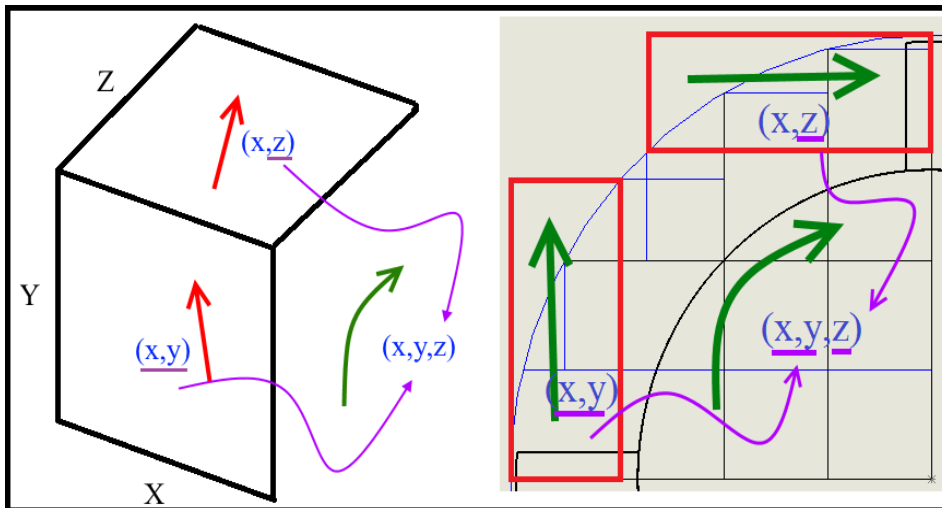
As mentioned before, this study is using a 2-D PIV system to acquire velocity vectors of flow field over a pump which consists of three parts (inducer, rotor, diffuser) which is going to be an axial-flow LVAD. A 2-D PIV system illuminates a very thin layer of flow with an illumination source and acquires images from the flow using one camera. This means that the outcome from 2-D PIV experiment is the flow field in two dimensions. However, because fluid accelerating part (rotor) is rotating, it imparts rotational energy and as a result, fluid flows both in axial and tangential manners. The flow field and streamlines of water particles along the pump are known from virtual step. Figure 2.36 is illustrating the streams that particles use to cover in order to get out of the pump. In physical stage, PIV technique is used to validate the flow field and velocity vectors from CFD (Ansys). However, a 2-D PIV system which has one camera looking at the pump cannot acquire information about third dimension. The innovation that this thesis uses and makes itself unique in its own kind is as following. In this study after acquiring information from one side of the pump, the location of camera and LED light sheet are exchanged and the same test is done from other side of the pump. Acquiring images from one side would reveal the velocity vectors in a 2-dimensional manner. And after doing the same test in another view, second two dimensional velocity vectors would be revealed. Illustrated in figure 2.37, two 2-D velocity vectors information can be combined to produce one 3-D velocity vector. This is accomplished by combining the 2<sup>nd</sup> velocity component of one side with 2 velocity components from the other side.

**Figure 2.36: Virtual Representation of Velocity Streamlines**



Source: Made by Sina Dadgar

**Figure 2.37: 3-D Reconstruction from two 2-D Vectors**



Source: Made by Sina Dadgar

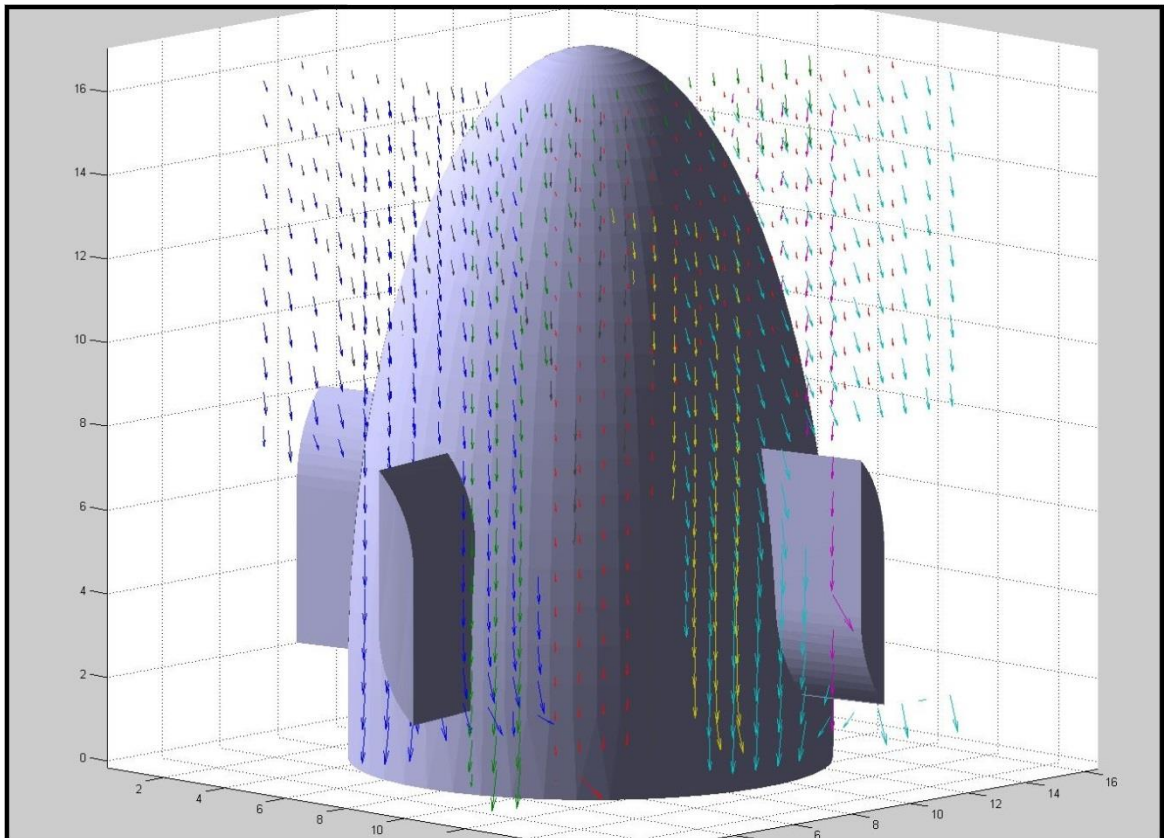
After post-processing images, the software can convert the velocity vectors to excel format where they have 2-D coordinates and velocities. By adding the third dimension ( $z$ ) from up view to velocity information from side view, velocity vectors can be illustrated in 3-dimensional manner.

Further, 3-dimensional data from excel files (which represent different planes and sub-regions) are transferred to Matlab and `quiver3` function is used to plot them in matrix form. This Matlab function plots vectors with directions which are determined by velocity components ( $u,v,w$ ) at the points  $(x,y,z)$ . Simultaneously, using `stlread` function, SolidWork drawing of each part has evoked to Matlab. Thus three-dimensional object in the presence of velocity vectors are acquired which gives the chance to compare streamlines acquired from Ansys with PIV.

It must be noted that this method is used for the parts where the flow is not laminar. (i.e. diffuser and rotor)

For inducer part, where the flow is completely laminar and since the fluid is axially flowing, 2-D vectors from different planes from side and up view are plotted over the inducer in MATLAB. Figure 2.38 illustrates how water particles cover the inducer part in four planes from side and up.

**Figure 2.38: Illustration of Velocity Streamlines Over Inducer**



**Source: Made by Sina Dadgar**

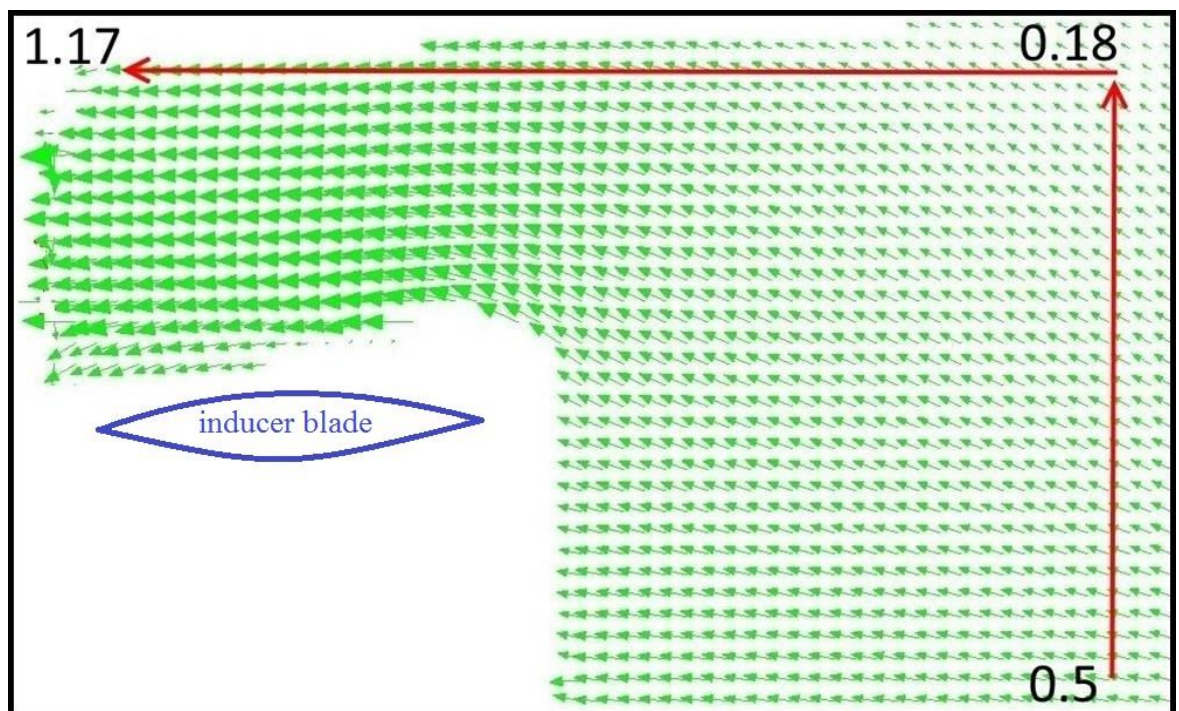
### 3. RESULTS

#### 3.1 INDUCER

Four-bladed inducer leads the flow parallel to its blades avoiding any rotation in rotor inlet. Based on this and results from CFD, it was expected to find the similar velocity vectors in PIV where all particles travel in parallel with blades without any tangential velocities. PIV tests for inducer part were accomplished in four consecutive planes. It must be noted that since the radius of inducer is 8 mm and the width of the light sheet is 2mm, inducer part can only be divided into 4 planes. PIV images from inducer were taken from a 18mm x 13 mm region (ROI=18mm) while rotor spinning approximately at 8240 RPMs pumping 5 liters per minute at a pressure difference rate of 100 mmHg.

The results from PIV test reveals that the fluid is flowing without any turbulence all over the inducer. Figure 3.1 illustrates the velocity vectors over the inducer part. The velocity of particles is increasing from left (inducer's entrance) to right (rotor's entrance). This increase is due to the suction of rotor which increases the velocity from 0.18 m/s to 1.17 m/s at the entrance of rotor.

**Figure 3.1: Velocity Vector Illustration over the Inducer**



*Source: Made by Sina Dadgar*



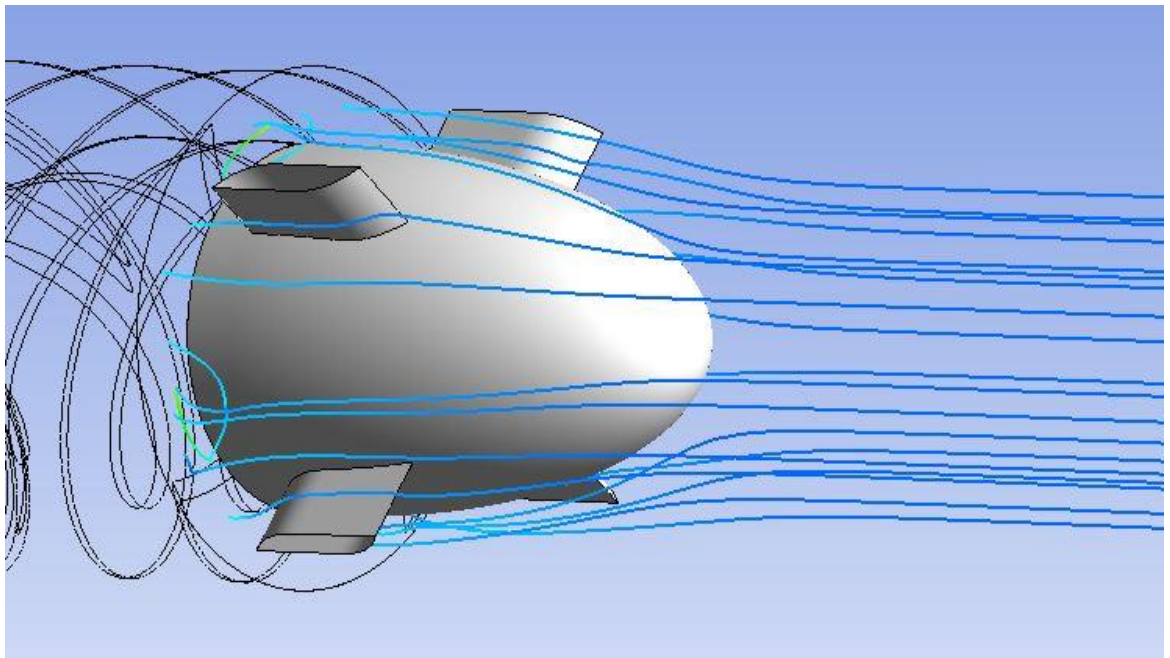
In parallel, acquired velocity from PIV tests meet the calculated velocity from CFD. Since the cross-section area of inducer is  $105.56 \text{ mm}^2$  and considering a flow rate of 5 L/min, the velocity can be calculated using equation 3.1 which turns out to be 1.2 m/s.

$$Q = V \times A \quad 3.1$$

Furthermore, it's known that the velocity of fluid is always larger in the center of a pipe than its walls. The same concept was reported in PIV tests. As seen in figure 3.1, the velocity of fluid is 0.5 m/s in the center of the tube and it gets slower while getting closer to walls (0.18 m/s). Also, the average velocity is faster in the planes closer to center than the planes close to walls.

Virtual velocity streamlines from virtual step is known. These vectors represent the streams that water particles cover in order to pass the inducer and reach rotor which are illustrated in figure 3.2.

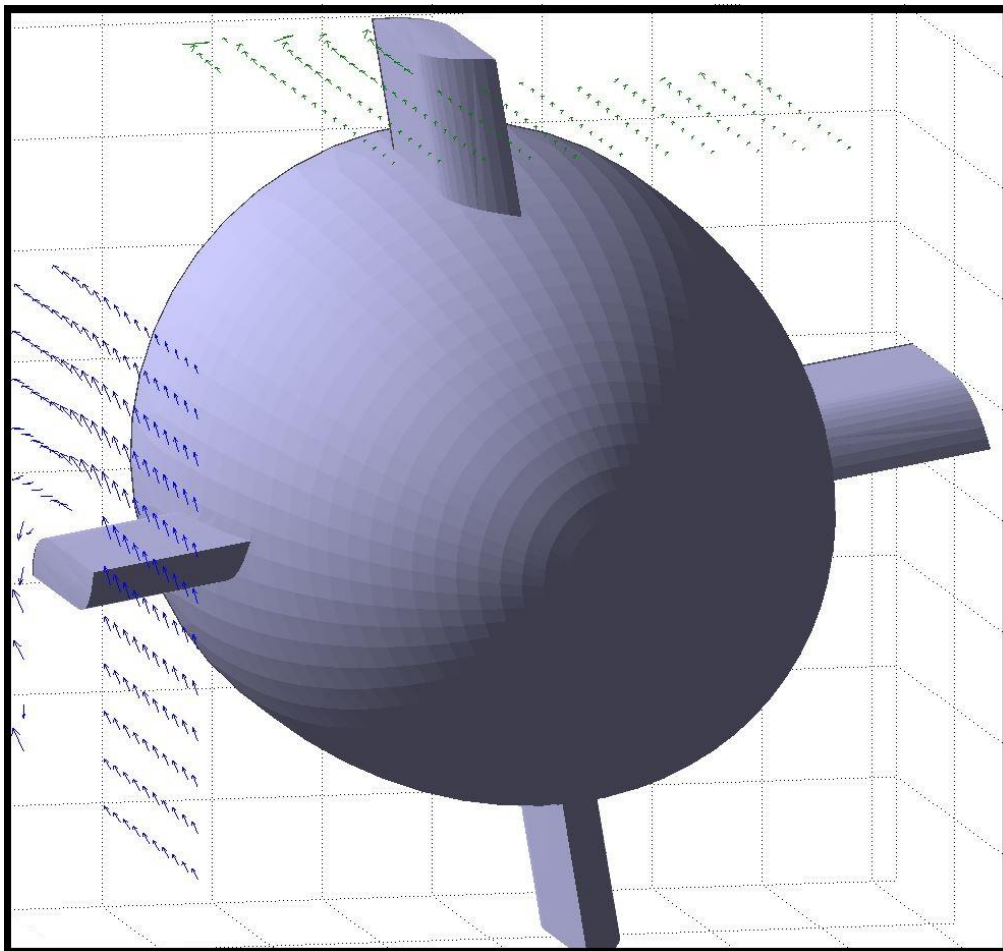
**Figure 3.2: Virtual Velocity Streamlines over the Inducer**



*Source: Made by Sina Dadgar*

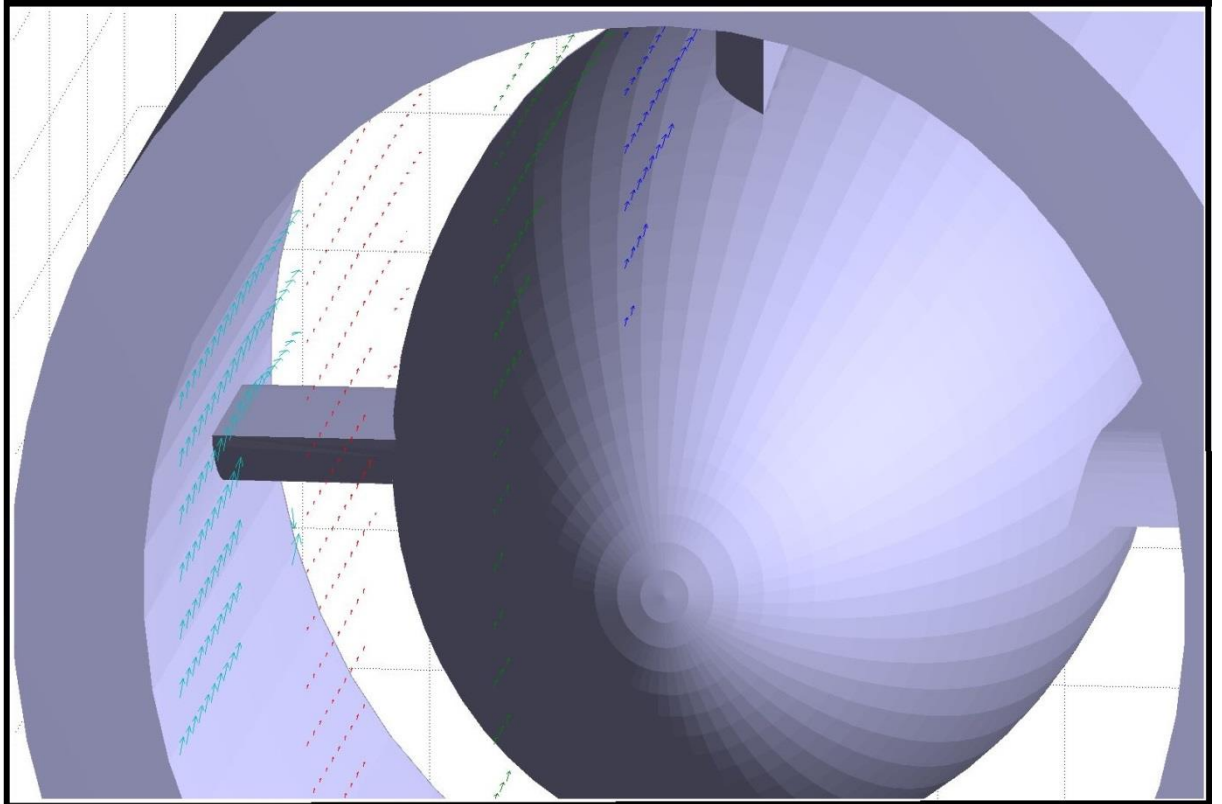
To acquire the streamlines from physical stage, illumination system illuminates the inducer from top while camera looks at particles from sides and next, the location of camera and LED is exchanged to acquire information from two different views. Using quiver3 and stlread functions, SolidWork drawing of inducer, 4 planes of velocity vectors from top view and 4 planes of vectors from side view are plotted in MATLAB. Figure 3.3 illustrates the plotted planes and drawing all together which represents physical velocity streamlines. For simplicity of visualization, only one plane from each side has chosen to be represented. Figure 3.4 and 3.5 are illustrating the flow field over inducer in the presence of housing shroud.

**Figure 3.3: Physical Velocity Streamlines over the Inducer**



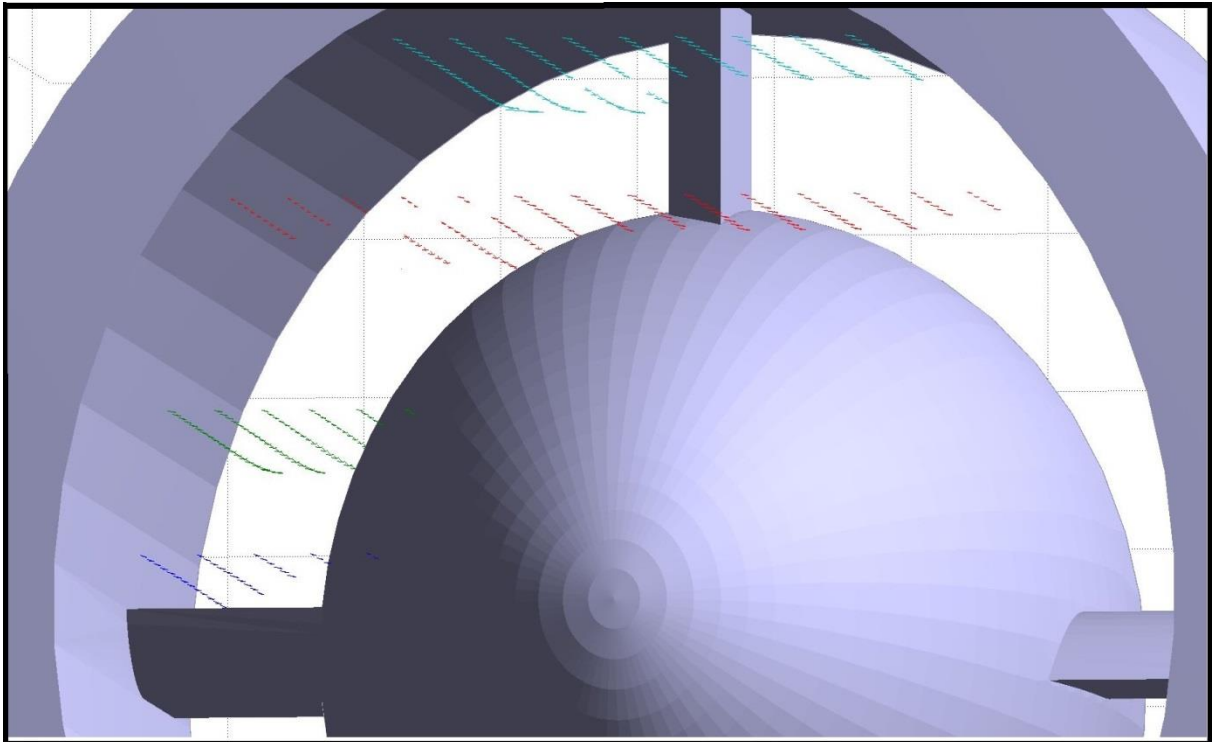
*Source: Made by Sina Dadgar*

**Figure 3.4: Physical Velocity Streamlines over the Inducer**



*Source: Made by Sina Dadgar*

**Figure 3.5: Physical Velocity Streamlines over the Inducer**

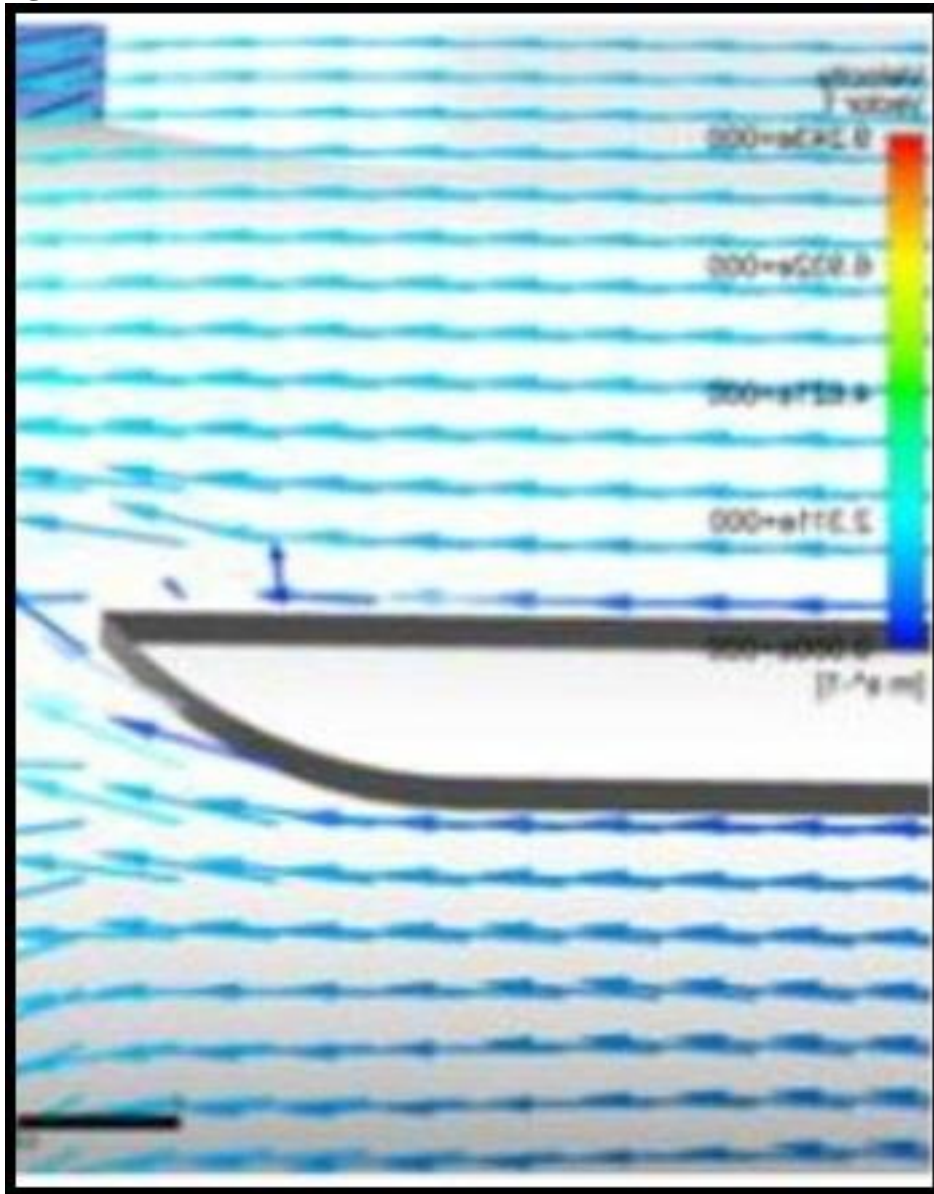


*Source: Made by Sina Dadgar*



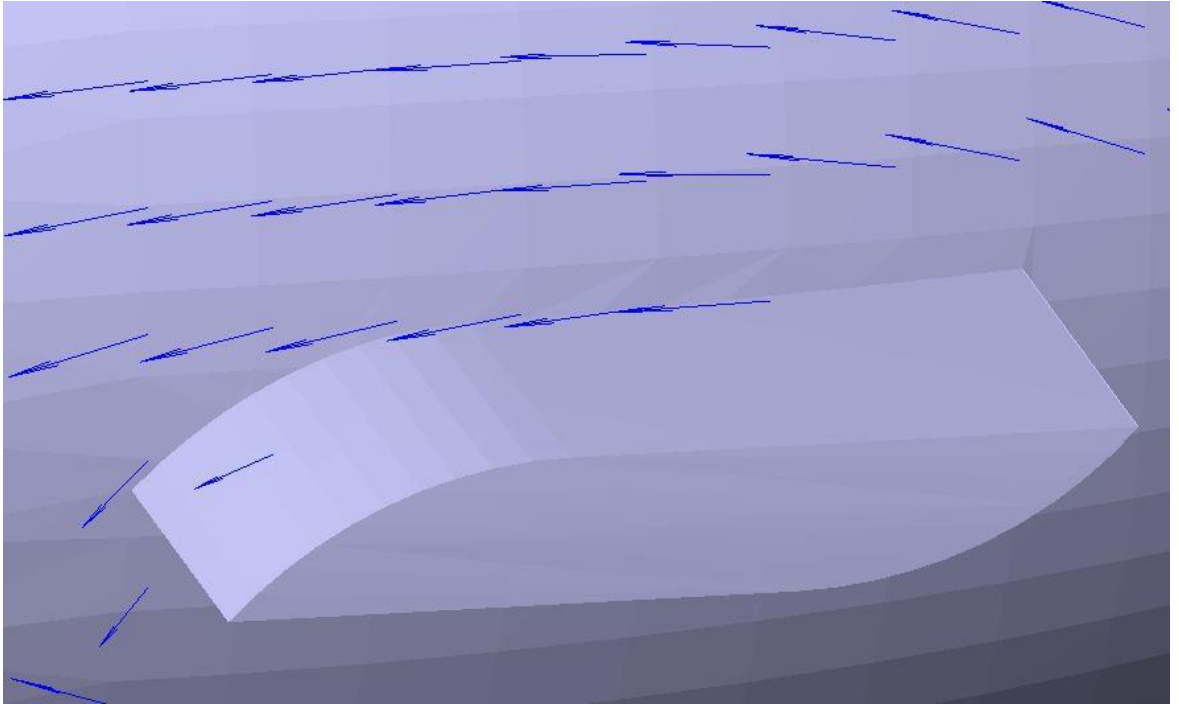
PIV results are also validating the results from CFD about the effect of inducer blade over particles. Figure 3.6 and 3.7 illustrate the effect of inducer blade on particles respectively from CFD and PIV.

**Figure 3.6: Inducer Blade Effect on Particles from CFD**



Source: Toptop's Thesis [14]

**Figure 3.7: Inducer Blade Effect on Particles from PIV**



*Source: Made by Sina Dadgar*

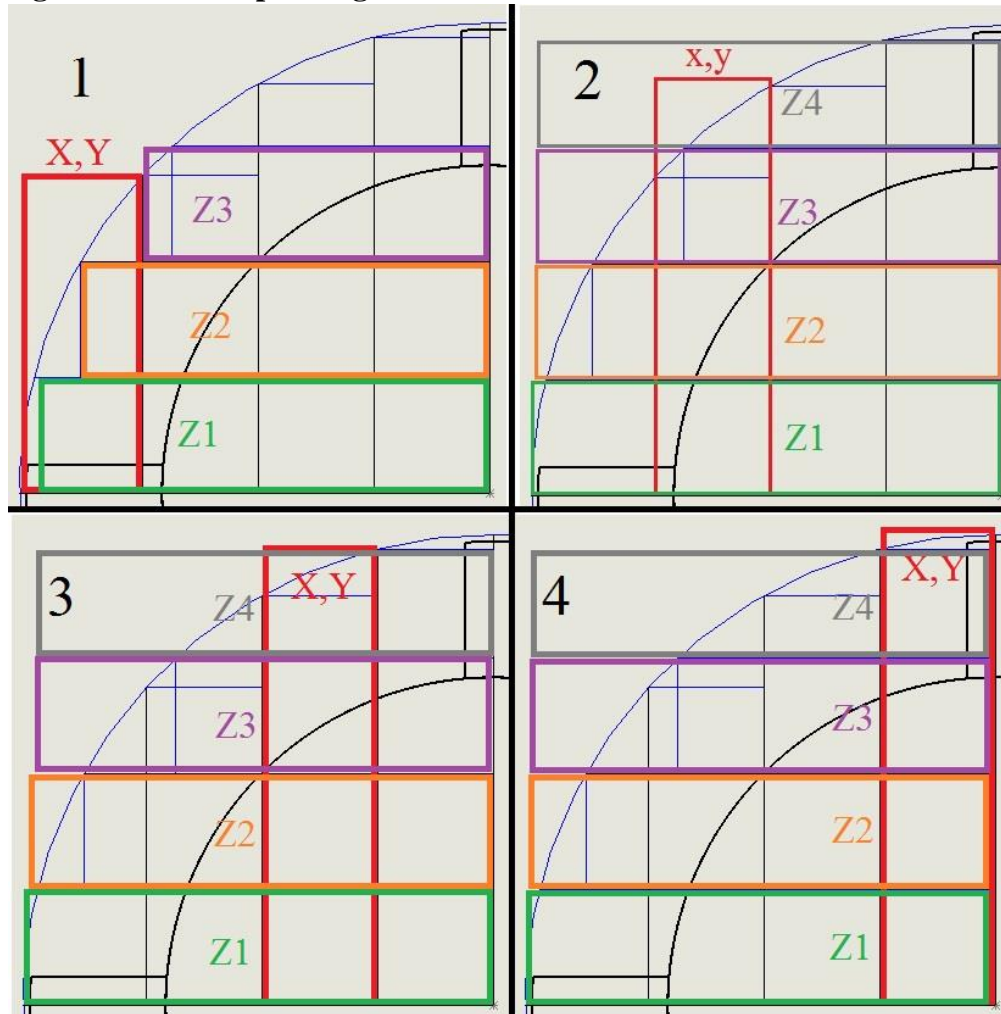
### **3.2 ROTOR**

Rotor imparts kinetic energy to fluid with its blades to generate enough pressure difference and flow rate. Because of the curved nature of these blades, it accelerates the fluid not only axially, but also tangentially. In other words, the rotation of curved-bladed-rotor makes the particles to travel in three dimensions. Thus, the PIV experiments in this section were done in two sides to study both axial and tangential velocities.

As explained in section 2.6, tangential velocity vectors are acquired by considering second velocity component planes illuminated from side as the third velocity component in each respective plane. Figure 3.8 illustrates corresponding horizontal and vertical planes in order to 3-D refinement.

Refined 3-D arrows in rotor are acquired by the combination of 2-D vectors in corresponding planes.

**Figure 3.8: Corresponding vertical and Horizontal Planes**



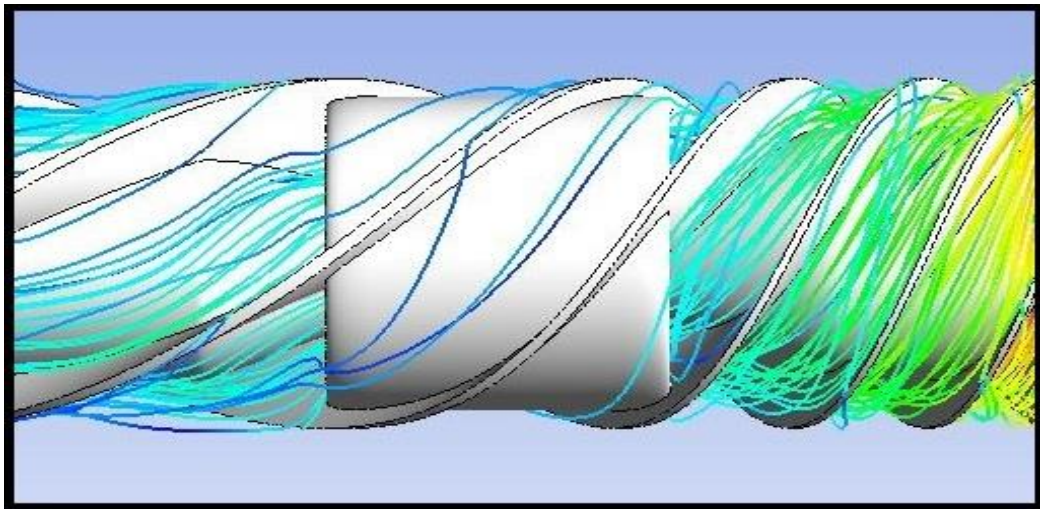
*Source: Made by Sina Dadgar*

Due to the large dimensions of spinning part which is 40 mm, PIV tests has been done in three sub-regions of rotor all with ROI of 16mm. Rotating approximately at 8240 RPMs and pumping 5 liters per minute at a pressure difference rate of 100 mmHg.

Figure 3.9 illustrates velocity streamlines over the rotor acquired from ANSYS and figure 3.10 illustrates velocity vectors in 3 different planes and 3 different sub-regions. Figure 3.10 was plotted by MATLAB software using quiver3 function to characterize the velocity vectors and stread to read the drawing of rotor. Velocity vectors and the SolidWorks drawing are numerically corresponded in correct addresses.

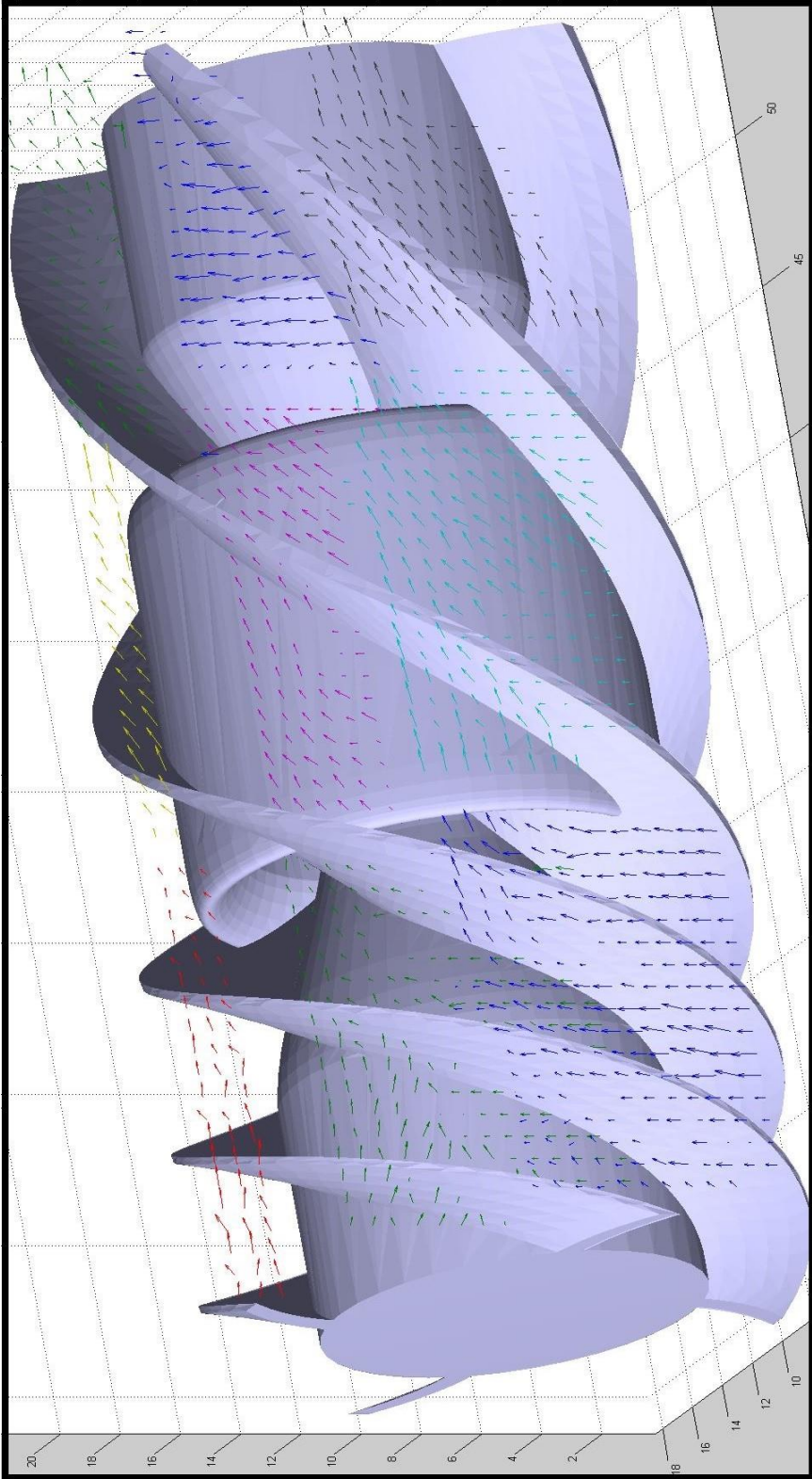
It must be noted that due the reason mentioned in section 2.4, acquiring 200 consecutive image pairs of the behavior of particles in rotor failed. Shown results are all acquired from only one image pair which reduces the accuracy of result (i.e. the velocity vectors are not exactly unidirectional)

**Figure 3.9: Virtual Velocity Streamlines over the Rotor acquired by ANSYS**



*Source: Made by Sina Dadgar*

**Figure 3.10: Physical Velocity Streamlines over the Rotor**



**Source: Made by Sina Dadgar**

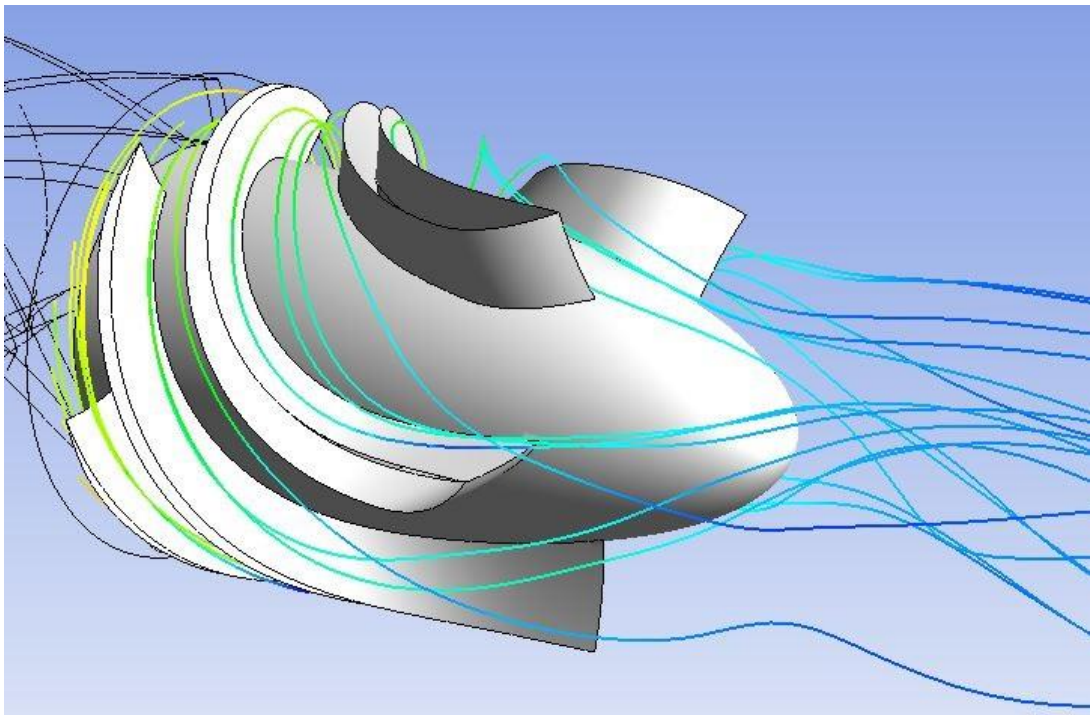


### 3.3 DIFFUSER

Fluid leaving the rotor contains a large velocity and less pressure. Hemodynamics of human cardiovascular system doesn't need fast blood flow, but pressurized flow. To convert the kinetic energy to potential energy by decelerating the fluid, LVADs are equipped with the third part which is stationary and is called diffuser. Diffuser of the first Turkish Axial-Flow LVAD has a complicated design which makes the fluid to travel through with a tangential manner. Add to this, the inlet of diffuser which is connected to the outlet of rotor is under an unsteady and extremely fast moving flow.

Based on CFD, it is expected that in real world (PIV tests) diffuser convert this kinetic energy to potential energy between blade paths without any backflow or vortex. Figure 3.11 illustrates the paths and velocity streamlines that water particles use in order to get out of diffuser.

**Figure 3.11: Virtual Velocity Streamlines over Rotor know from ANSYS**

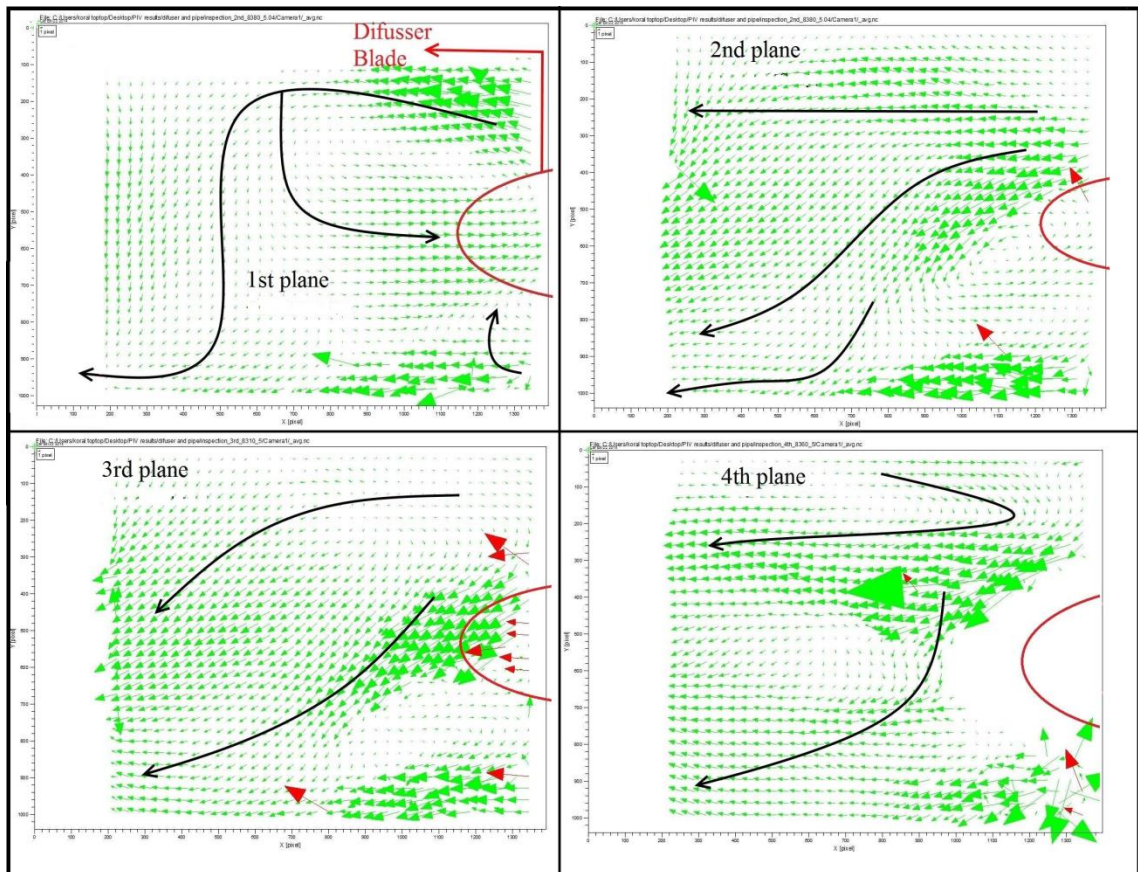


*Source: Made by Sina Dadgar*

PIV images from diffuser were taken from a 18mm x 13 mm region (ROI=18mm) while rotor spinning approximately at 8240 RPMs pumping 5 liters per minute at a pressure difference rate of 100 mmHg.

Preliminary PIV tests over diffuser revealed major turbulences in the flow in different regions of diffuser. Vortices and backflows was reported everywhere in between diffuser blades and output with different and strange velocities which didn't match any results from CFD stage. These tests were conducted in 4 horizontal and vertical light planes. Post-processed results of those planes are represented in figure 3.12.

**Figure 3.12: Preliminary results over Diffuser (First Housing)**

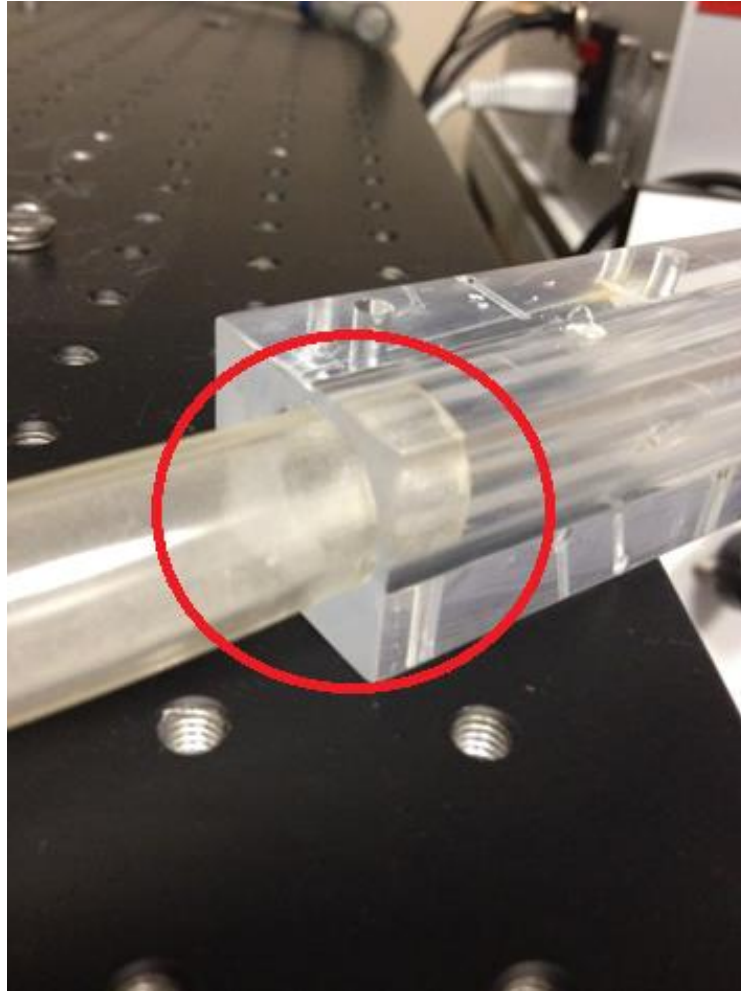


**Source:** Made by Sina Dadgar

It was revealed that vortices are located right after the diffuser curve where the fluid is almost entering the pipe (i.e. the backflow was reported in the region between diffuser and outlet of transparent shroud).

It was first considered that observed unsteady behavior of flow is because of physical reasons. Figure 3.12 illustrates the flow field when the housing shroud didn't have any output. The outlet of the first design of shroud was directly connected to the pipe. Figure 3.13 illustrates first housing shroud.

**Figure 3.13: First Housing Shroud**

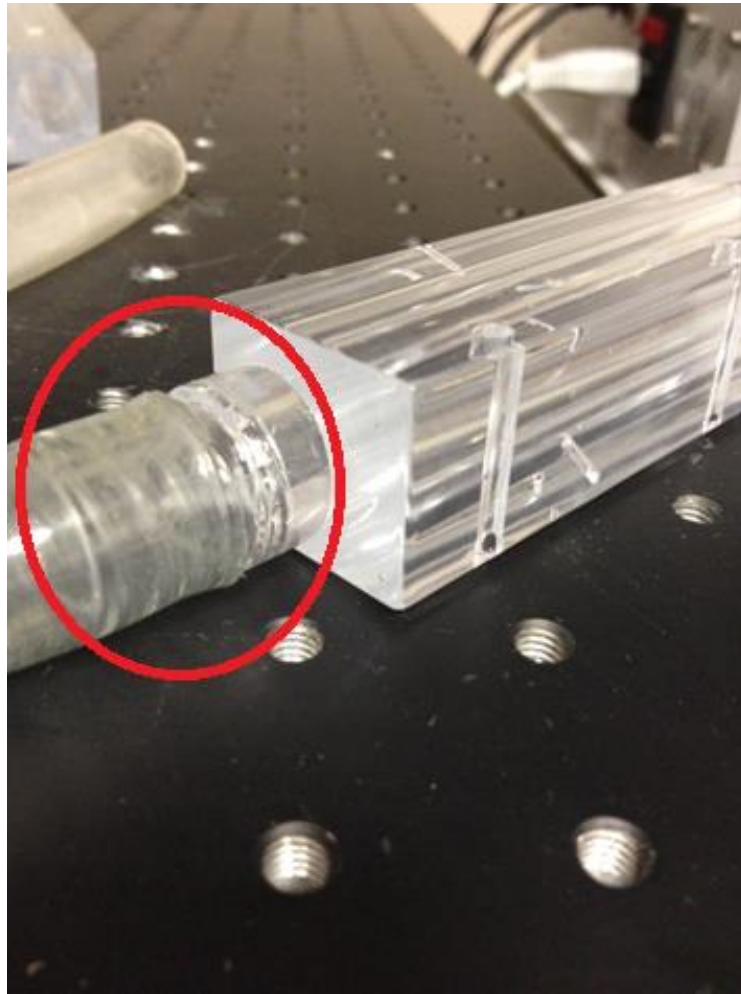


*Source: Made by Sina Dadgar*

So a new transparent shroud was manufactured where the output of housing stayed inside the pipe. It was considered maybe this is the source of backflow and vortices. New design of shroud is illustrated in figure 3.14.



**Figure 3.14: Second Housing Shroud**

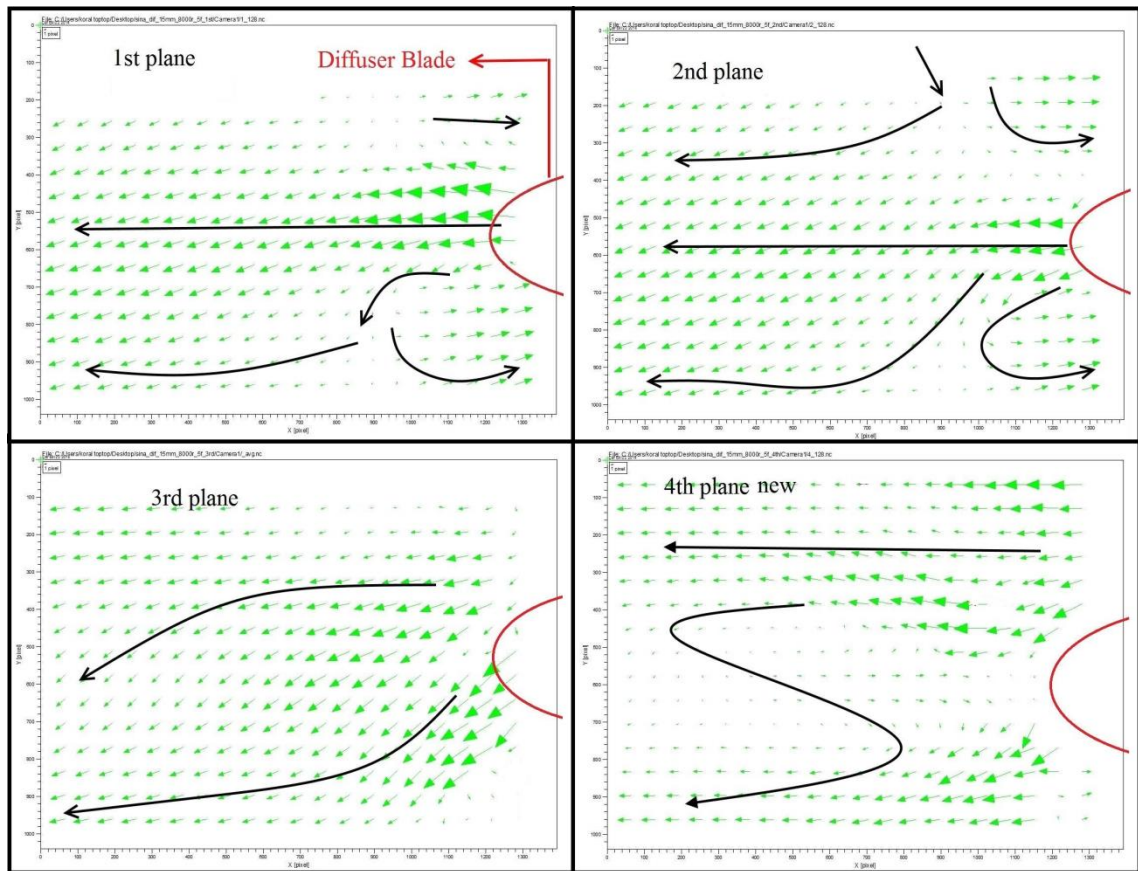


*Source: Made by Sina Dadgar*

Just like the first prototype of shroud, PIV tests for the second shroud were accomplished for a region of 18mm x 13 mm region (ROI=18mm) while rotor spinning approximately at 8240 RPMs pumping 5 liters per minute at a pressure difference rate of 100 mmHg.

The post processed outcome from PIV results had weird turbulences all over the diffuser again. However, comparison between first, second, third, and forth planes from new prototype with old prototype reveals that the change in physical structure of housing altered the flow. Figure 3.15 illustrates post-processed velocity vectors over diffuser.

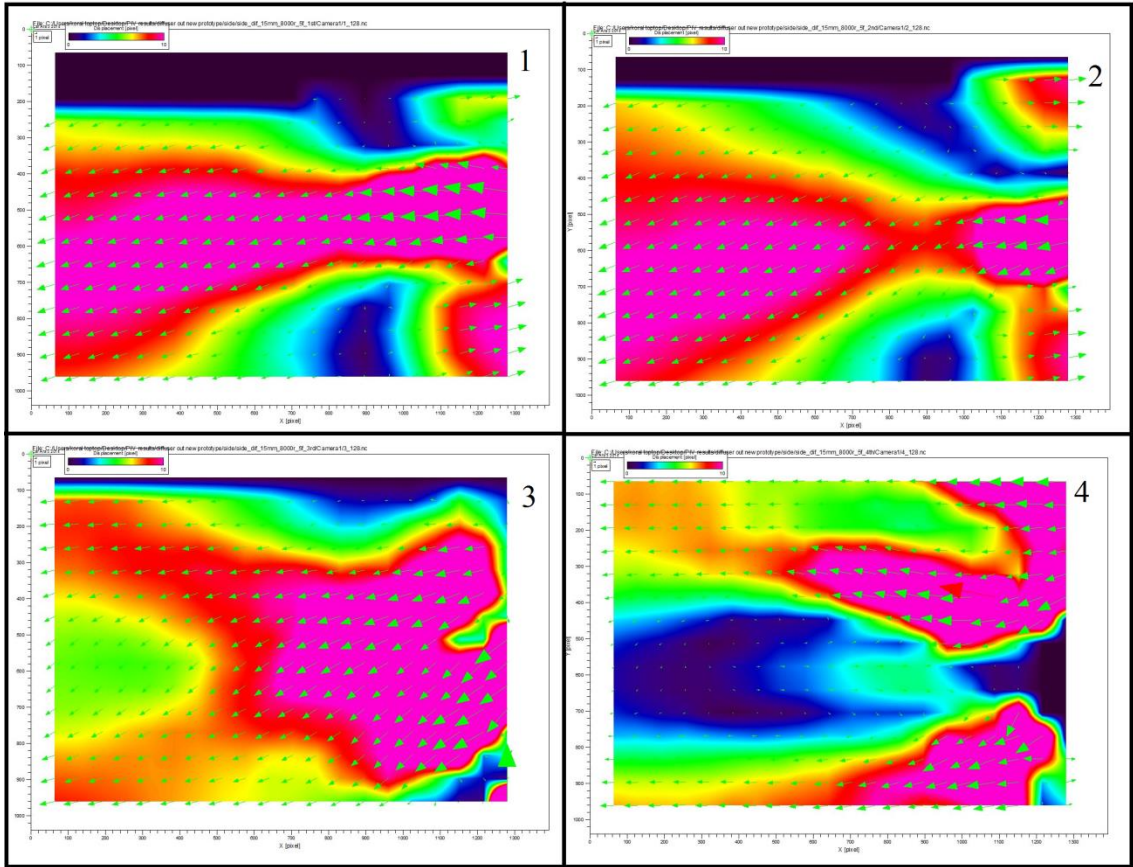
**Figure 3.15: Velocity Vectors over Diffuser (Second Housing)**



**Source:** Made by Sina Dadgar

Also, the magnitude of velocity in different planes of diffuser varies in a large scale. Figure 3.16 illustrates velocity contours over diffuser from 4 planes. All in all, the results over inducer are not satisfying and don't validate the virtual outcome. The source of error can be because of housing shroud and/or maybe the pump parts are not manufactured in scale.

**Figure 3.16: Velocity Contours over Diffuser in 4 planes**



*Source: Made by Sina Dadgar*

#### 4. CONCLUSION

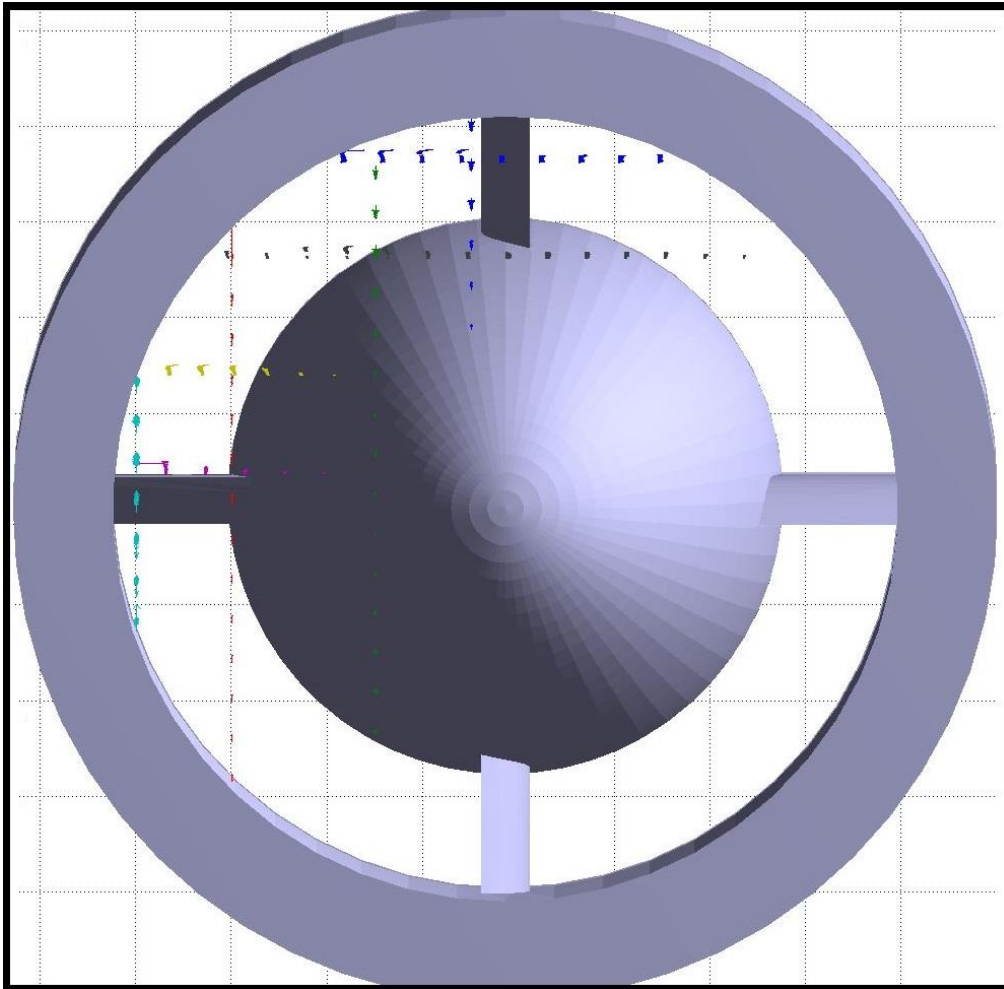
Particle Image Velocimetry (PIV) has been recognized as a useful method to characterize the flow field in a quantitative manner. Just like any project which fluid's physical behavior needs to be studied, current project also employed PIV to acquire velocity vectors of the pump in different regions to be able to validate the outcome from CFD.

PIV physical results over inducer and rotor parts of the pump reveal promising results validating CFD. However as discussed in next chapter (5. Discussion and Future Works), it is required to acquire trigger signal from rotor which enables camera to take photographs from spinning part in exact same location. This would highly increase the accuracy of the velocity vectors over rotor. In diffuser part, PIV tests over turbulent flow were accomplished from two sides to conduct and acquire three dimensional (tangential) velocity vectors in order to detect the source of backflows and vortices. Figures 4.1, 4.2, and 4.3 are respectively representing the flow field over inducer, diffuser, and rotor.

In almost all of similar researches, stereoscopic PIV setups are used to characterize the flow field where the fluid is flowing in three dimensions. Nowadays usual belief is that stereoscopic PIV systems are able to acquire three velocity components and monoscopic ones are not. However, the researchers in current study insist that using 2-D PIV system it is still possible to do exact same objectives that 3-D systems do. As a result, it can be avoided to use 3-D setups which are much more expensive than 2-D setups. Explanations regarding to the accomplishment of 3-D flow field characterization using 2-D PIV system has been explained in details throughout this thesis.

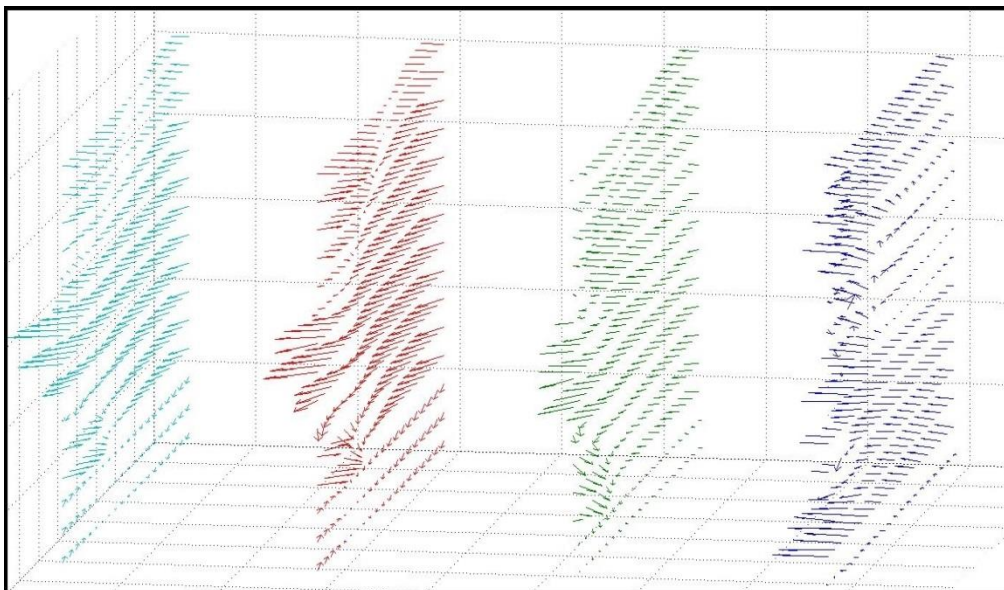


**Figure 4.1: Physical Velocity Streamlines over the Inducer (all planes)**



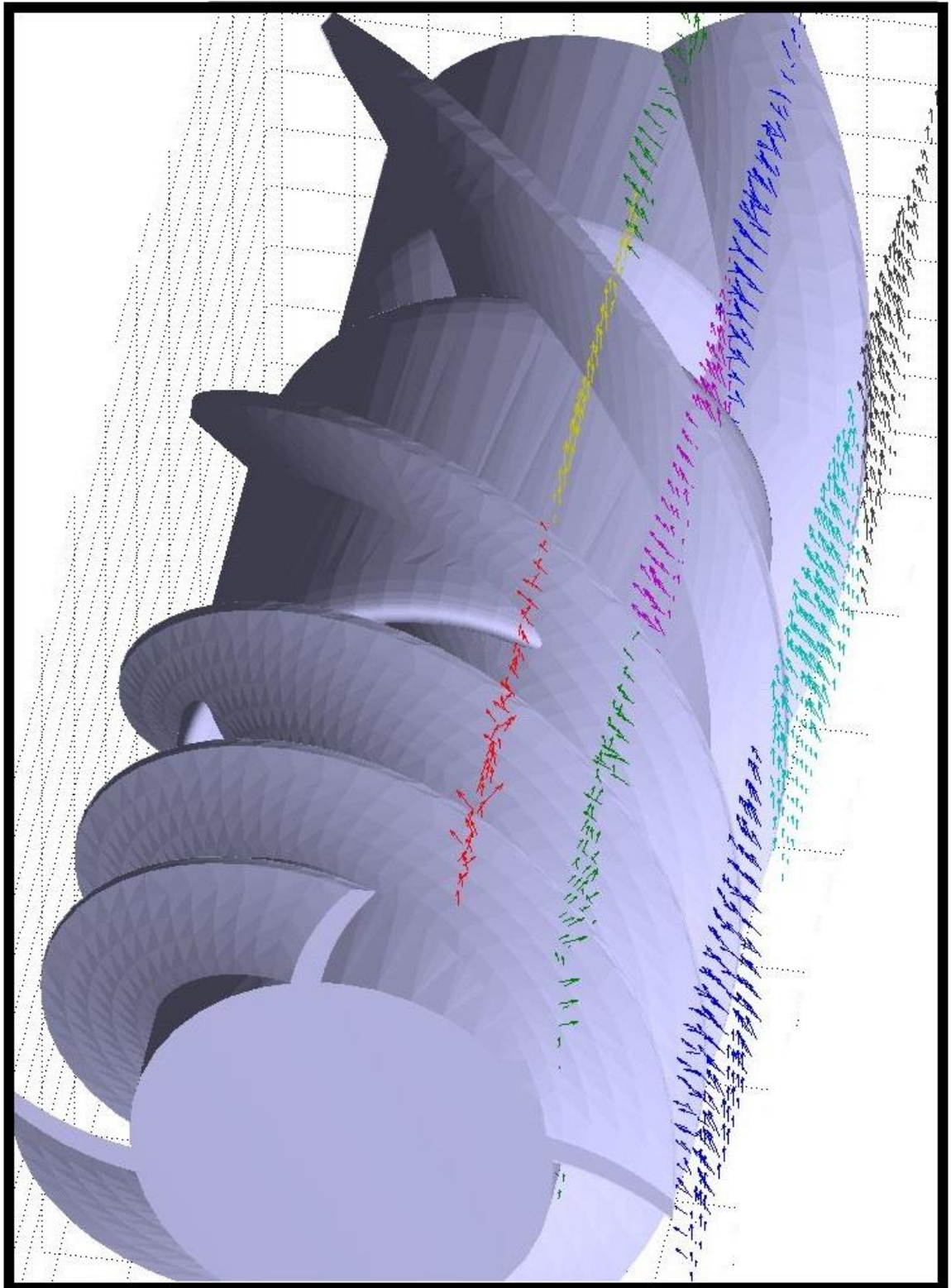
*Source: Made by Sina Dadgar*

**Figure 4.2: Physical Velocity Streamlines over the Diffuser**



*Source: Made by Sina Dadgar*

**Figure 4.3: Physical Velocity Streamlines over the Rotor**



*Source:* Made by Sina Dadgar

## 5. DISCUSSION AND FUTURE WORKS

All data, results, conclusion, and comment in this thesis are revealed for the flow field characterization of an LVAD using water. Since the viscosity of blood is higher than water, the fluid in the whole system must be replaced with glycerin-water in order to realistically study the flow field.

Furthermore, in order to image different layer of light sheets from side and up in a precise manner, EDM must be equipped with a precise sliding rail to be able to exactly correspond them. This is necessary for the accuracy of results and revealing small vortices.

In order to acquire exact and unidirectional velocity streamlines in spinning part, calculating the background image is necessary. However, since the rotor is spinning all the time, calculated background is not constant. A clear background for rotor requires an external trigger signal to set the fire to camera to acquire images in exact same location so that background calculation can be accomplished. However, currently the system is not spinning in the exact same rotation speed all the time and this is precisely why the revealed results from rotor are from only one image pair. Unsteady rotational speed of pump can be because of the gaps in the lack of the calculation of preload and afterload. It can also be because of some errors in EDM.

Last but not least, mathematical modeling of this study needs to be improved in order to get physical velocity streamlines to validate virtual velocity streamlines. Axial and tangential streamlines can be mathematically modeled to represent more similar physical streamlines to virtual ones.

## 6. REFERENCES

- 
- [1] **Klein, Andrew A. Lewis, Clive J. and Madsen, Joren C.** *Organ Transplantation A clinical guide*. New York : CAMBRIDGE university press, 2011. 978-0-521-19753-3.
- Clinical guide*. New York : CAMBRIDGE university press, 2011. 978-0-521-19753-3.
- [2] **McDonagh, Theresa A, et al., et al.** *Oxford Text Book of Heart Failure*. New York : Oxford University Press, 2011.
- [3] **Zaret, Barry L., Moser, Marvin and Cohen, Lawrence S.** *YALE University school of medicine HEART BOOK*. New York : YALE university school of Medicine, 1992. 0-688-09719-7.
- [4] *Heart Disease and Stroke Statistics—2012 Update: A Report From the American Heart Association*. **L. Roger, Véronique, et al., et al.** Dallas, TX : American Heart Association, 2012. 10.1161/CIR.0b013e31823ac046.
- [5] *Chronic Coronary Artery Disease: Diagnosis and Management*. **Cassar, Andrew, et al., et al.** s.l. : Mayo Foundation for Medical Education and Research, 2009. 10.4065/mcp.2009.0391.
- [6] **Ravitsky, Vardit, Fiester, Autumn and Caplan, Arthur L.** *The Penn Center Guide to Bioethics*. New York : Springer, 2009. 978-0-8261-1731-1.
- [7] *The influence of HLA compatibility on graft survival after heart transplantation*. **Opelz, Gerhad and Wujciak, Thomas.** 12, Heidelberg : THE NEW ENGLAND JOURNAL OF MEDICINE, 1994, Vol. 330. 04/1994; 330(12):816-9.
- [8] *ISHLT*. [Online] The international society for heart & lung transplantation , 2013. [Cited: April 07, 2014.] <https://www.isHLT.org/registries/slides.asp?slides=heartLungRegistry>.
- [9] *Explaining the decline in coronary heart disease mortality in Turkey between 1995 and 2008*. **Unal, Belgin, et al., et al.** 1135, s.l. : BMC Public Health , 2013, BMC Public Health , Vol. 13. 1471-2458-13-1135.
- [10] *Mechanical Circulatory Support and heart transplantation* . **R, Hetzer, et al., et al.** 81, Berlin : Europe PubMed Central , 1992, The journal of heart and lung transplantation , Vol. 175. 1515436.
- [11] *Long-Term use of a Left Ventricular Assist Device for end-stage heart failure*. **Rose, Eric.A, et al., et al.** 20, s.l. : THE NEW ENGLAND JOURNAL OF MEDICINE, 2001, Vol. 345. 345:1435-1443.



---

[12] **Estafanous, Fawzy G, Barash, Paul G and Reves, J.G.** *Cardiac Anesthesia Principles and Clinical Practice* . Philadelphia : Lippincott Williams & Wilkins, 2001. 0-7817-2195-4.

[13] **Miller, Kormos.** *Mechanical circulatory support; A companion to BRAUNWALD's HEART DISEASE.* Philadelphia : ELSEVIER SAUNDERS, 2012. 978-1-4160-6001-7.

[14] **K. Toptop,** "Computational Fluid Dynamic Analysis Of Axial-Flow Left-Ventricular Assist Device," *Bahcesehir University*, 2013.

[15] **R. C. Starling,** "Advanced heart failure: Transplantation, LVADs, and beyond," *Cleveland Clinic journal of medicine*, vol. 80, pp. 33-40, 2013.

[16] *Axial Flow Blood Pumps.* **SONG, XINWEI, et al., et al.** 355-364, s.l. : Asaio Journal, July 2003, Asaio, Vol. 49. 10.1097/01.MAT.0000074117.00332.0D.

[17] Office of the Chief Technologist  
[http://spinoff.nasa.gov/Spinoff2011/shuttle\\_spinoffs.html](http://spinoff.nasa.gov/Spinoff2011/shuttle_spinoffs.html)

[18] **Yildiz, Cenk Eray.** Ventricular Assist Devices for Pediatric Heart Disease. [book auth.] Guillermo Reyes. *New Aspects of Ventricular Assist Devices.* s.l. : InTech, 2011.

[19] **E.J. Birks** , Left Ventricular Assist Devices, Harefield, Middlesex 2009 Technology and guidelines

[20] CFD Analysis of MicroMed DeBakey pump and hemolysis prediction. **M. Behbhani, M. Behr, D.Arora, O. Coronado, M. Pasquili.** 14th. Congress of the International Society for Rotary Blood Pumps, Leuven, Belgium, August 31-September 2, 2006

[21] **İ.B. Aka,** "Design of a platform for physical performance testing of an Axial-Flow Left-Ventricular Assist Device", Bahcesehir University, 2014

[22] **Raffel, M; Willert, C; Wereley, S; Kompenhans, J** 'PARTICLE IMAGE VELOCIMETRY; A Practical Guide' New York 2007 Springer

[23] **Emir Gokberk Eken,** "DESIGN of LEFT VENTRICLE for CARDIOVASCULAR SYSTEM MOCK CIRCUIT" Bahcesehir University, 2013

[24] *Comparison between Tomographic PIV and Stereo PIV.* **Dirk Michaelis, Bernhard Wieneke** 14th Symp on Application of Laser Techniques to Fluid Mechanics Lisbon, Portugal, 07-10 July, 2008

---

[25] *Particle Image Velocimetry Measurements of Blood Velocity in a Continuous Flow Ventricular Assist Device*. **Steven W. Day, James C. McDaniel, et al.** ASAIO Journal August 2001- 47(4):406-11

[26] A Prototype HeartQuest Ventricular Assist Device for Particle Image Velocity Measurements. **Steven W. Day, James C. McDaniel, et al.** Blackwell Publishing Inc. International Society for Artificial Organs August 2001- 26(11):1002-1005

[27] *Multiplane Scanning Stereo-PIV Measurement of Flow inside a Spiral Vortex Pulsatile Blood Pump*. **Takanobu Yagi, William Yang, et al.** 13th Symp on Application of Laser Techniques to Fluid Mechanics Lisbon, Portugal, 26-29 June, 2006

[28] **ADRIAN, Ronald J and WESTERWEEL, Jerry.** *Particle Image Velocimetry*. New York : Cambridge University Press, 2001. 978-0-521-44008-0.

[29] **Zourob, M., Lakhtakia, A. and Urban, G.** *Optical Guided - Wave Chemical and Biosensors I*. New York : Springer , 2010. 10.1007/978-3-540-88242-8.

[30] Web Page of EVONIK industries  
<http://www.vestosint.com/product/vestosint/en/products-services/pages/default.aspx>

[31] Infinity Micro/Macro & Long-Distance Microscope Technology -  
<http://www.infinity-usa.com/products/Instruments/Model-K2-DistaMax.aspx>

[32] **Ludwig Reimer ; Helmut Kohl** ‘Transmission Electron Microscopy; Physics of Image Formation’ New York 2008 Springer

[33] **Douglas E. Chandler ; Robert W. Roberson** ‘Bio-imaging Current Concepts in Light and Electron Microscopy’ USA - 2009 - Jones and Bartlett

[34] *Salt and Pepper Noise Removal from Document Images*. **Hasan S.M. Al-Khaffaf, Abdullah Zawawi Talib, Rosalina Abdul** : Visual Informatics: Bridging Research and Practice - Springer , Volume 5857, 2009, pp 607-618

[35] **Bala Muralikrishnan and Jay Raja.** *Computational Surface and Roundness Metrology*. Antioch / California : Springer, 2009. 978-1-84800-296-8.

[36] Refractive Index Matching Methods For Liquid Flow Investigations - R.BUDWIG - Springer-Verlag 1994

[37] Reframing Photography-Theory and Practice – R. Modrak, B. Anthes, Routledge 2nd edition 2011 New York – USA